c. Tsunami Arraival Time Distribution

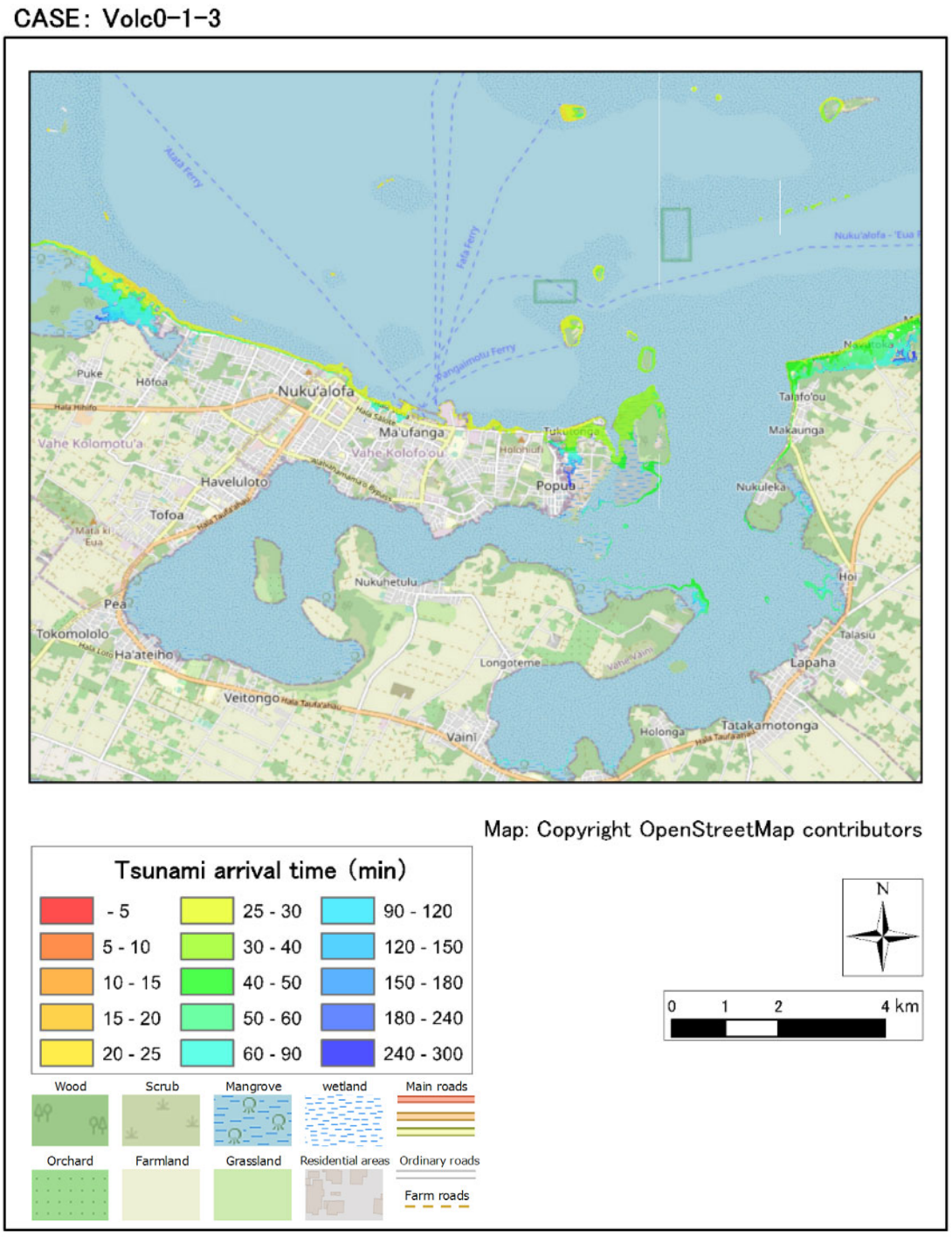

Source: JICA Study Team

Figure 2.6.299 Tsunami Arraival Time Distribution (Hunga Tonga-Hunga Ha'pai, H=30m Raised Seawall M.S.L.+4.0m)

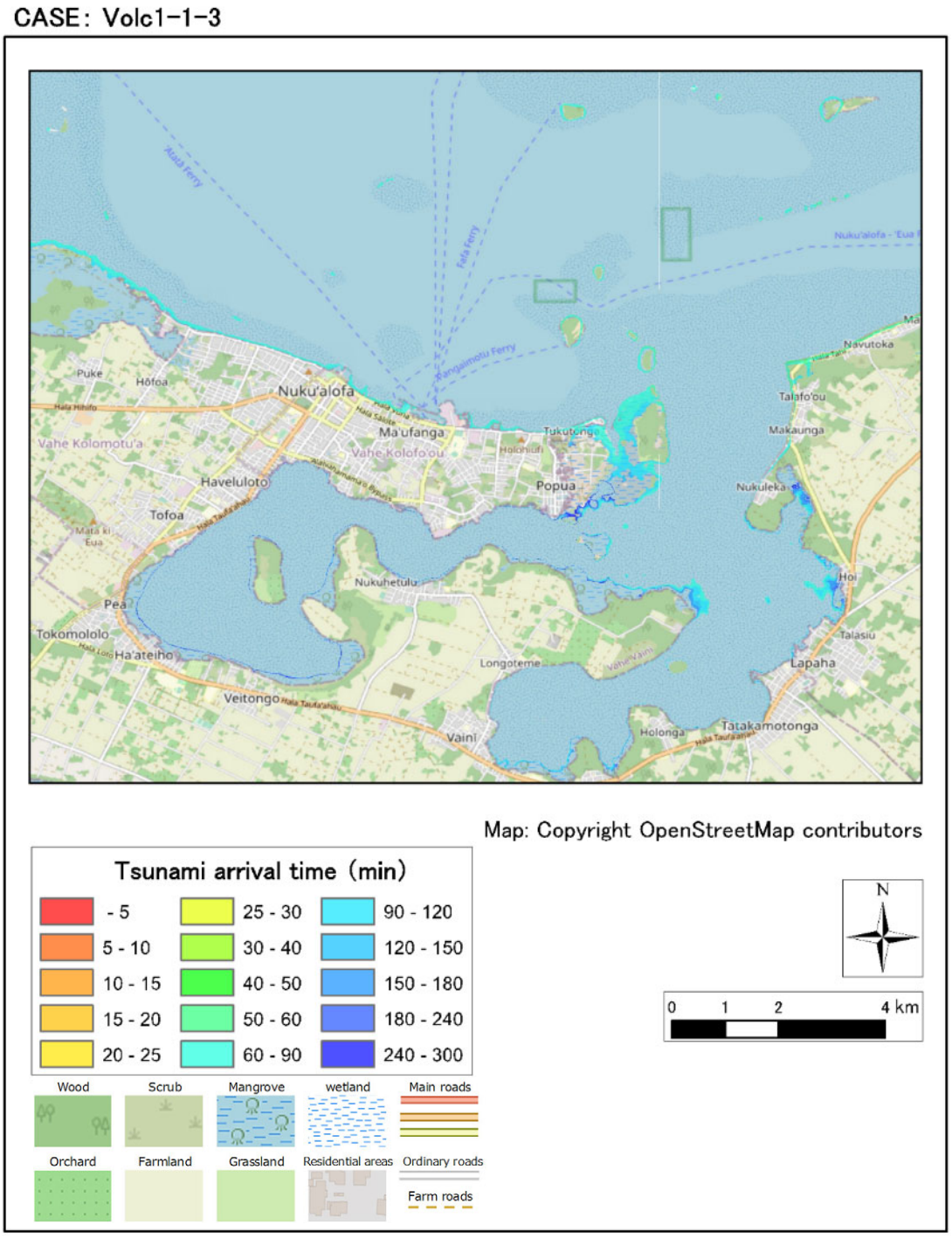

Source: JICA Study Team

Figure 2.6.300 Tsunami Arraival Time Distribution (Unnamed1, H=30m Raised Seawall M.S.L.+4.0m)

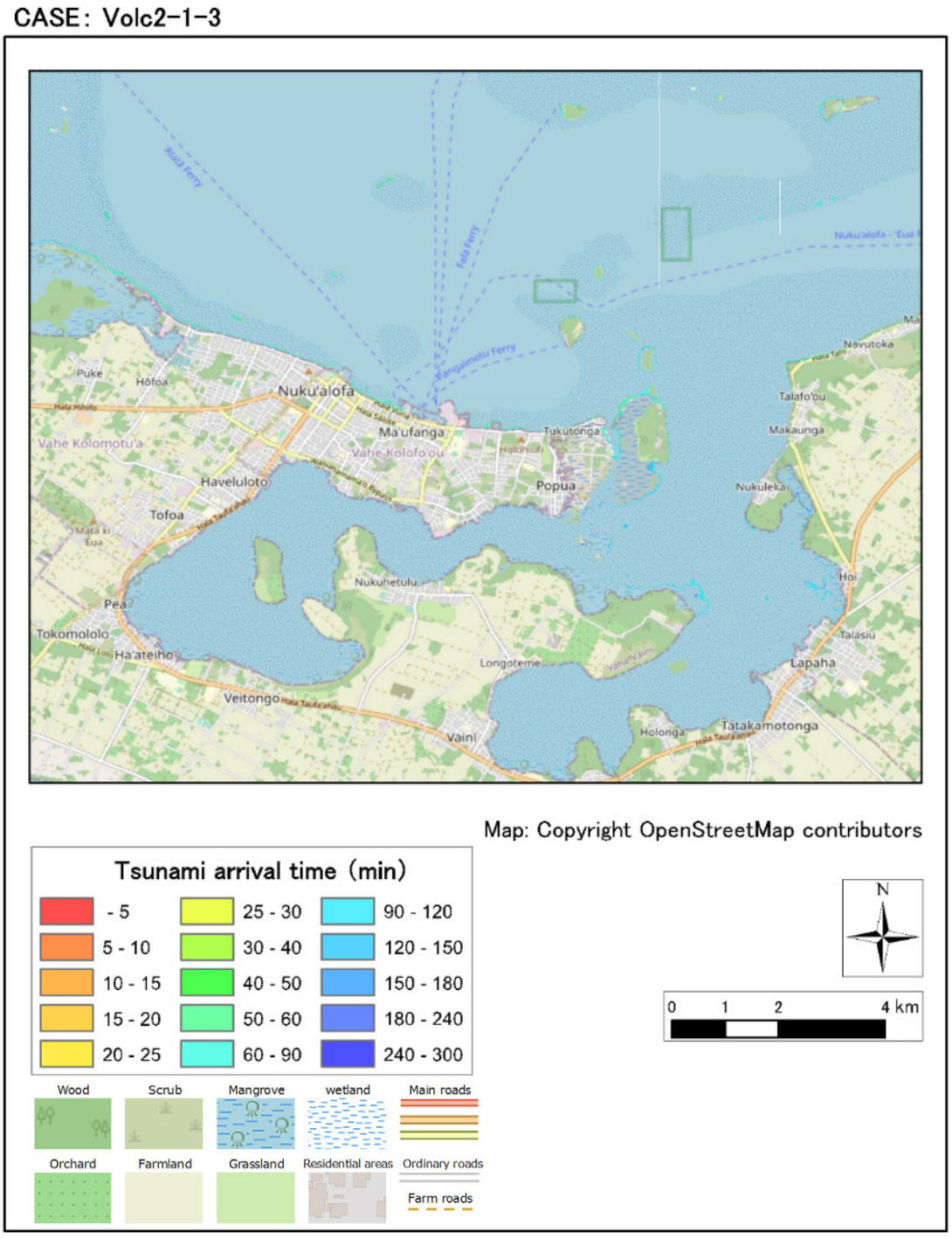

Source: JICA Study Team

Figure 2.6.301 Tsunami Arraival Time Distribution (HomeReef, H=30m Raised Seawall M.S.L.+4.0m)

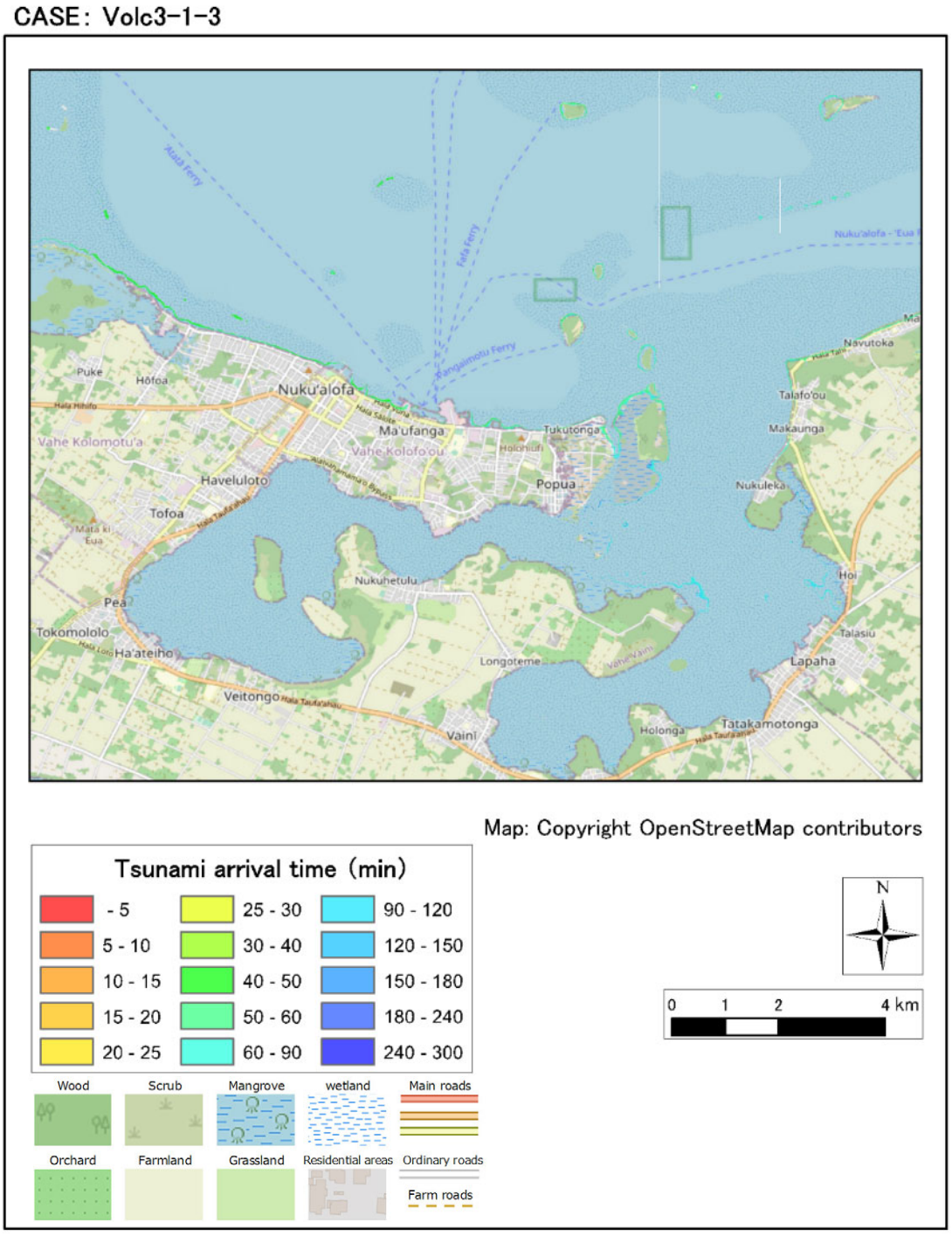

Source: JICA Study Team

Figure 2.6.302 Tsunami Arraival Time Distribution (Lateiki, H=30m Raised Seawall M.S.L.+4.0m)

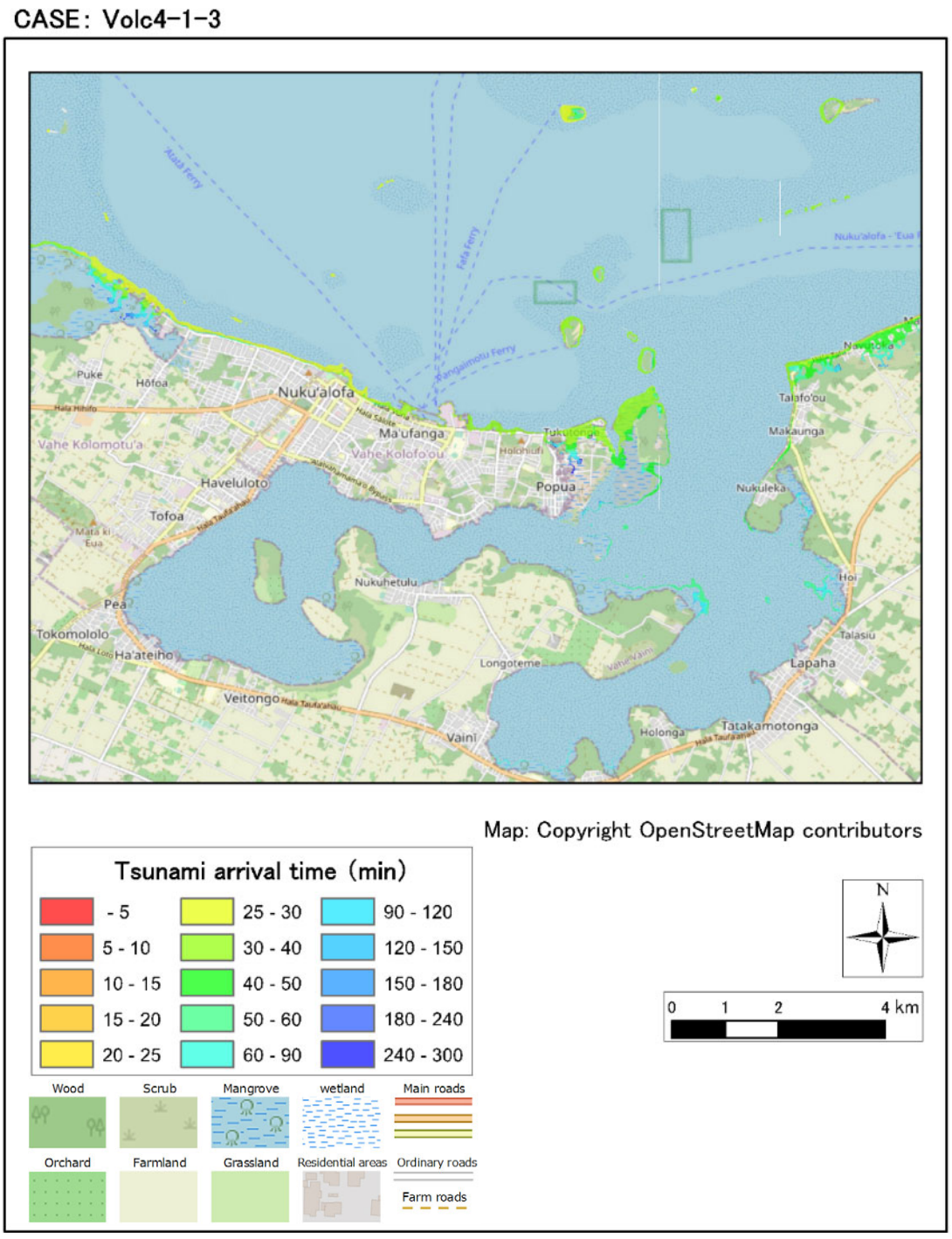

Source: JICA Study Team

Figure 2.6.303 Tsunami Arraival Time Distribution (Fonuafo'ou H=30m Raised Seawall M.S.L.+4.0m)

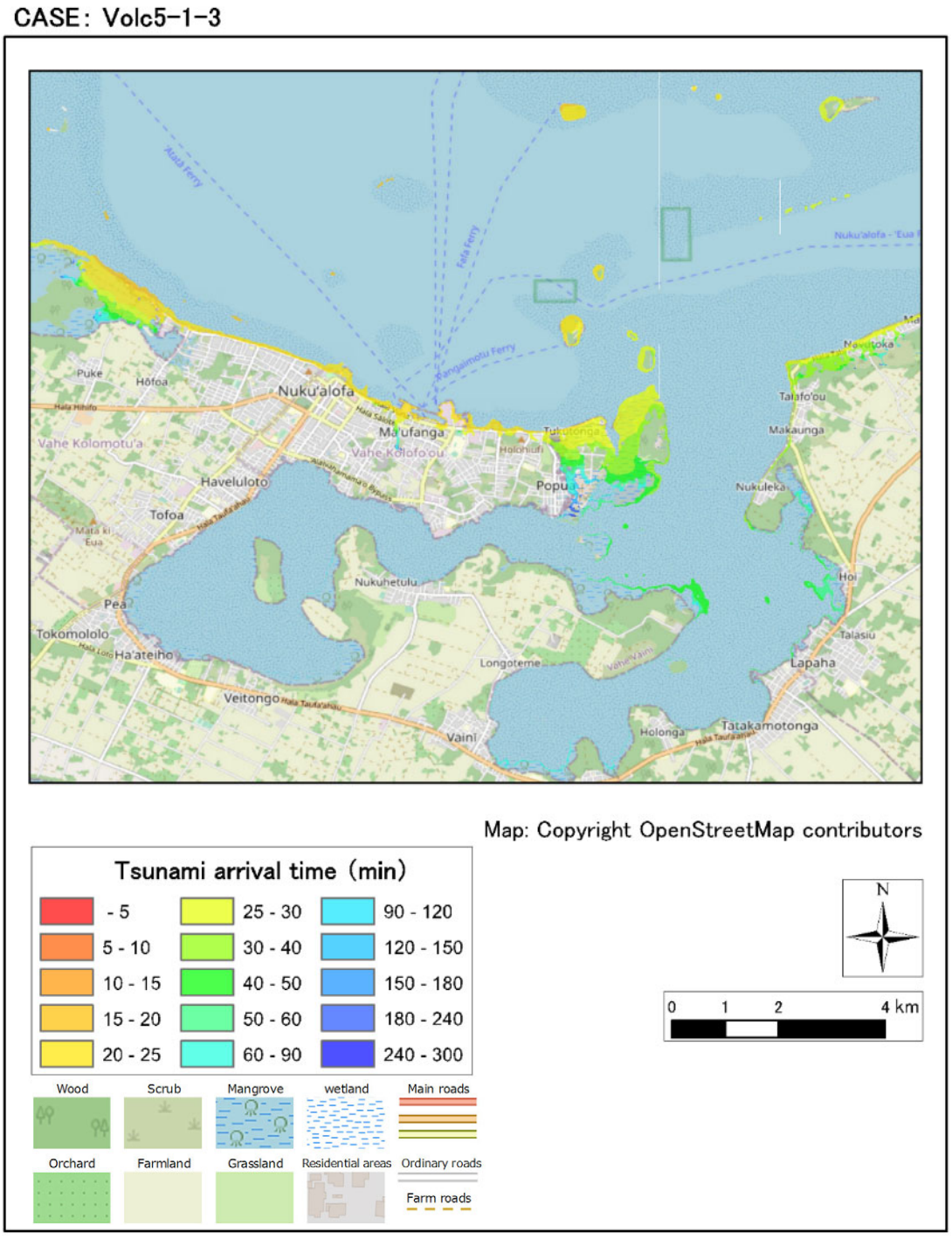

Source: JICA Study Team

Figure 2.6.304 Tsunami Arraival Time Distribution (Unamed2, H=30m Raised Seawall M.S.L.+4.0m)

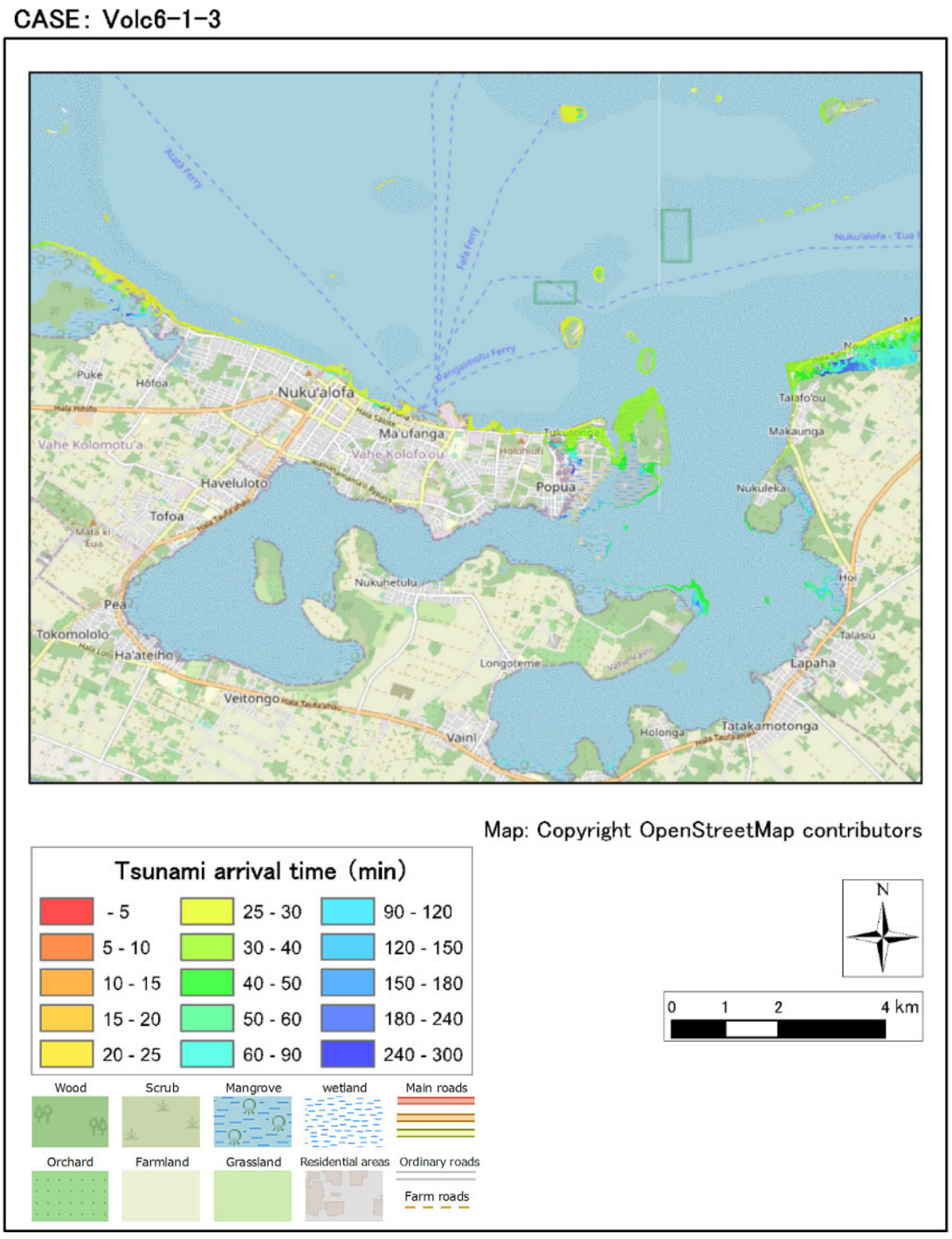

Source: JICA Study Team

Figure 2.6.305 Tsunami Arraival Time Distribution (Unamed3, H=30m Raised Seawall M.S.L.+4.0m)

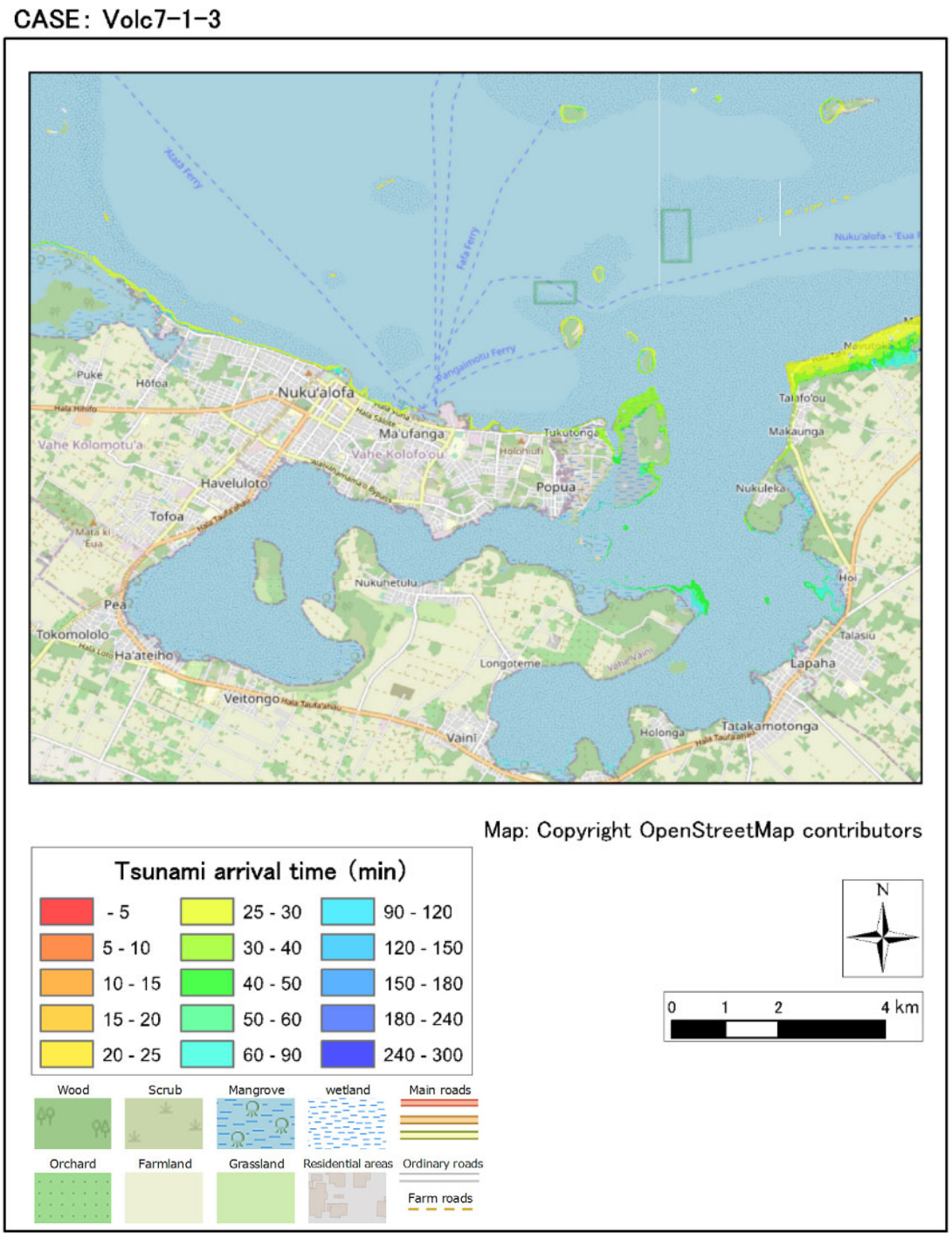

Source: JICA Study Team

Figure 2.6.306 Tsunami Arraival Time Distribution (Unamed4, H=30m Raised Seawall M.S.L.+4.0m)

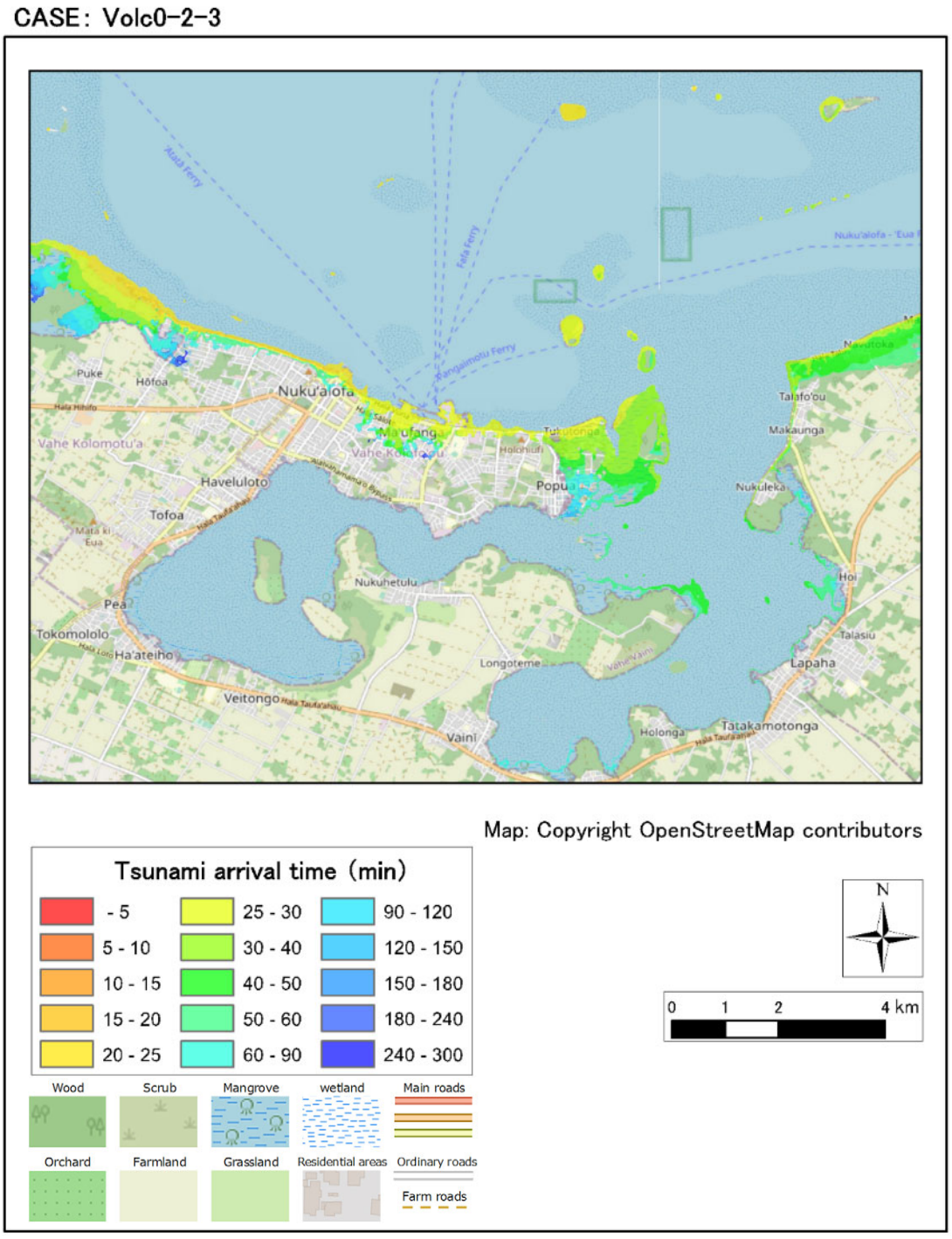

Source: JICA Study Team

Figure 2.6.307 Tsunami Arraival Time Distribution (Hunga Tonga-Hunga Ha'pai, H=60m Raised Seawall M.S.L.+4.0m)

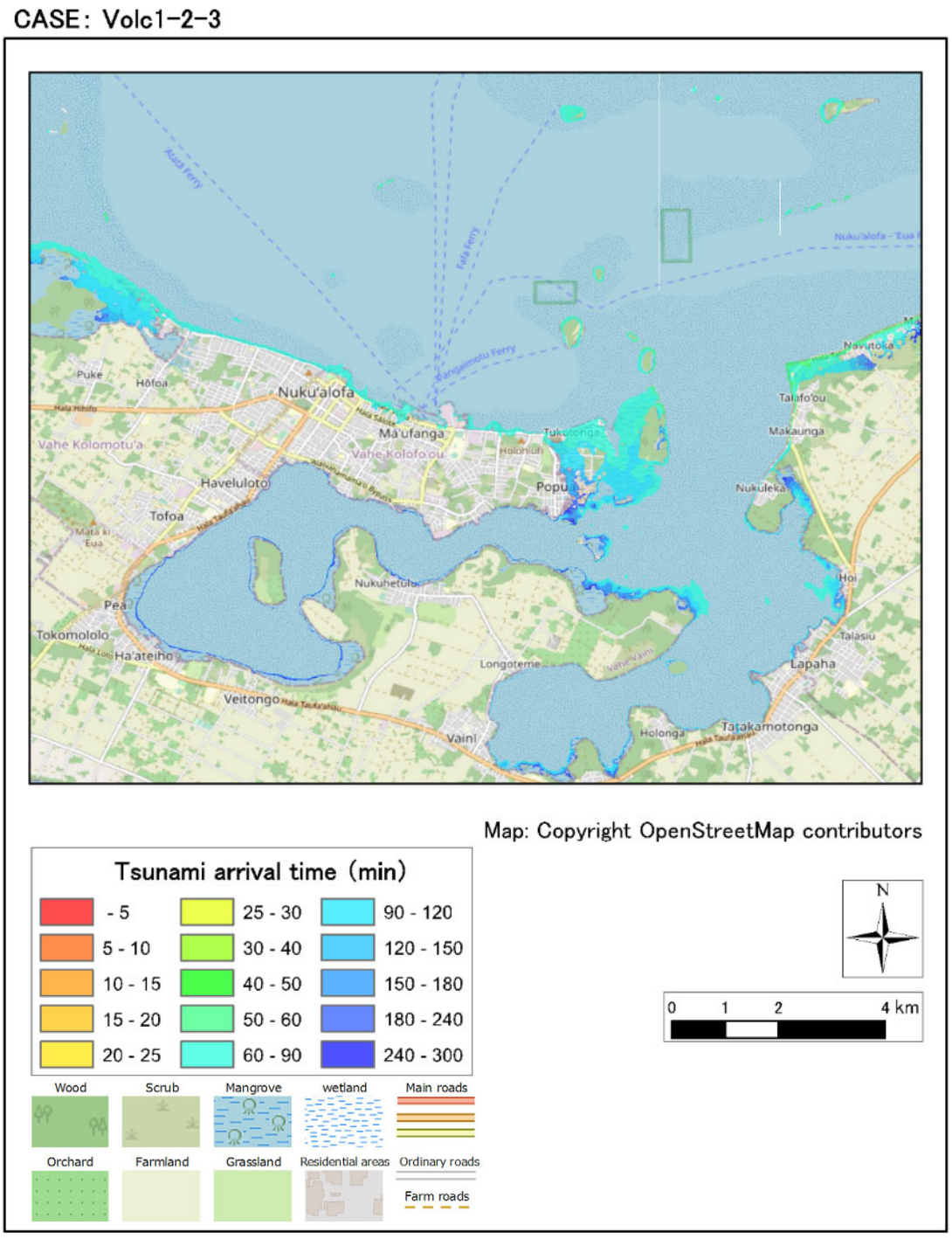

Source: JICA Study Team

Figure 2.6.308 Tsunami Arraival Time Distribution (Unnamed1, H=60m Raised Seawall M.S.L.+4.0m)

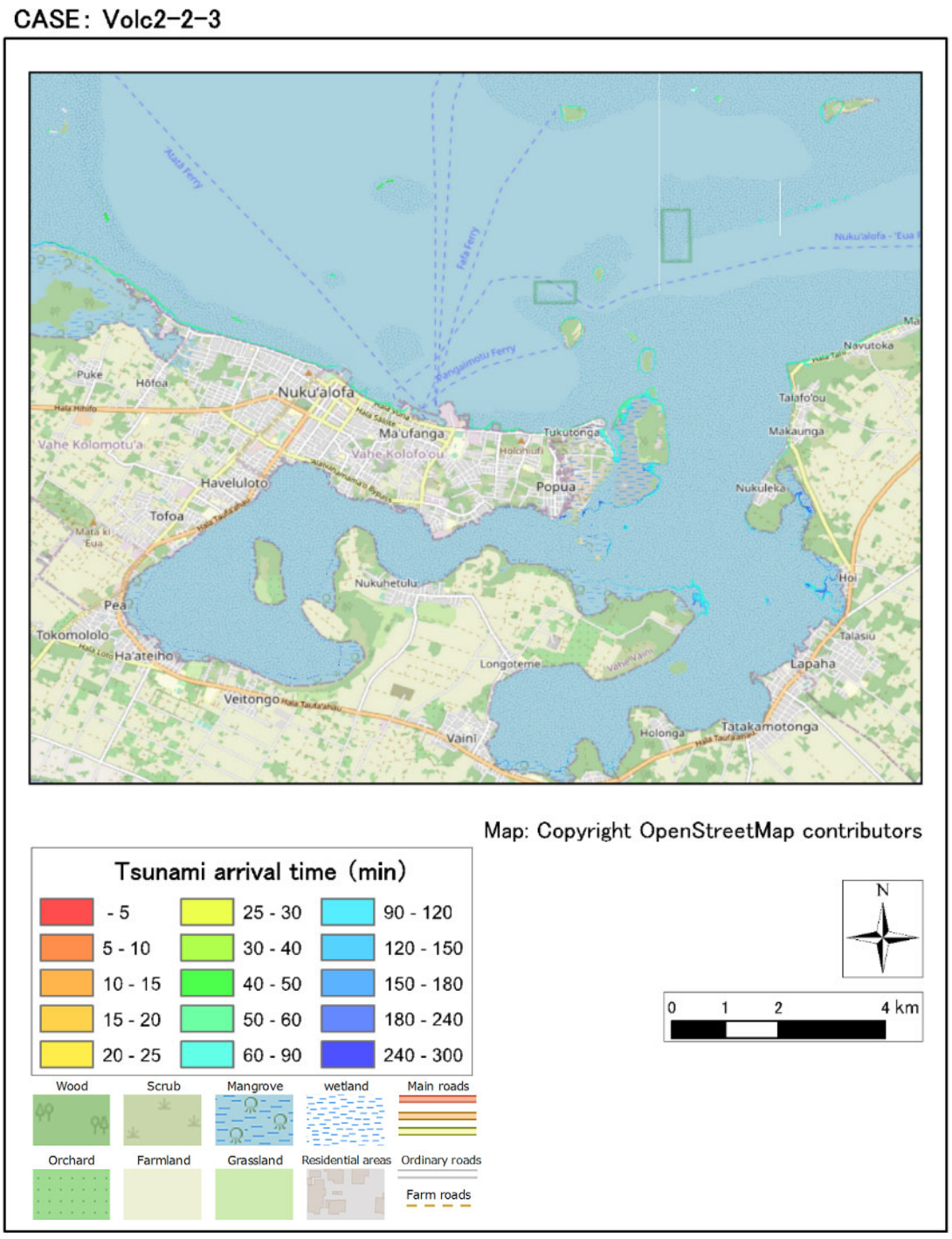

Source: JICA Study Team

Figure 2.6.309 Tsunami Arraival Time Distribution (HomeReef, H=60m Raised Seawall M.S.L.+4.0m)

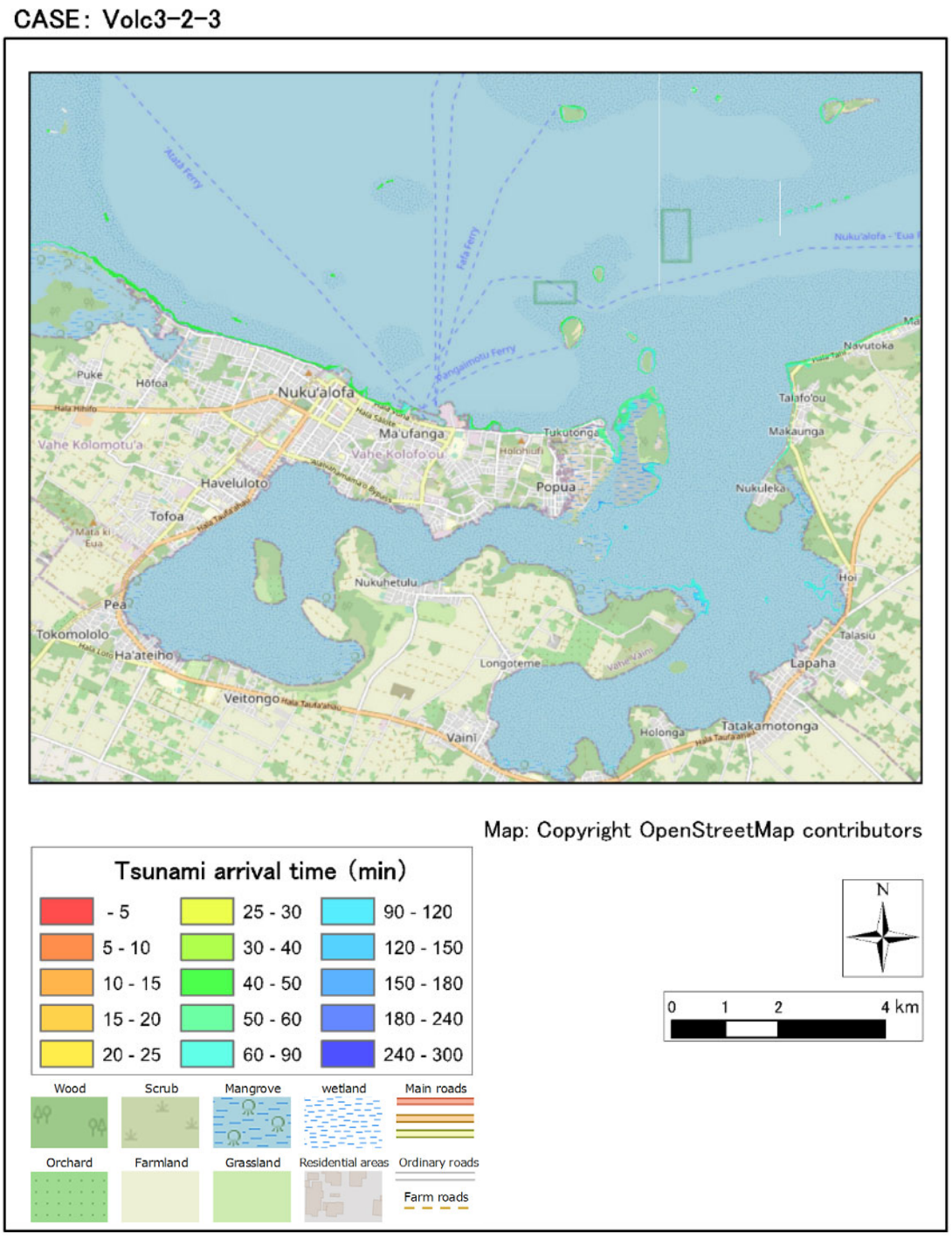

Source: JICA Study Team

Figure 2.6.310 Tsunami Arraival Time Distribution (Lateiki, H=60m Raised Seawall M.S.L.+4.0m)

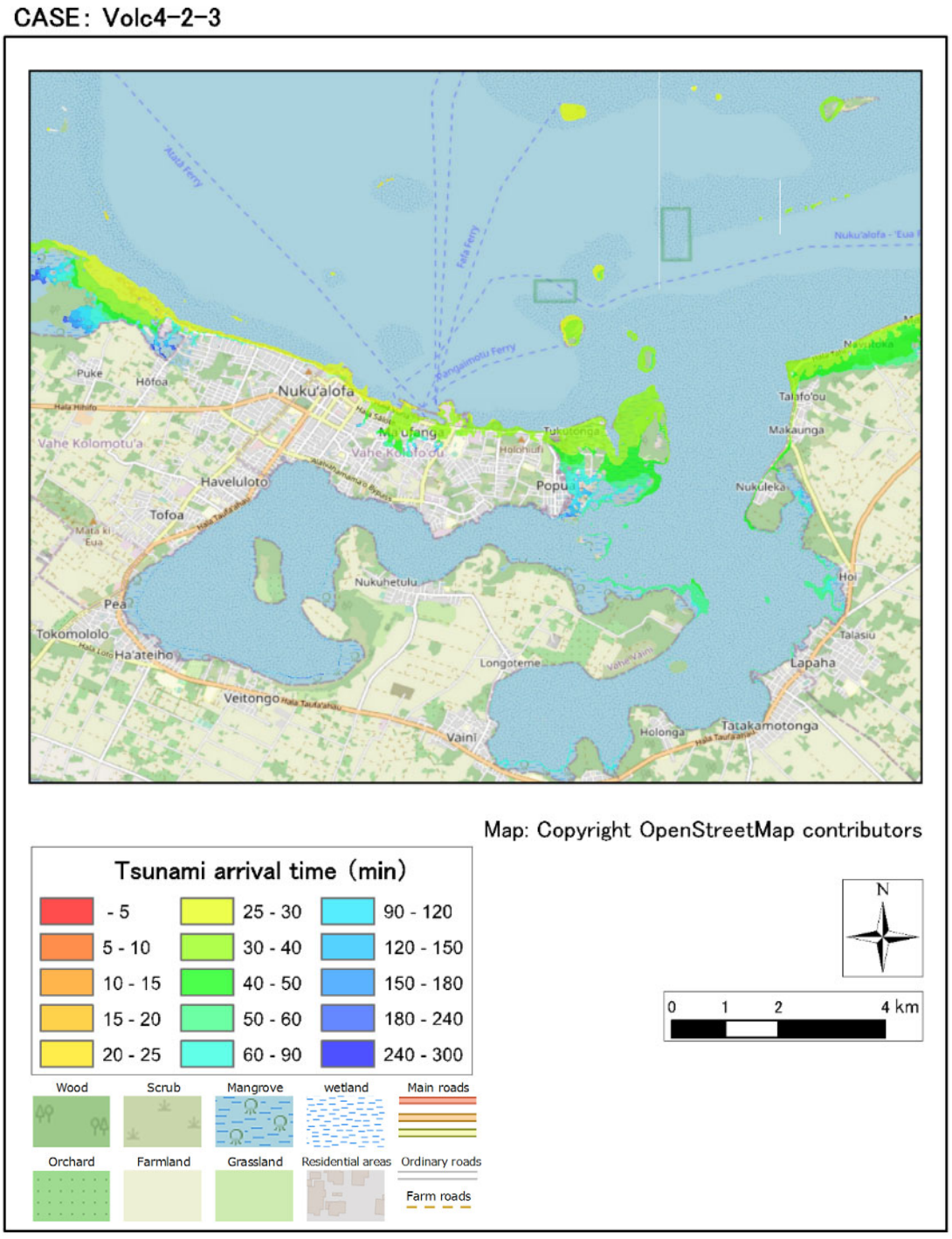

Source: JICA Study Team

Figure 2.6.311 Tsunami Arraival Time Distribution (Fonuafo'ou, H=60m Raised Seawall M.S.L.+4.0m)

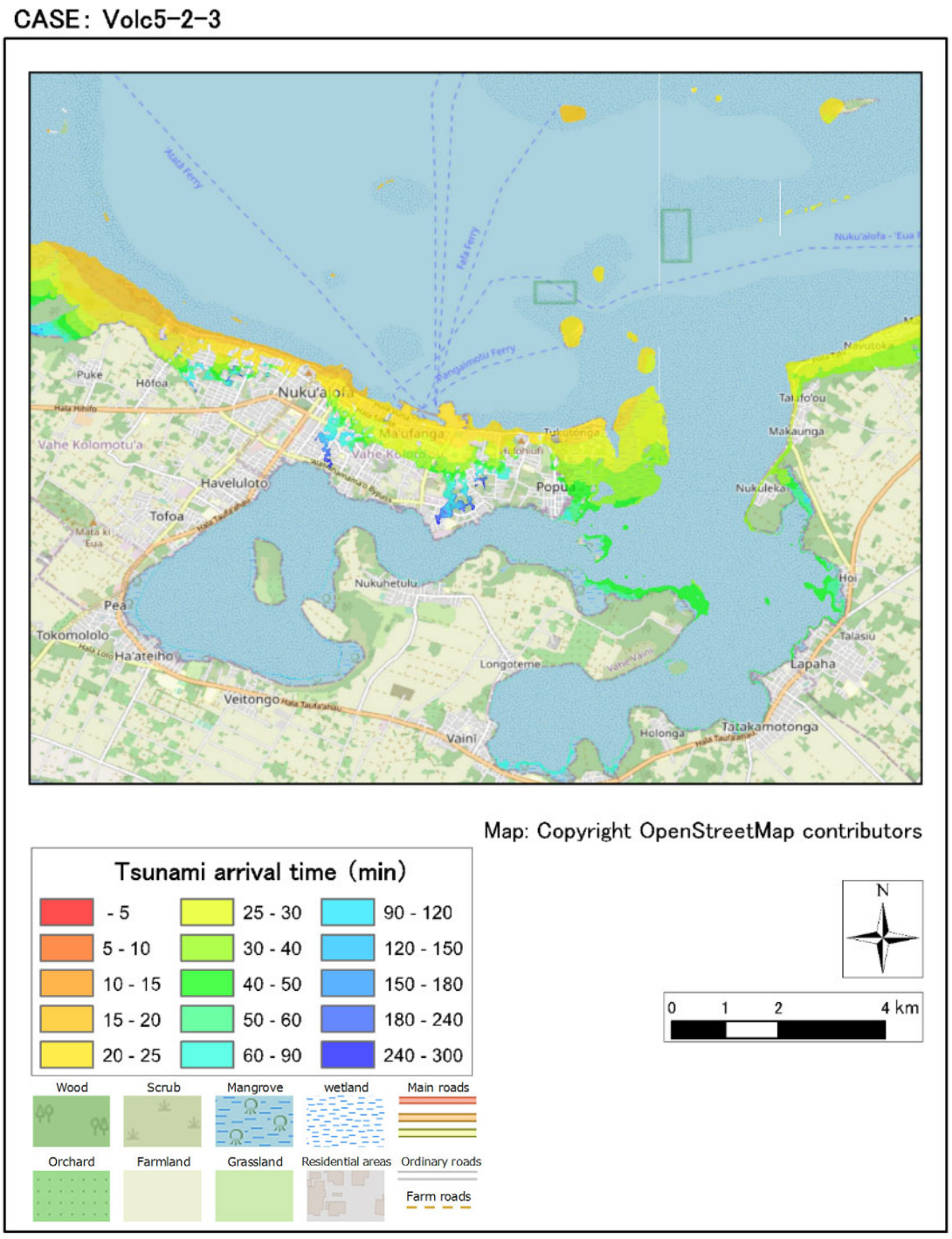

Source: JICA Study Team

Figure 2.6.312 Tsunami Arraival Time Distribution (Unamed2, H=60m Raised Seawall M.S.L.+4.0m)

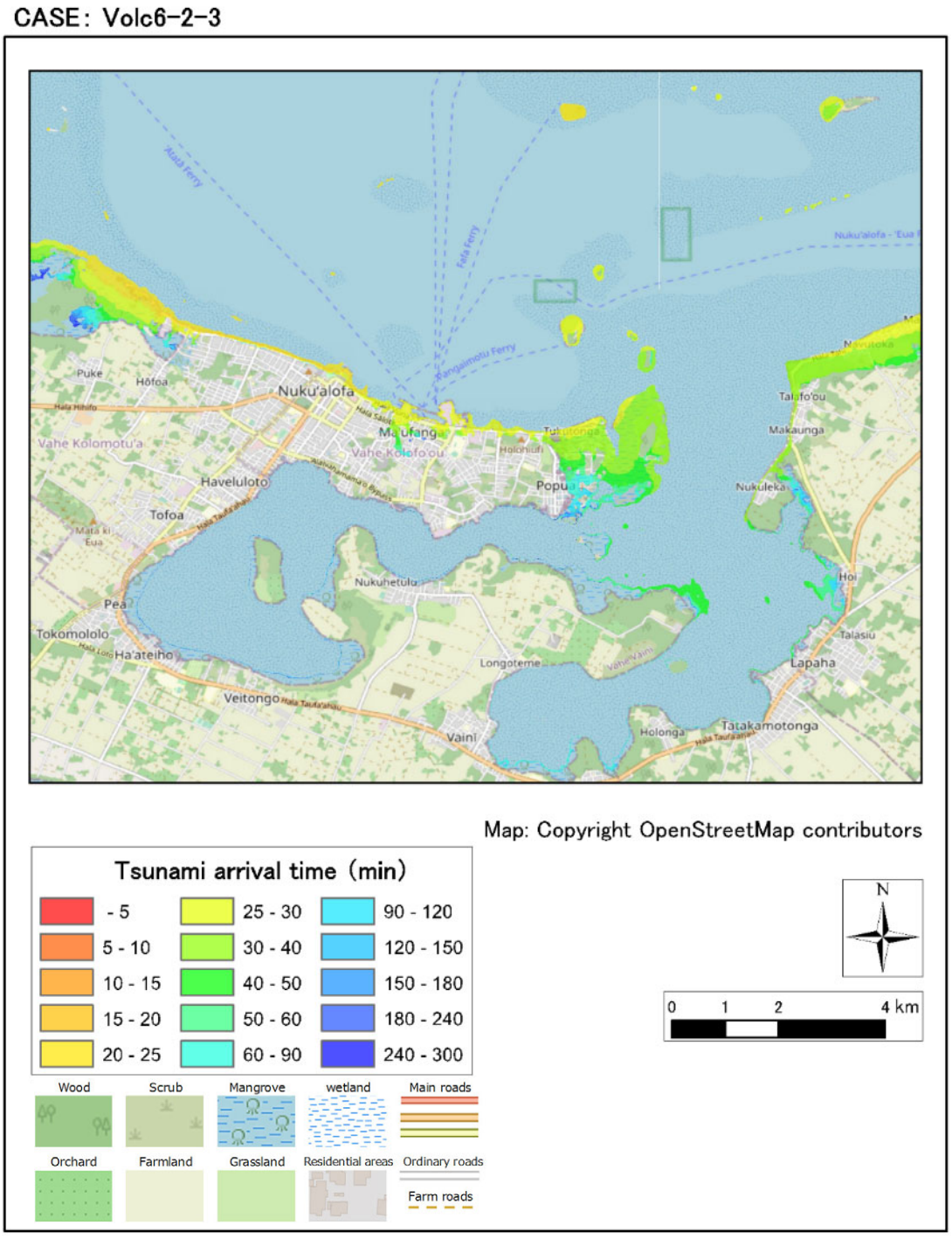

Source: JICA Study Team

Figure 2.6.313 Tsunami Arraival Time Distribution (Unamed3, H=60m Raised Seawall M.S.L.+4.0m)

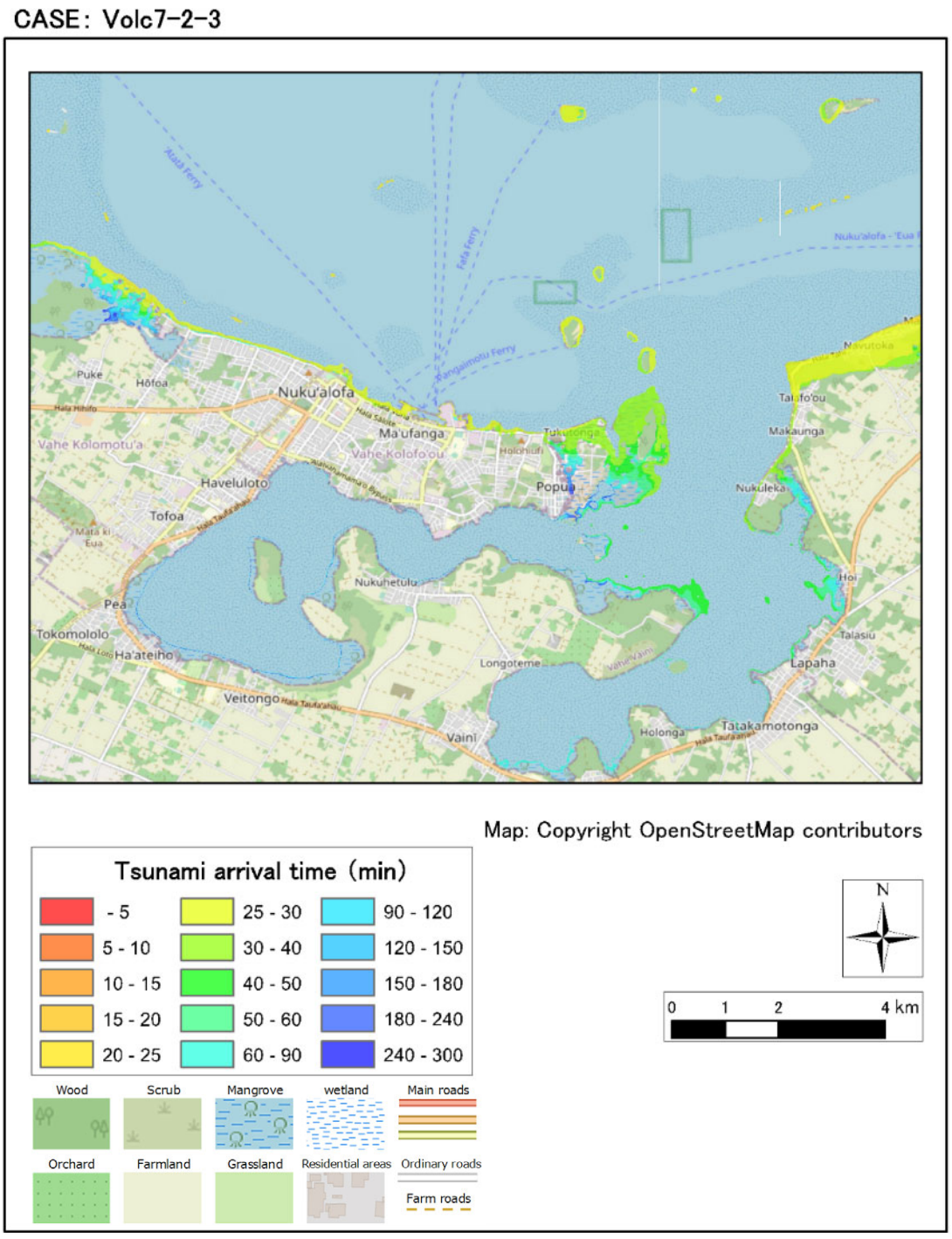

Source: JICA Study Team

Figure 2.6.314 Tsunami Arraival Time Distribution (Unamed4, H=60m Raised Seawall M.S.L.+4.0m)

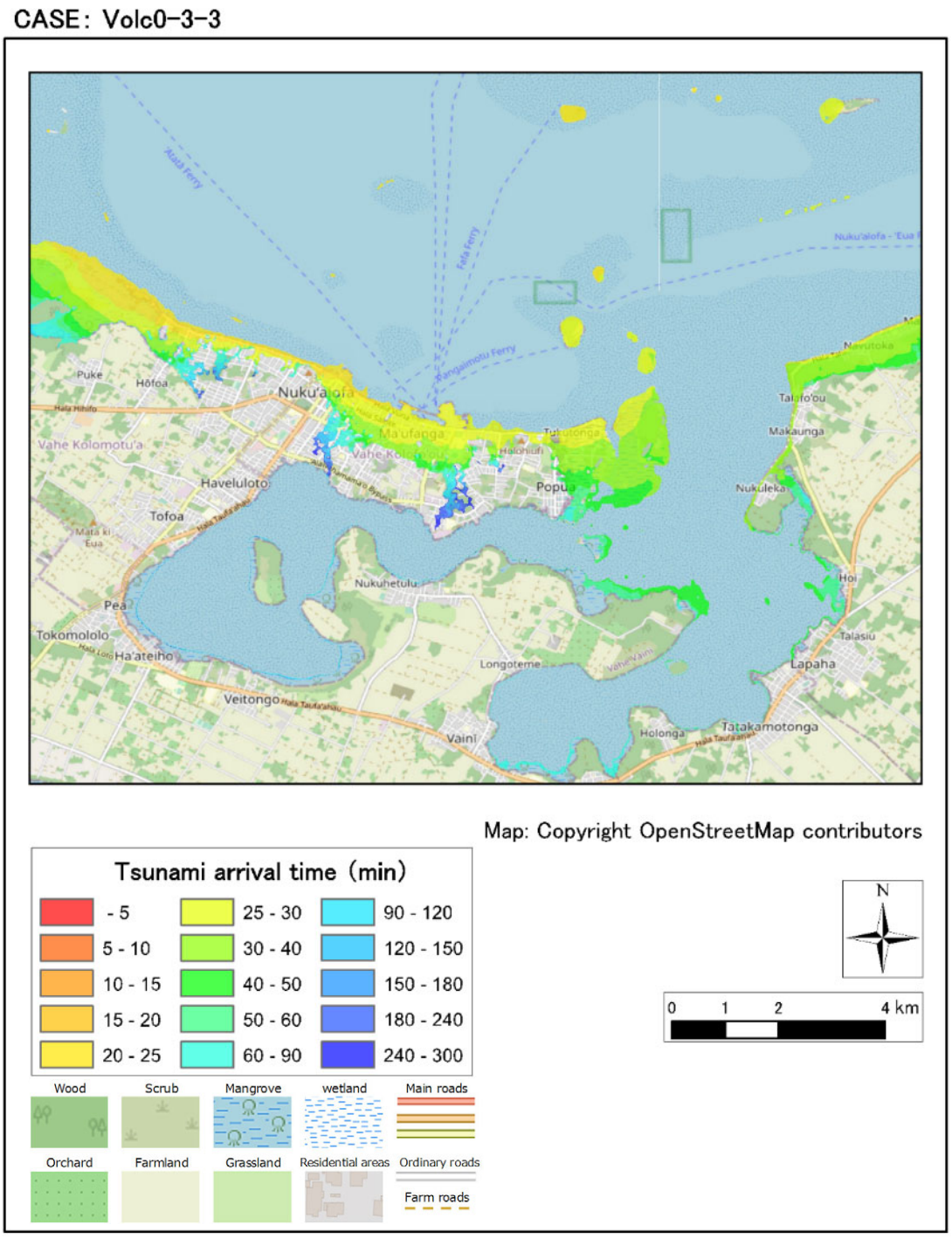

Source: JICA Study Team

Figure 2.6.315 Tsunami Arraival Time Distribution (Hunga Tonga-Hunga Ha'pai, H=90m Raised Seawall M.S.L.+4.0m)

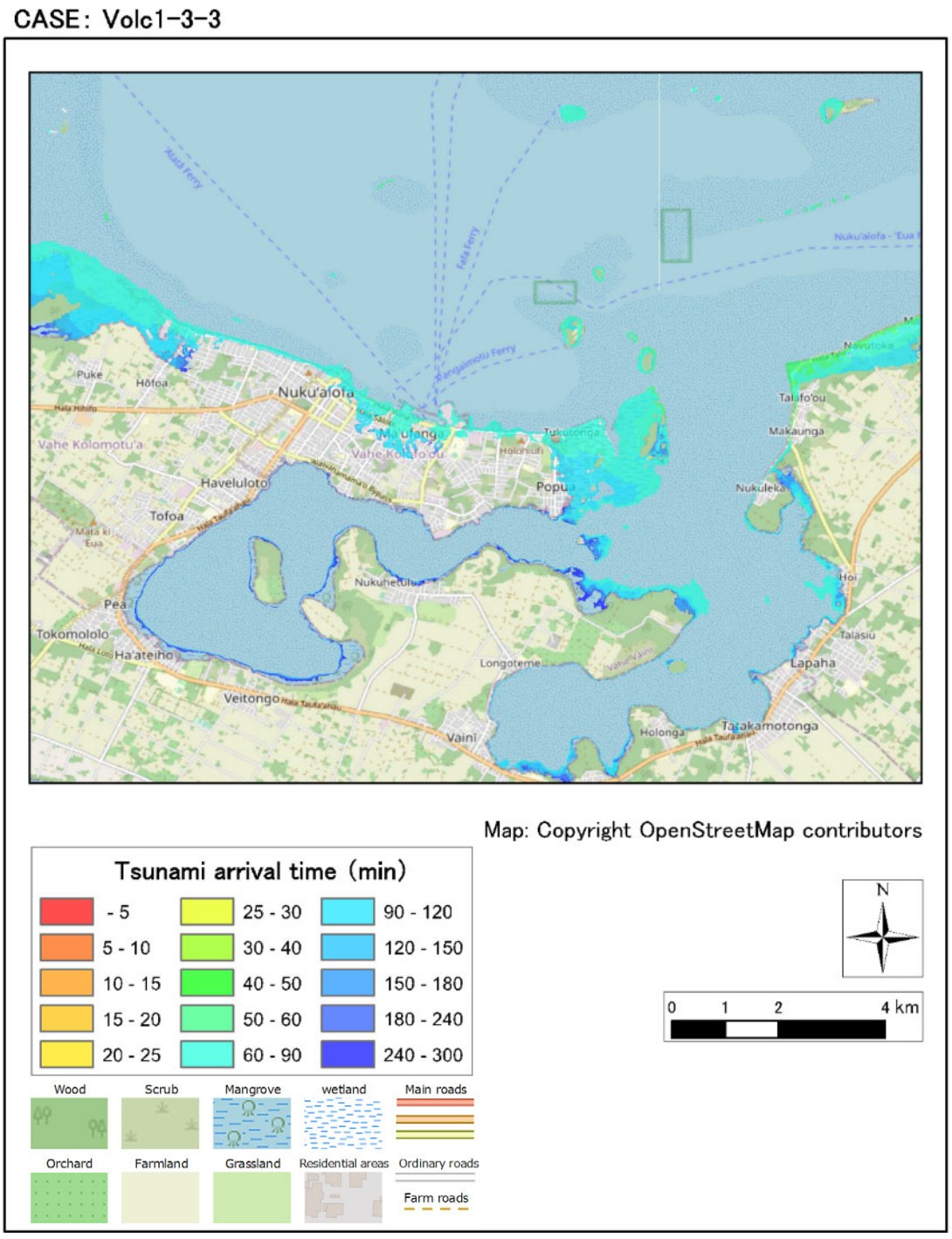

Source: JICA Study Team

Figure 2.6.316 Tsunami Arraival Time Distribution (Unnamed1, H=90m Raised Seawall M.S.L.+4.0m)

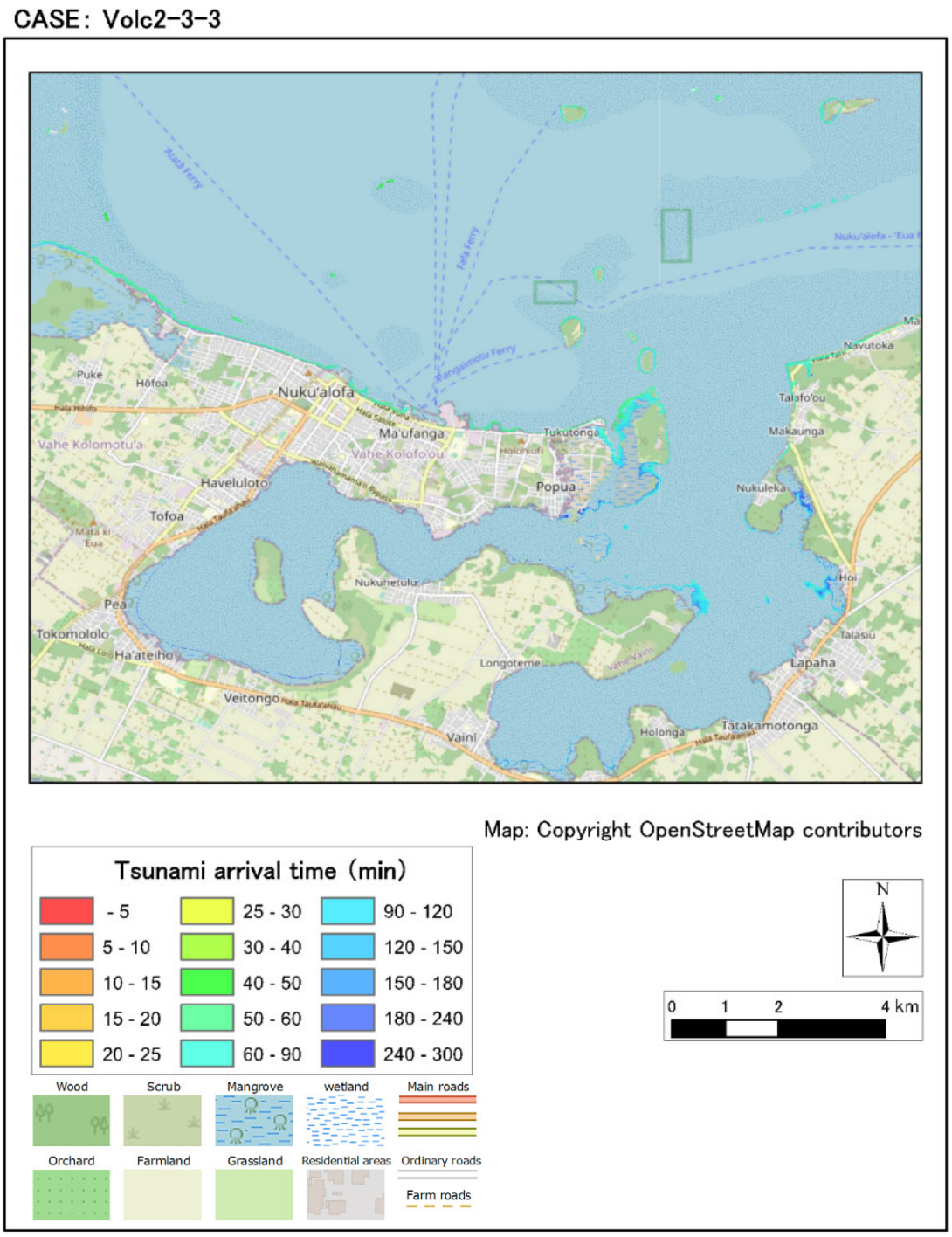

Source: JICA Study Team

Figure 2.6.317 Tsunami Arraival Time Distribution (HomeReef, H=90m Raised Seawall M.S.L.+4.0m)

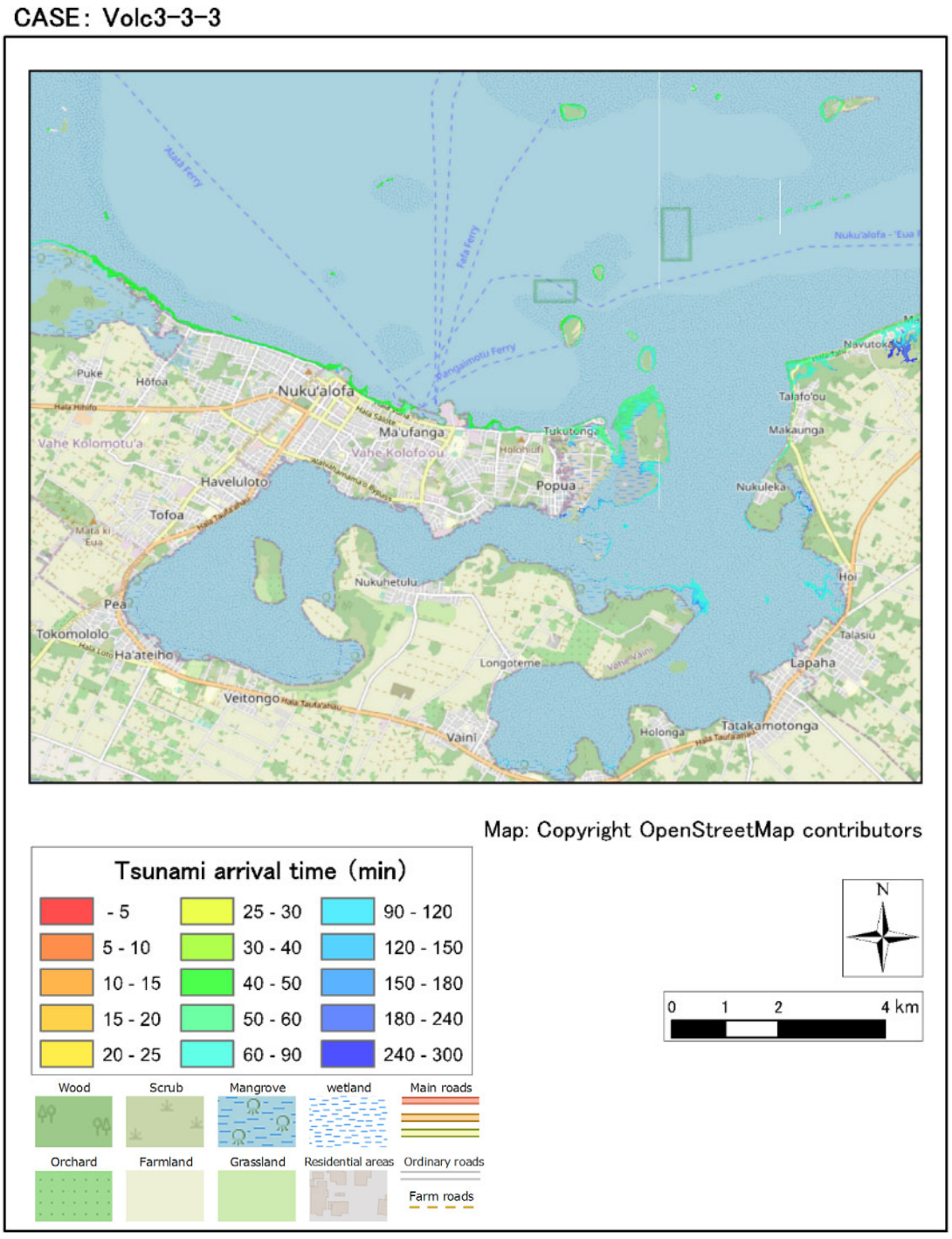

Source: JICA Study Team

Figure 2.6.318 Tsunami Arraival Time Distribution (Lateiki, H=90m Raised Seawall M.S.L.+4.0m)

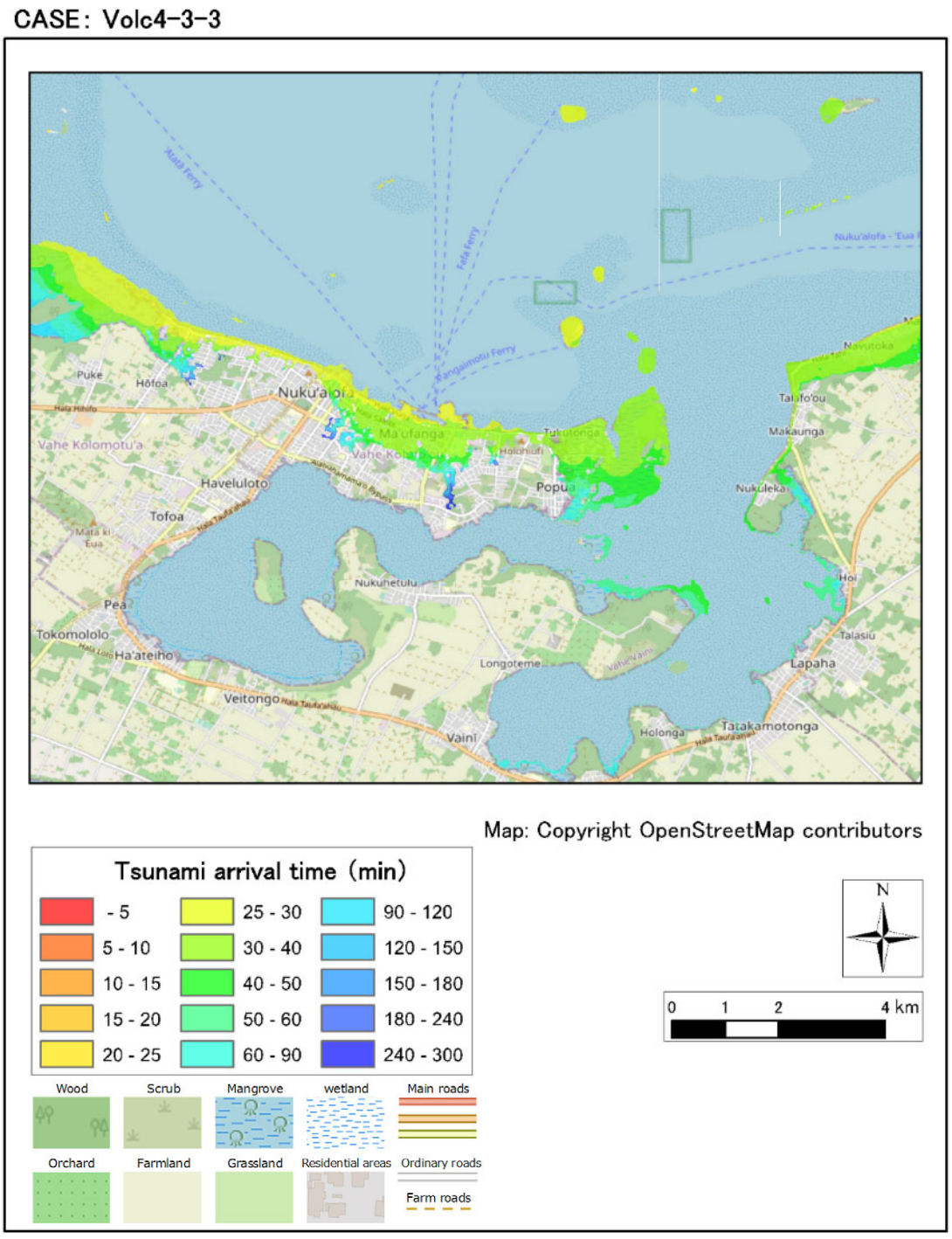

Source: JICA Study Team

Figure 2.6.319 Tsunami Arraival Time Distribution (Fonuafo'ou, H=90m Raised Seawall M.S.L.+4.0m)

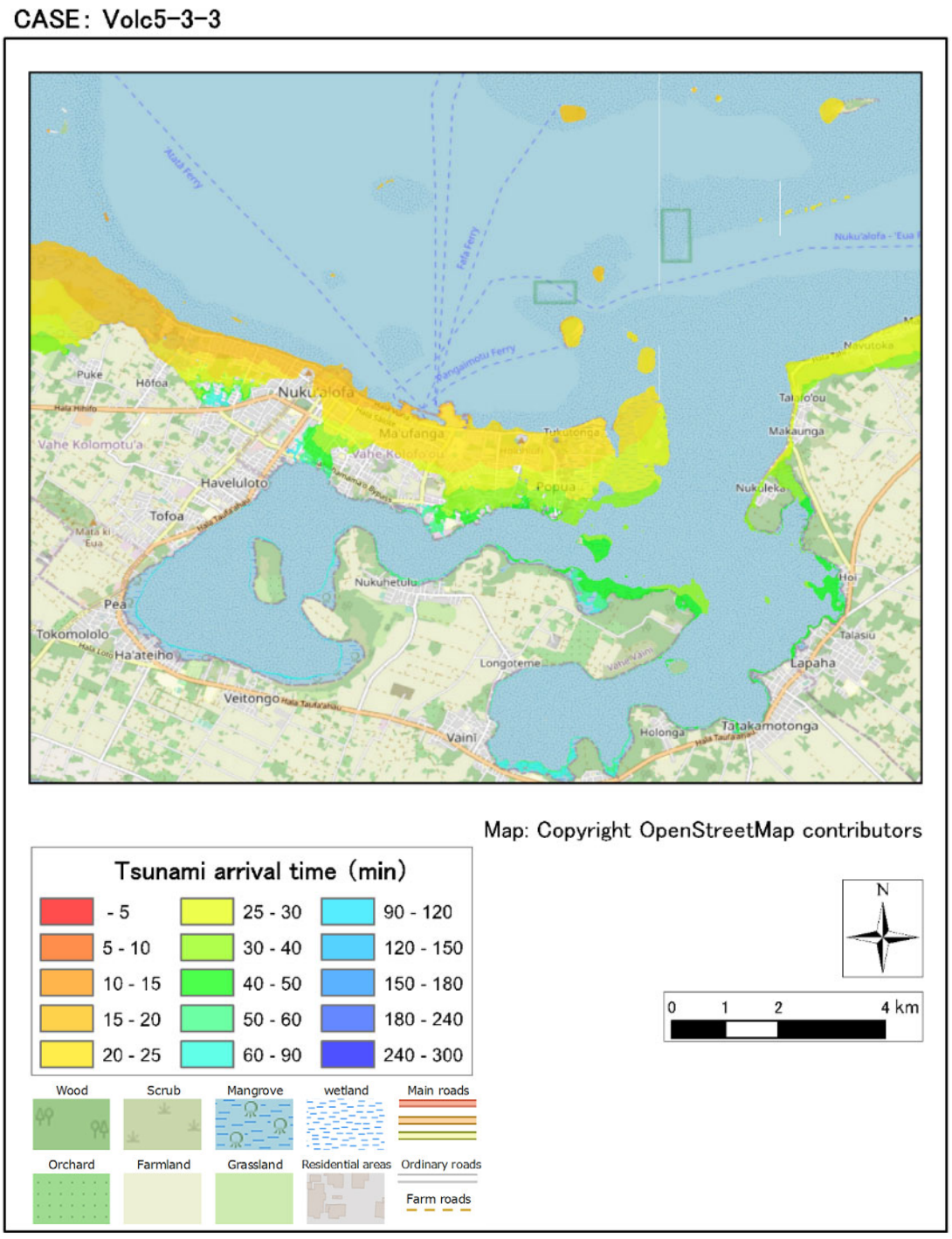

Source: JICA Study Team

Figure 2.6.320 Tsunami Arraival Time Distribution (Unamed2, H=90m Raised Seawall M.S.L.+4.0m)

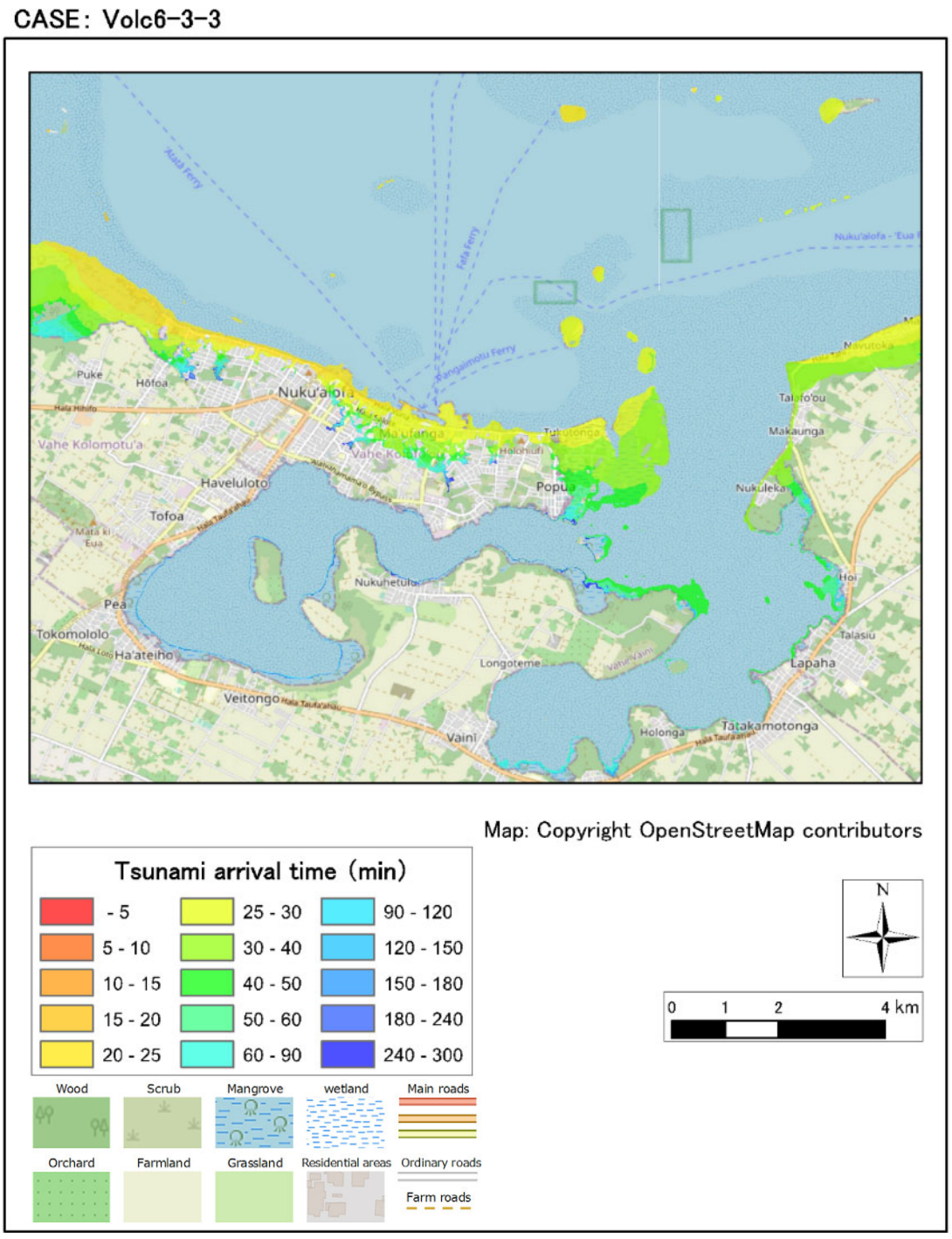

Source: JICA Study Team

Figure 2.6.321 Tsunami Arraival Time Distribution (Unamed3, H=90m Raised Seawall M.S.L.+4.0m)

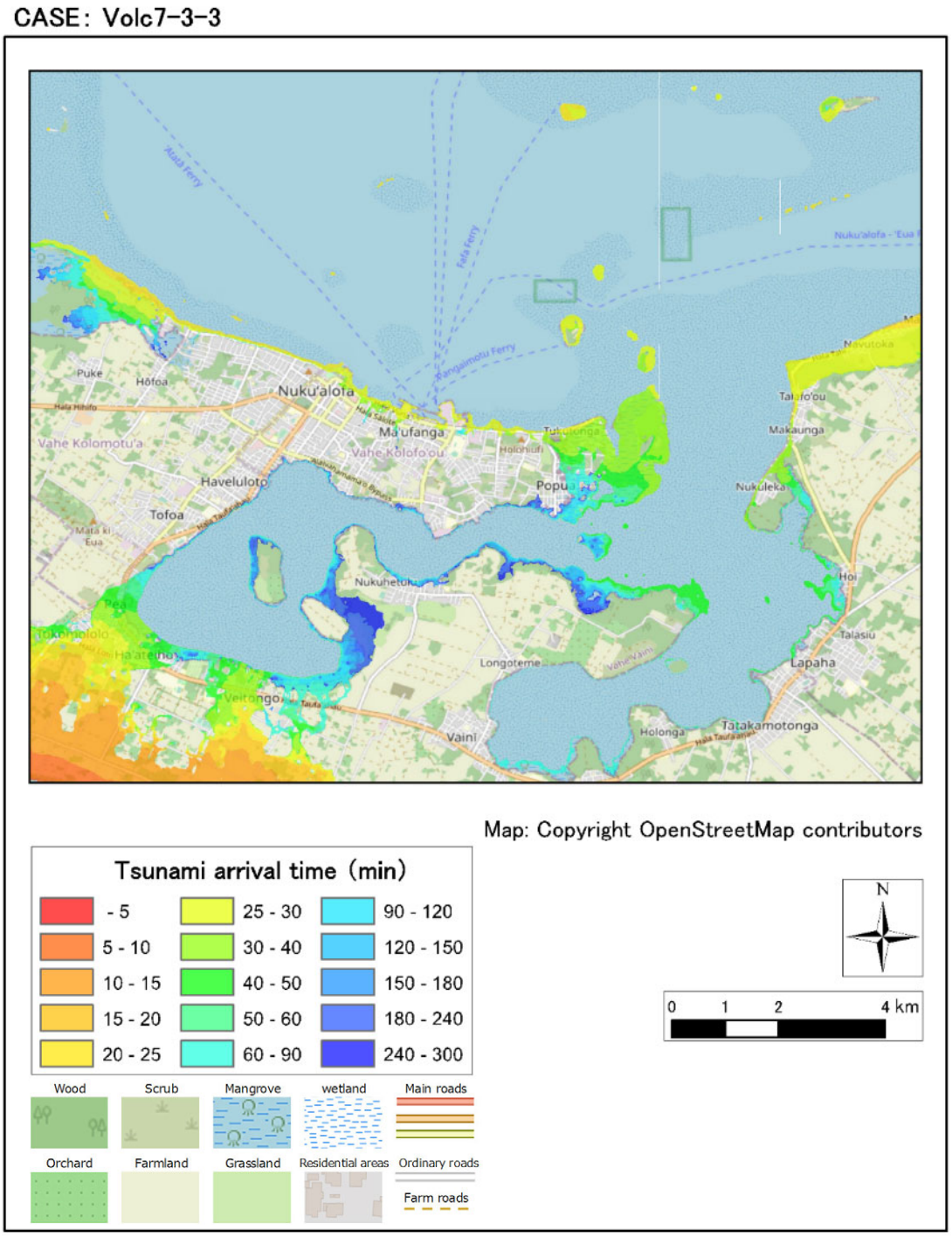

Source: JICA Study Team

Figure 2.6.322 Tsunami Arraival Time Distribution (Unamed4, H=90m Raised Seawall M.S.L.+4.0m)

2.7 Seismic Tsunami Analysis

2.7.1 Tsunami analysis with seismic faults as wave sources

Tsunami analysis with seismic faults is carried out for earthquakes of M8 or greater that have occurred in the past in the Tonga Trench and for which fault models can be set up.

(1) Target earthquakes.

The locations of past large-scale earthquakes in and around Tonga are shown in Figure 2.7.1. Table 2.7.1 lists the timing and location of each earthquake. From this, it can be seen that a large number of earthquakes have been recorded since 1913, and among them, earthquakes of M8.0 or higher, which are considered to cause large tsunamis, have occurred eight times. Therefore, the potential for the occurrence of seismic tsunamis is very great.

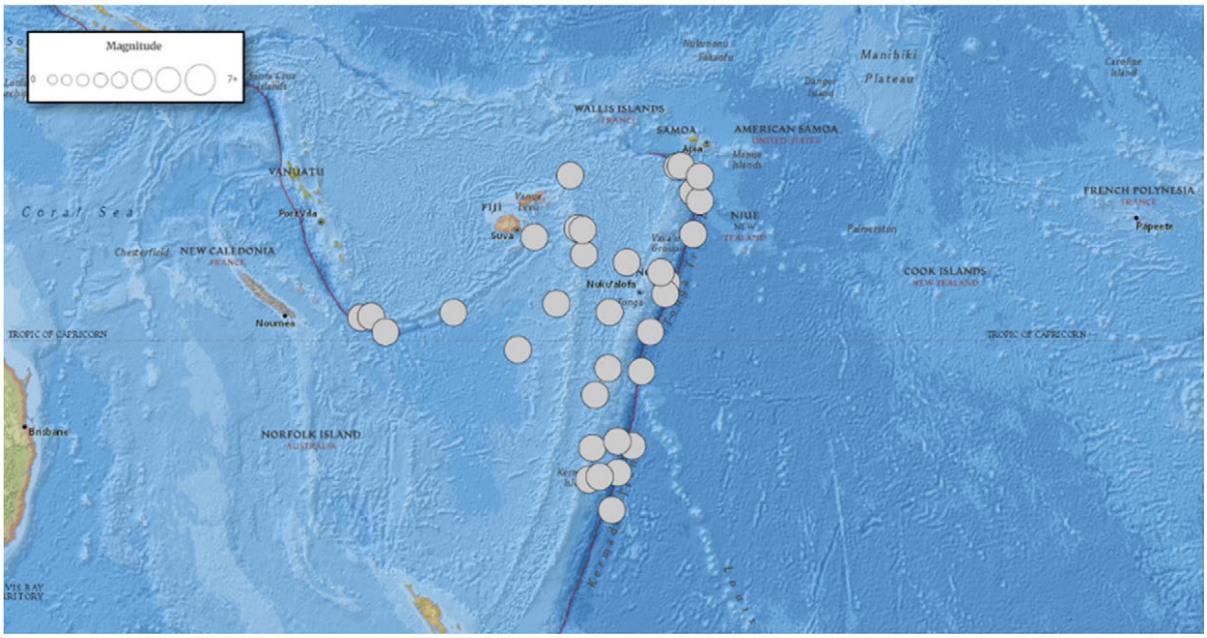

Source: USGS.

Figure 2.7.1 Location of Major Earthquakes in and around Tonga Country (1913-2022)

Table 2.7.1 List of Past Major Earthquakes

Time	Latitude	Longitude	Mag	MagType	Place
1913-06-26T04:57:18.290Z	-20.68	-173.808	7.79	mw	111 km SSE of Pangai, Tonga
1917-05-01T18:26:20.360Z	-31.195	-176.653	8.2	mw	Kermadec Islands region
1917-06-26T05:49:44.390Z	-14.996	-173.27	8	mw	120 km NNE of Hihifo, Tonga
1917-11-16T03:19:35.760Z	-29.849	-177.839	7.5	mw	Kermadec Islands, New Zealand
1919-01-01T03:00:34.460Z	-19.318	-178.08	7.8	mw	Fiji region
1919-04-30T07:17:16.970Z	-18.322	-172.442	8.1	mw	166 km ENE of Neiafu, Tonga
1928-03-16T05:01:05.850Z	-22.36	170.395	7.56	mw	274 km ESE of Tadine, New Caledonia
1948-09-08T15:09:14.220Z	-21.222	-173.891	7.5	mw	110 km E of ‘Ohonua, Tonga
1950-12-14T01:52:54.230Z	-19.705	-175.874	7.8	mw	159 km W of Pangai, Tonga
1955-02-27T20:43:27.880Z	-28.336	-175.599	7.52	mw	Kermadec Islands region
1956-05-23T20:48:32.710Z	-15.434	-178.803	7.6	mw	144 km SSW of Leava, Wallis and Futuna
1963-12-18T00:30:05.470Z	-24.749	-176.844	7.6	mw	south of the Fiji Islands
1975-10-11T14:35:15.000Z	-24.894	-175.119	7.8	ms	south of Tonga
1975-12-26T15:56:38.700Z	-16.264	-172.467	7.8	ms	146 km ESE of Hihifo, Tonga
1976-01-14T16:47:33.500Z	-28.427	-177.657	8	ms	Kermadec Islands region
1977-04-02T07:15:22.700Z	-16.696	-172.095	7.6	ms	199 km ESE of Hihifo, Tonga
1981-09-01T09:29:31.540Z	-14.96	-173.085	7.7	ms	133 km NE of Hihifo, Tonga
1986-10-20T06:46:09.980Z	-28.117	-176.367	7.7	mw	Kermadec Islands region
1990-03-03T12:16:27.960Z	-22.122	175.163	7.6	mw	south of the Fiji Islands
1994-03-09T23:28:06.780Z	-18.039	-178.413	7.6	mw	240 km E of Levuka, Fiji
1997-10-14T09:53:18.150Z	-22.101	-176.772	7.8	mwb	192 km WSW of Haveluloto, Tonga
1998-01-04T06:11:58.970Z	-22.301	170.911	7.5	mwc	southeast of the Loyalty Islands
2002-08-19T11:01:01.190Z	-21.696	-179.513	7.7	mwc	Fiji region
2002-08-19T11:08:24.310Z	-23.884	178.495	7.7	mwc	south of the Fiji Islands
2006-05-03T15:26:40.290Z	-20.187	-174.123	8	mwc	47 km SSE of Pangai, Tonga
2007-12-09T07:28:20.820Z	-25.996	-177.514	7.8	mwc	south of the Fiji Islands
2009-03-19T18:17:40.470Z	-23.043	-174.66	7.6	mwc	191 km S of ‘Ohonua, Tonga
2009-09-29T17:48:10.990Z	-15.489	-172.095	8.1	mwc	168 km SSW of Matavai, Samoa
2011-07-06T19:03:18.260Z	-29.539	-176.34	7.6	mww	Kermadec Islands region
2018-08-19T00:19:40.670Z	-18.1125	-178.153	8.2	mww	267 km E of Levuka, Fiji
2018-09-06T15:49:18.710Z	-18.4743	179.3502	7.9	mww	45 km S of Levuka, Fiji
2021-02-10T13:19:55.530Z	-23.0511	171.6566	7.7	mww	southeast of the Loyalty Islands
2021-03-04T19:28:33.178Z	-29.7228	-177.279	8.1	mww	Kermadec Islands, New Zealand

☐ : Earthquakes of Mw 8.0 and above, Red: earthquakes to be calculated

Source: USGS.

Objective analysis in this project will be extracted the earthquakes with the highest moment magnitude (Mw) among the earthquakes that occurred after 1913 from the Earthquake Catalog of the United States Geological Survey (USGS). Targeting the top 5 extracted earthquakes, set Fault Parameters and perform tsunami analysis.

Figure 2.7.2 shows the epicenter map of the target earthquake. Earthquakes before 1975 are excluded from the study because there is little information such as CMT solutions and aftershock distribution, and it is difficult to set Fault Parameters.

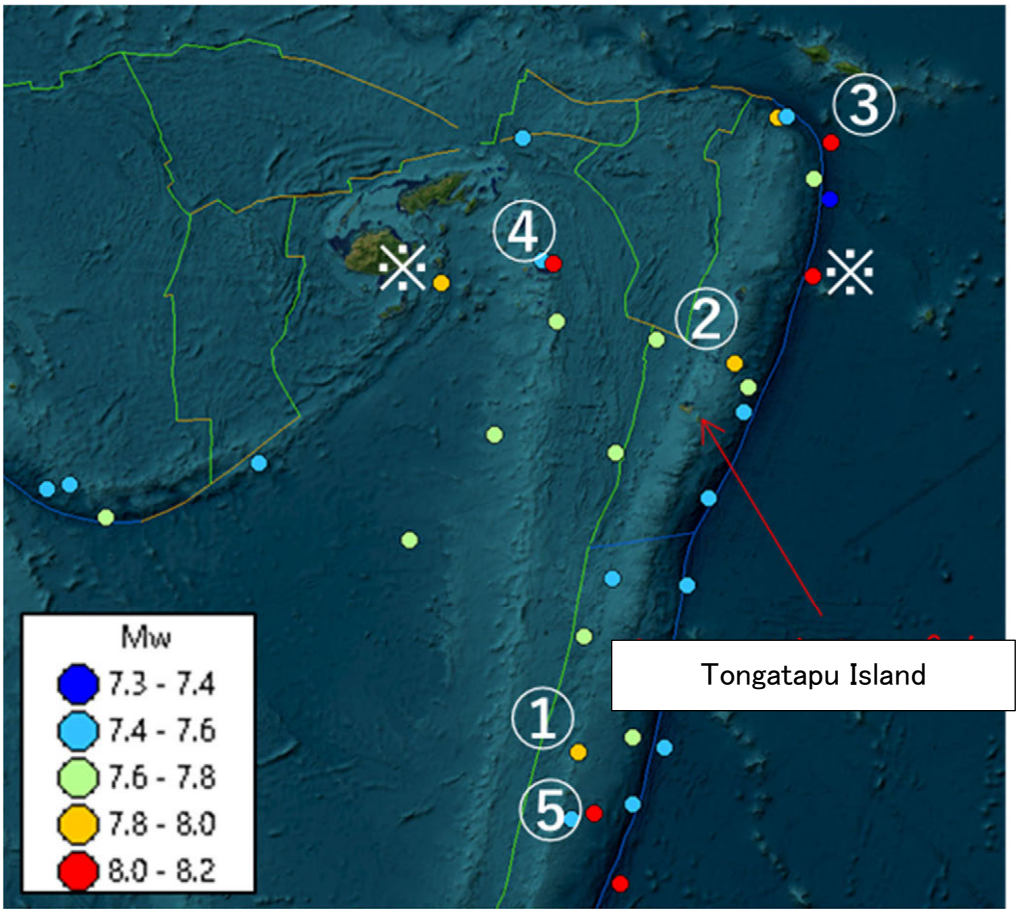

Source: JICA Study Team

Figure 2.7.2 Location of Epicenter

(2) Overview of fault parameterisation

In modeling the tsunami fault of the target earthquake, the fault plane is approximated by a single rectangular fault. In setting the fault model, the parameters in Table 2.7.3 are set based on the USGS Earthquake Catalog, the Earthquake Research Promotion Institute's "Strong Ground Motion Prediction Methodology for Earthquakes with Specified Source Faults (hereinafter referred to as 'Recipe')" (March 2020) and JSCE's "Nuclear Power Plant Tsunami Evaluation Technology 2016 ' (September 2016) are used as a basis for the setting.

A conceptual diagram of the Fault Parameters is shown in Figure2.7.3. The specific setting policy for each parameter is given in the following pages.

Table 2.7.2 Fault Parameters to be Set

Parameter (units)	Symbol
Latitude of origin (°)	Lat
Latitude of origin (°)	Long
Upper end depth (km)	d
Fault length (km)	L
Fault width (km)	W

Parameter (units)	Symbol
Fault area (km2)	S(=W×L)
Strike (°)	Strike
Inclination (°)	Dip
Slip angle (°)	Rake
Slip volume (m)	D
Moment magnitude	Mw
Seismic moment (N/m)	M0
Rigidity of the medium (N/m2)	M0

Source: JICA Study Team

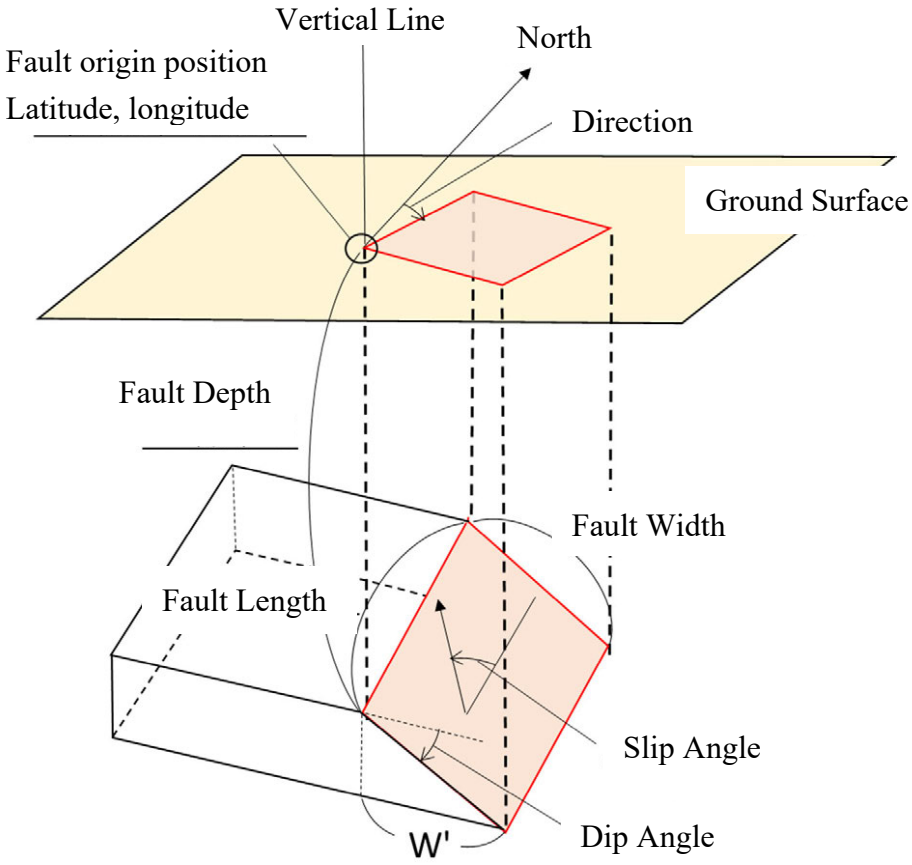

Source: JICA Study Team

Figure 2.7.3 Conceptual Diagram of Fault Parameters

(3) Methods for setting Fault Parameters

The moment magnitude Mw is set from the USGS Earthquake Catalog. Examples of descriptions in the USGS Earthquake Catalog are shown in Figure 2.7.4

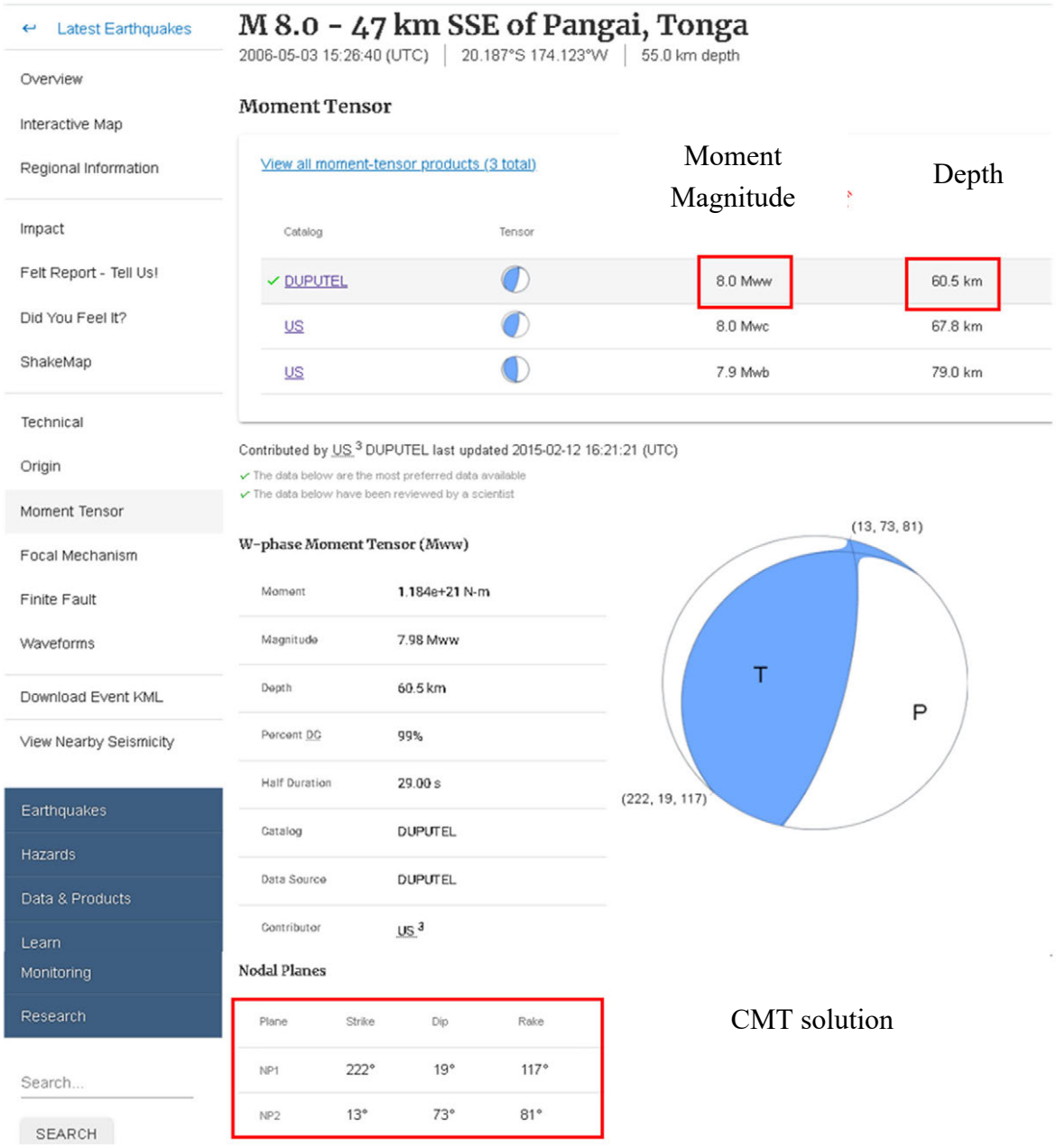

Source：USGS: Earthquake Catalog https://earthquake.usgs.gov/earthquakes/search/

Figure 2.7.4 USGS Example from the USGS Earthquake Catalog

The fault location (origin coordinates) should be set so that as many aftershocks as possible overlap with the fault plane. For the aftershock distribution, earthquakes that occurred in the vicinity of the target earthquake (mainshock) within one month of its occurrence are extracted from the USGS Earthquake Catalog.

The upper and lower depths of the fault are set to the shallowest and deepest epicentre depths, respectively, of the aftershocks that overlap the fault plane.

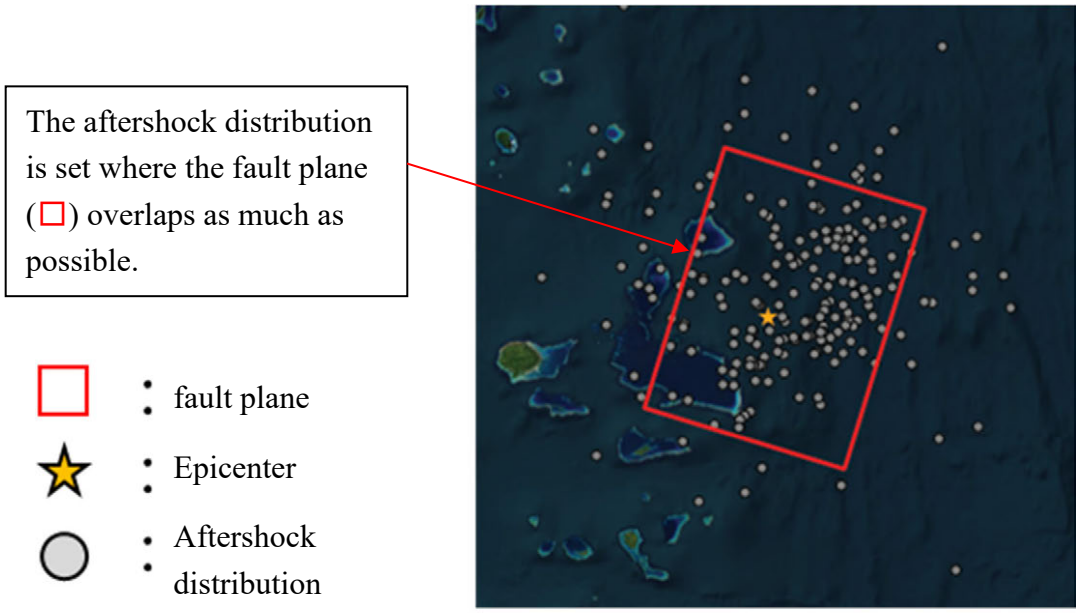

Source: JICA Study Team

Figure 2.7.5 Example of Fault Location Setting

The seismic moment M0 is calculated from the following equation

$$M_W = 2 / 3 (\log_{10}(M_O) - 16.1) \quad (2.7.5)$$

The fault area S is calculated from the following empirical equation of Yamanaka and Shimazaki (1990), based on the 'recipe'[3]

$$\log_{10}S = 2 / 3 \log_{10}(M_0) - 14.87 \quad (2.7.6)$$

The fault width W is calculated from the fault depth and tilt angle as follows

$$W = d_1 / \sin \delta \quad (2.7.7)$$

d1 ：depth at the bottom of the fault - depth at the top of the fault

δ ：Inclination angle

The fault length L is calculated from S and W obtained above as follows

$$S = W \times L \quad (2.7.8)$$

[3] Methodology for Predicting Strong Ground Motions of Earthquakes with Identified Source Faults ('Recipe')', Headquarters for Earthquake Research and Promotion, March 2020.

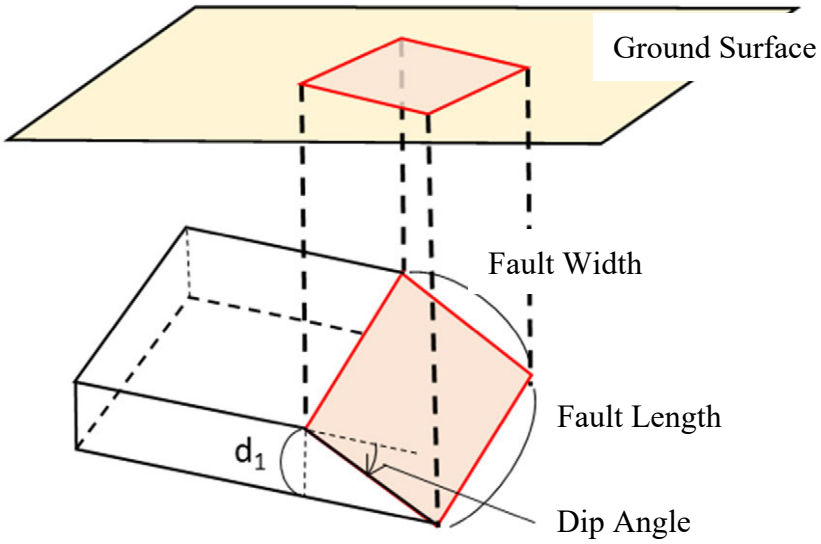

Source: JICA Study Team

Figure 2.7.6 Relationship between Fault Depth, Fault Width and Length

The average slip D is calculated from the following relationship based on the 'recipe'[4]

$$D = M_O / (\mu \cdot S) \quad \text{.....(2.7.9)}$$

The stiffness factor μ is set from Table 2.7.3 according to the depth of the fault plane as follows

If the entire fault plane is present at depths greater than 20 km:

$\mu = 7.0 \times 1010$ N / m^2

If the fault plane spans the depths below and above 20 km:

$\mu = 5.0 \times 1010$ N / m^2

[4] Strong-motion prediction method for earthquakes with identified source faults ('Recipe')', Headquarters for Earthquake Research and Promotion, March 2020.
https://www.jishin.go.jp/main/chousa/20_yosokuchizu/recipe.pdf

Table 2.7.3 Rigidity of the Medium Near the Epicenter

Sea Area	Basis	Rigidity
Within the Southwest Japan Sea Plate Eastern margin of the Sea of Japan	Vp=6.0km/s Vp/Vs=1.6～1.7 ρ =2.7～2.8g/cm^3 In this case μ =3.36×10^{10}～3.94×10^{10} N/m^2 Intermediate value.	3.5×10^{10} N/m^2 (3.5×10^{11} dyne/cm^2)
within the oceanic plate At the plate boundary (if the entire fault plane is located at 20 km)	Vp=8.0～8.1km/s Vp/Vs=1.75～1.80 ρ =3.2～3.5g/cm^3 In this case μ =6.31×10^{10}～7.50×10^{10} N/m^2 Intermediate value.	7.0×10^{10} N/m^2 (7.0×10^{11} dyne/cm^2)
Central part of the plate layer (when the fault plane spans depths of 20 km or more and shallower)	The value shall be intermediate between shallow and deep.	5.0×10^{10} N/m^2 (5.0×10^{11} dyne/cm^2)

Source: 'Tsunami assessment technology for nuclear power plants 2016', Annex,.
Subcommittee on Tsunami Assessment, Committee on Nuclear Engineering and Civil Engineering, JSCE, September 2016. Available at: https://committees.jsce.or.jp/ceofnp/node/84

(4) Fault model setting

The Fault Parameters and ground deformation distribution set up in this work are shown in Figure 2.7.7 to Figure 2.7.18. Note that the ground deformation distribution was calculated using the formula of Okada (1985).

Table 2.7.4 Fault Parameters (Earthquake occured 14/1/1976)

Latitude（°）	Lat	-28.29
Longitude（°）	Long	-177.15
Depth at Top（km）	d	23
Length（km）	L	83.496
Width（km）	W	83.5
Strike（°）	strike	189
Angle of Slope（°）	dip	11
Slide Angle（°）	rake	71
Slip Amount（m）	D	2.41
Moment Magnitude	Mw	7.9

Source: JICA Study Team

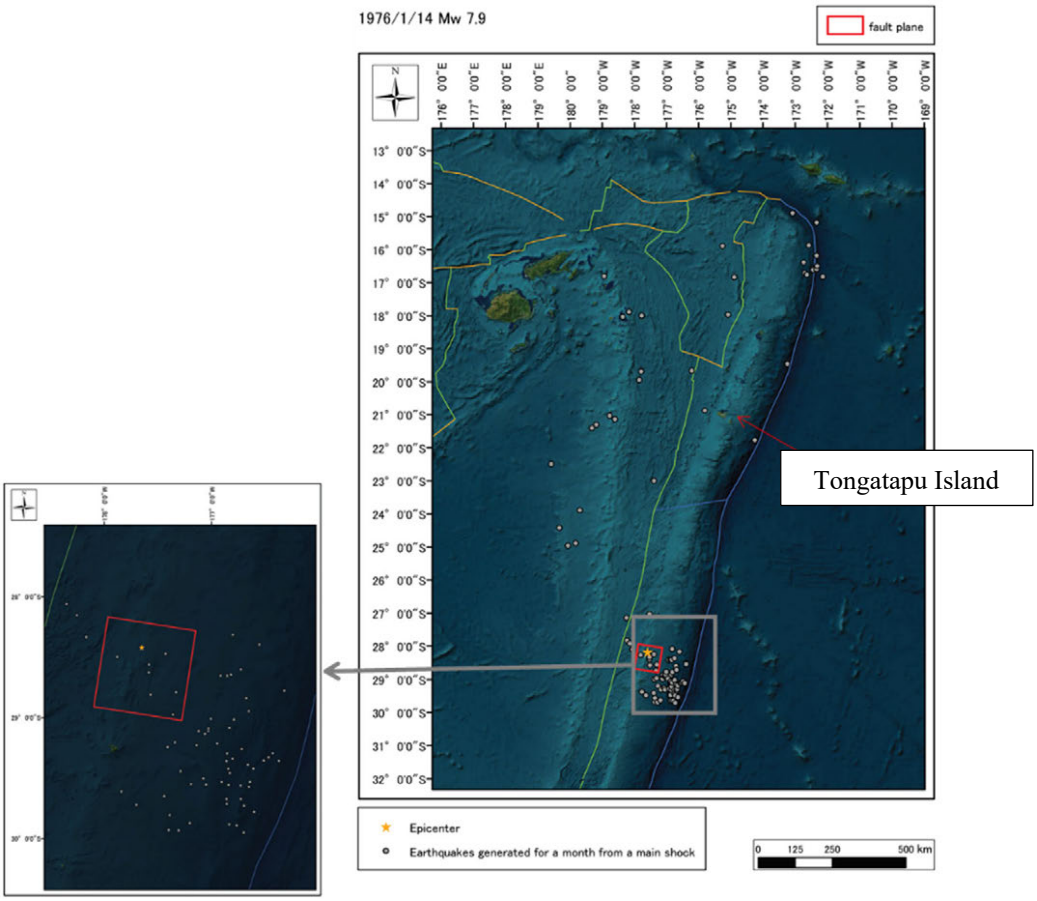

Source: JICA Study Team

Figure 2.7.7 Epicentre location and Aftershock Distribution of the 14/1/1976 Earthquake

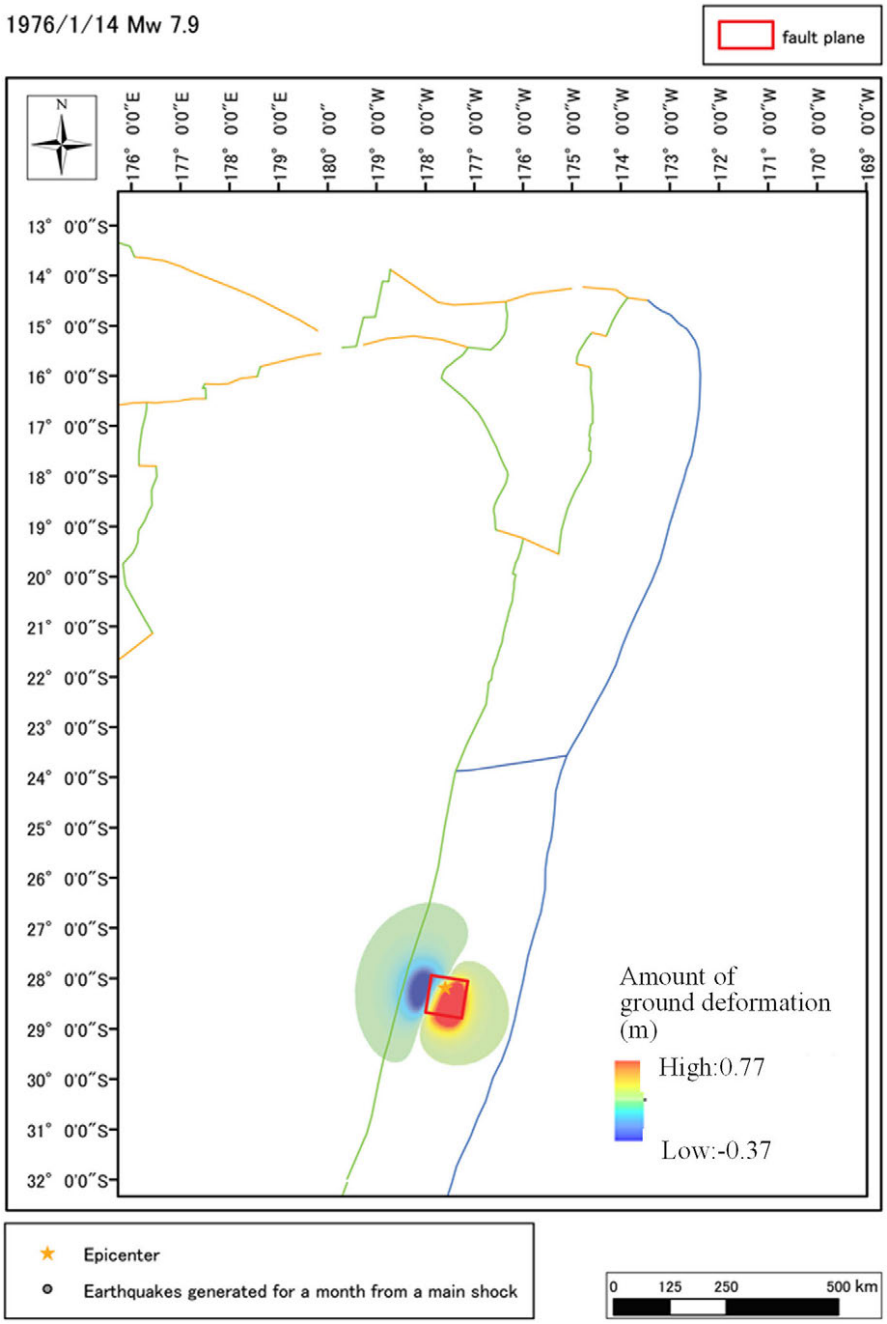

Source: JICA Study Team

Figure 2.7.8 Distribution of Ground Deformation (1976/1/14earthquake)

Table 2.7.5 Fault Parameters (2006/5/3earthquake) ①

Latitude（°）	Lat	-20.39
Longitude（°）	Long	-173.56
Depth at Top（km）	d	6.9
Length（km）	L	49.412
Width（km）	W	147.74
Strike（°）	strike	222
Angle of Slope（°）	dip	19
Slide Angle（°）	rake	117
Slip Amount（m）	D	3.45
Moment Magnitude	Mw	8

Source: JICA Study Team

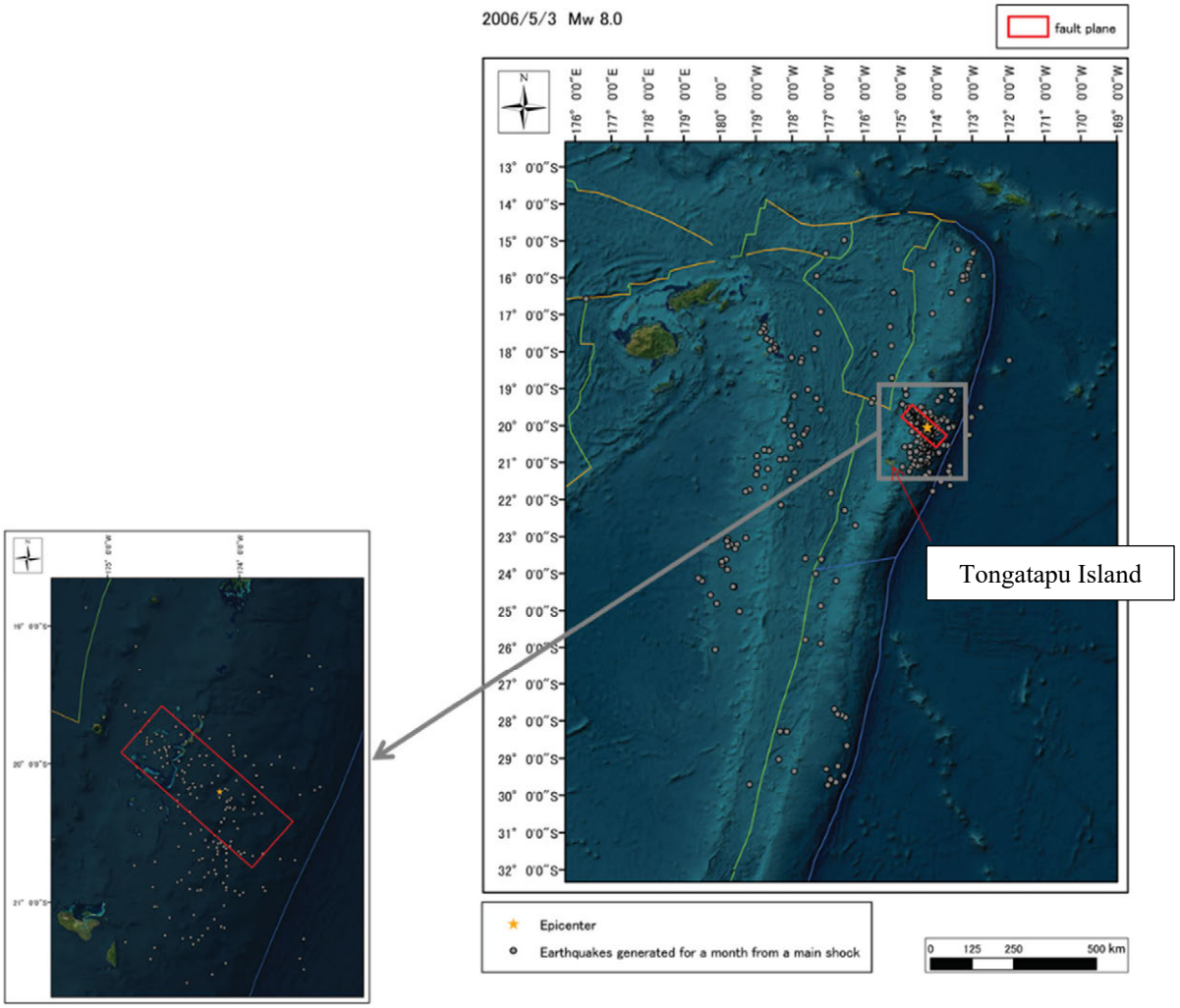

Source: JICA Study Team

Figure 2.7.9 Epicentre Location and Aftershock Distribution of the 3 May 2006 earthquake①

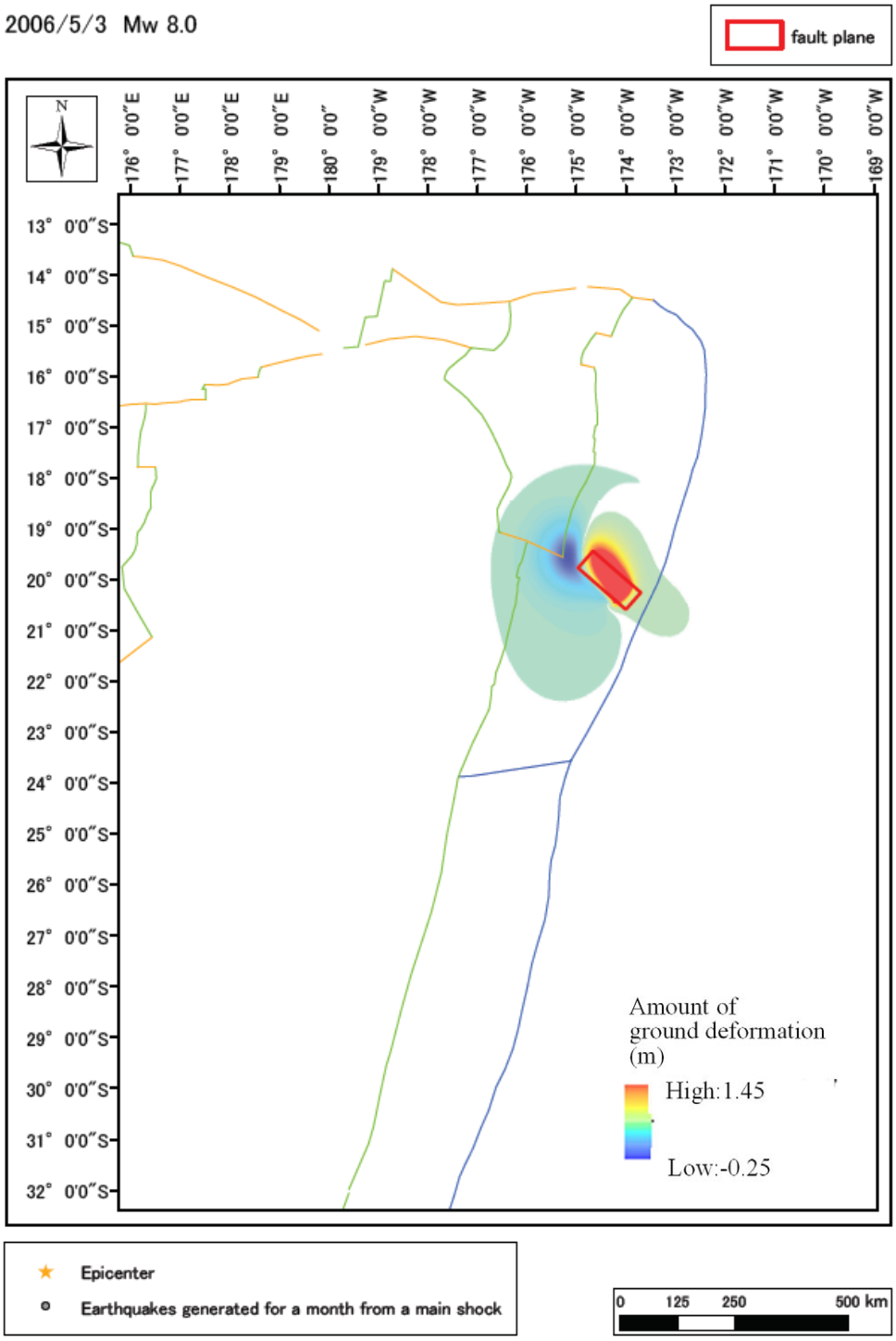

Source: JICA Study Team

Figure 2.7.10 Distribution of Ground Deformation (2006/5/3earthquake) ①

Table 2.7.6 Fault Parameters (2006/5/3earthquake) ②

Latitude（°）	Lat	-20.94
Longitude（°）	Long	-174.37
Depth at Top（km）	d	6.9
Length（km）	L	145.139
Width（km）	W	50.298
Strike（°）	strike	13
Angle of Slope（°）	dip	73
Slide Angle（°）	rake	81
Slip Amount（m）	D	3.45
Moment Magnitude	Mw	8

Source: JICA Study Team

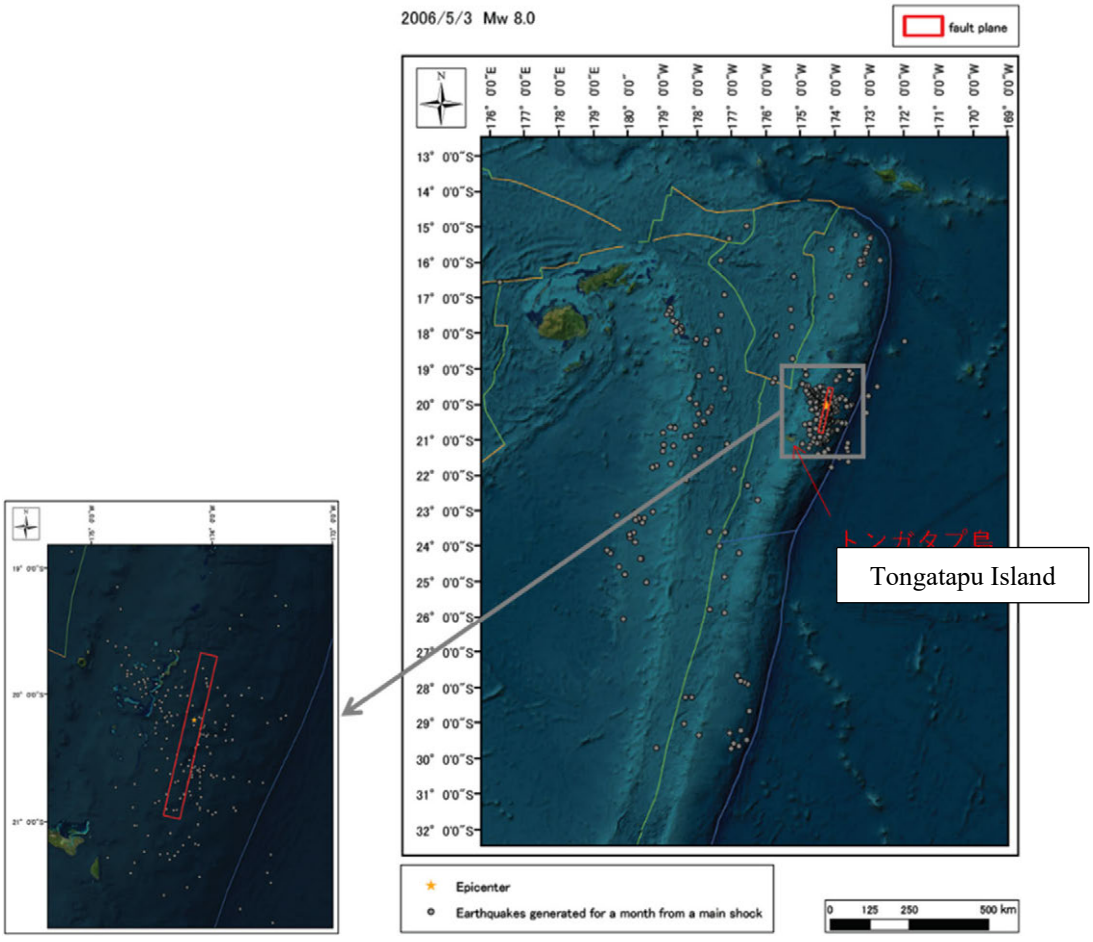

Source: JICA Study Team

Figure 2.7.11 Epicentre Location and Aftershock Distribution of the 3 May 2006 earthquake②

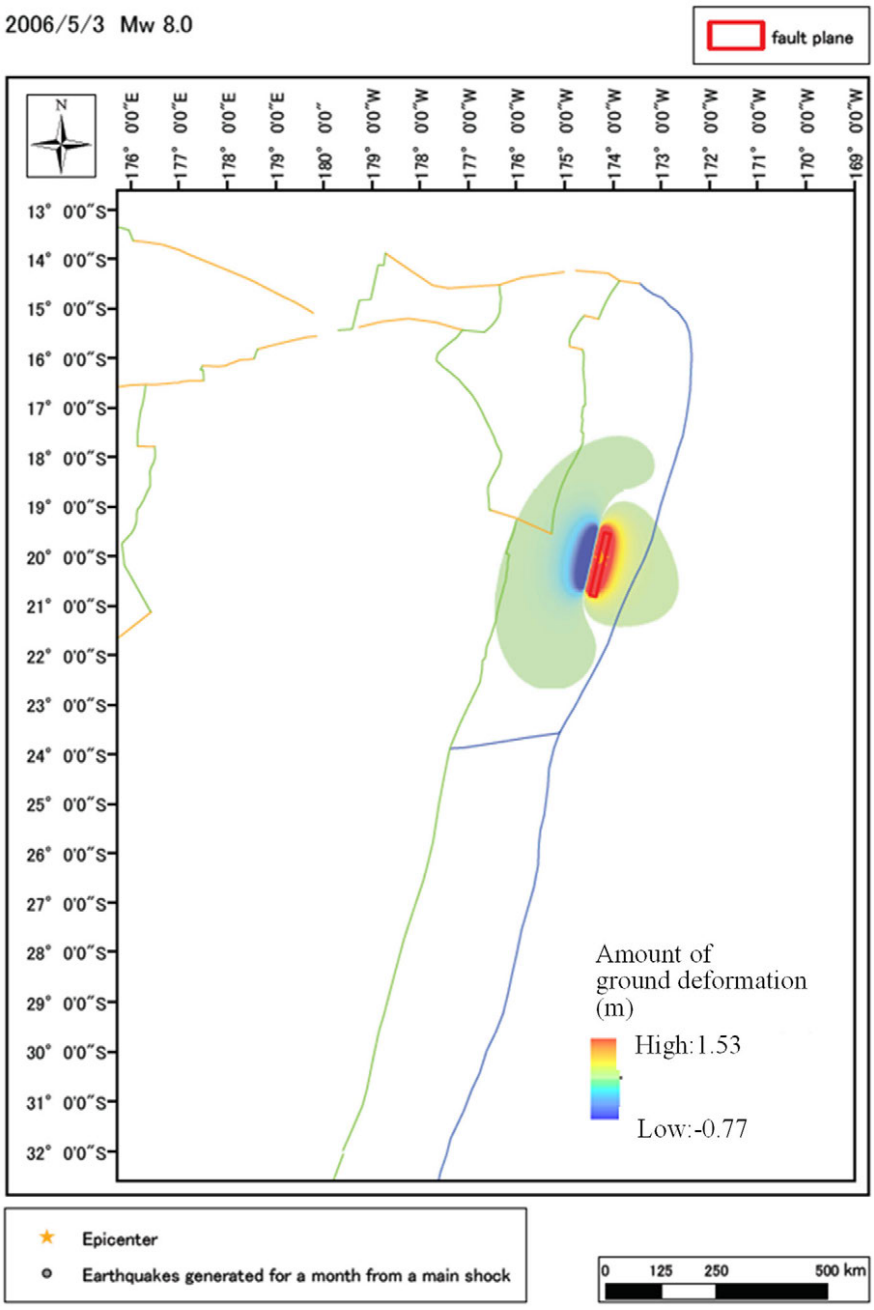

Source: JICA Study Team

Figure 2.7.12 Distribution of Ground Deformation (2006/5/3earthquake) ②

Table 2.7.7 Fault Parameters (2009/9/29earthquake)

		Fault①	Fault②
Latitude（°）	Lat	-16.061	-15.408
Longitude（°）	Long	-172.234	-172.382
Depth at Top（km）	d	13	18
Length（km）	L	114.0	109.0
Width（km）	W	28.0	90.0
Strike（°）	strike	352	175
Angle of Slope（°）	dip	48	16
Slide Angle（°）	rake	319	85
Slip Amount（m）	D	8.6	4.1
Moment Magnitude	Mw	7.9	8.0

Source：from Baeven et al., 2010 Fault Parameters

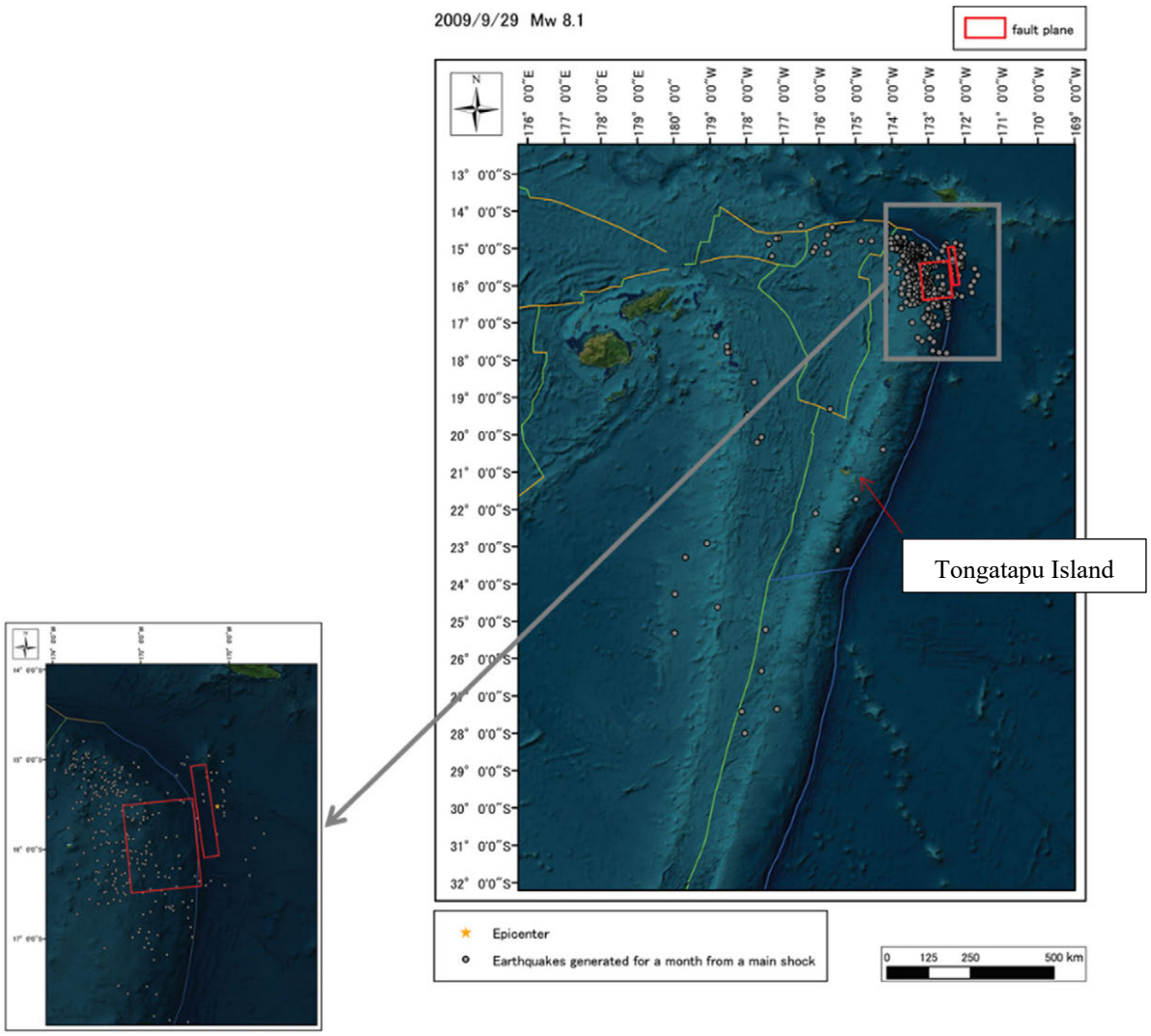

Source: JICA Study Team

Figure 2.7.13 Epicentre Location and Aftershock Distribution of the 29 Sept 2009 earthquake

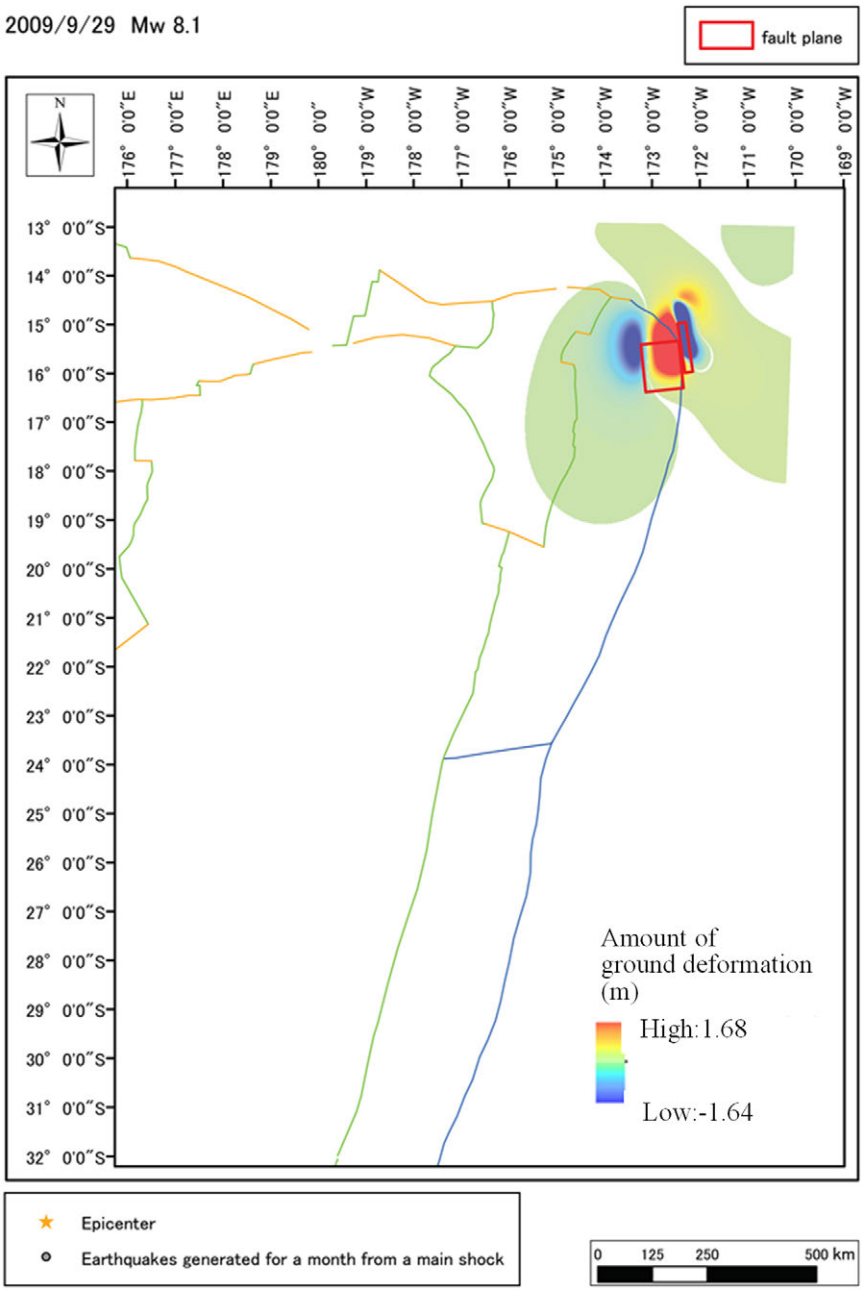

Source: JICA Study Team

Figure 2.7.14 Distribution of Ground Deformation (2009/9/29earthquake)

Table 2.7.8 Fault Parameters (2018/8/19earthquake)

Latitude（°）	Lat	-18.33
Longitude（°）	Long	-178.47
Depth at Top（km）	d	489.97
Length（km）	L	73.46
Width（km）	W	157.5
Strike（°）	strike	18
Angle of Slope（°）	dip	69
Slide Angle（°）	rake	266
Slip Amount（m）	D	3.1
Moment Magnitude	Mw	8.2

Source: JICA Study Team

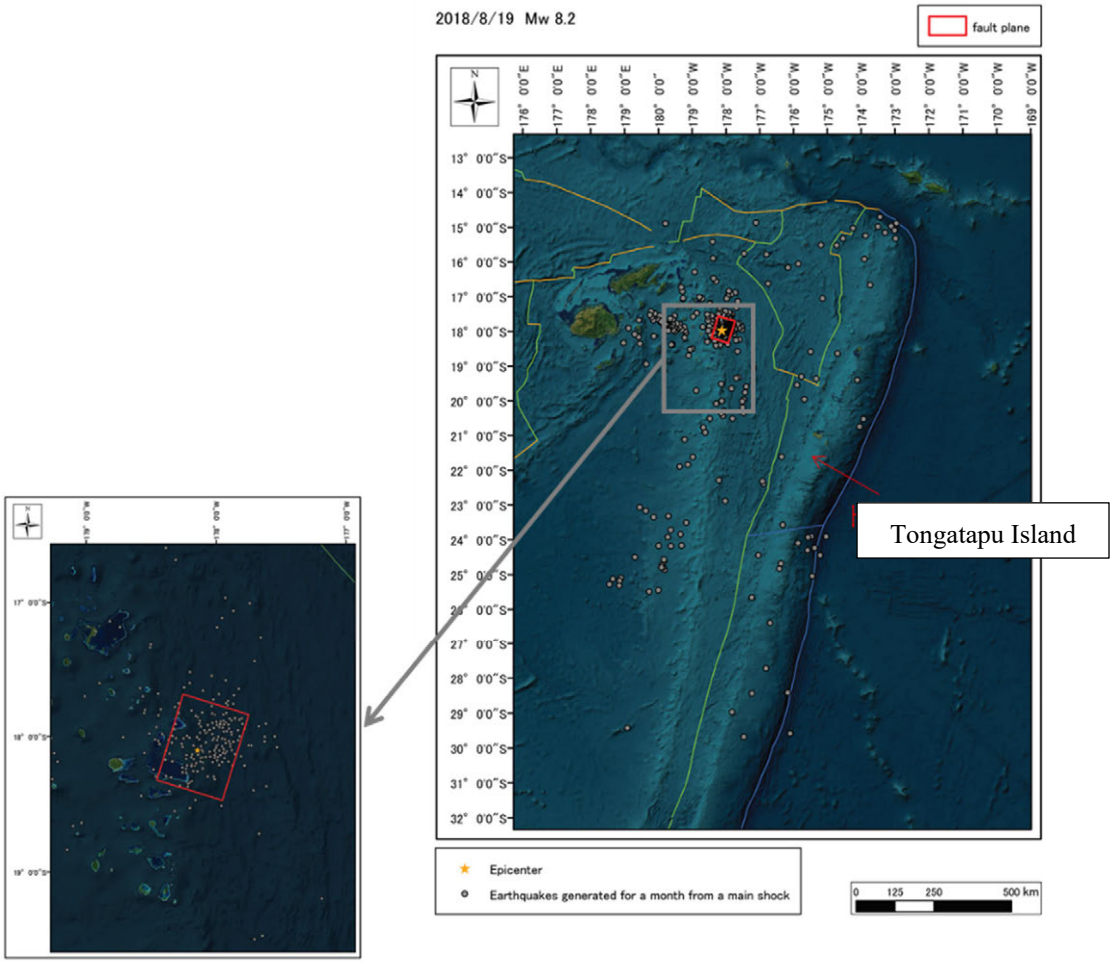

Source: JICA Study Team

Figure 2.7.15 Epicentre Location and Aftershock Distribution of the 19 Aug 2018 earthquake

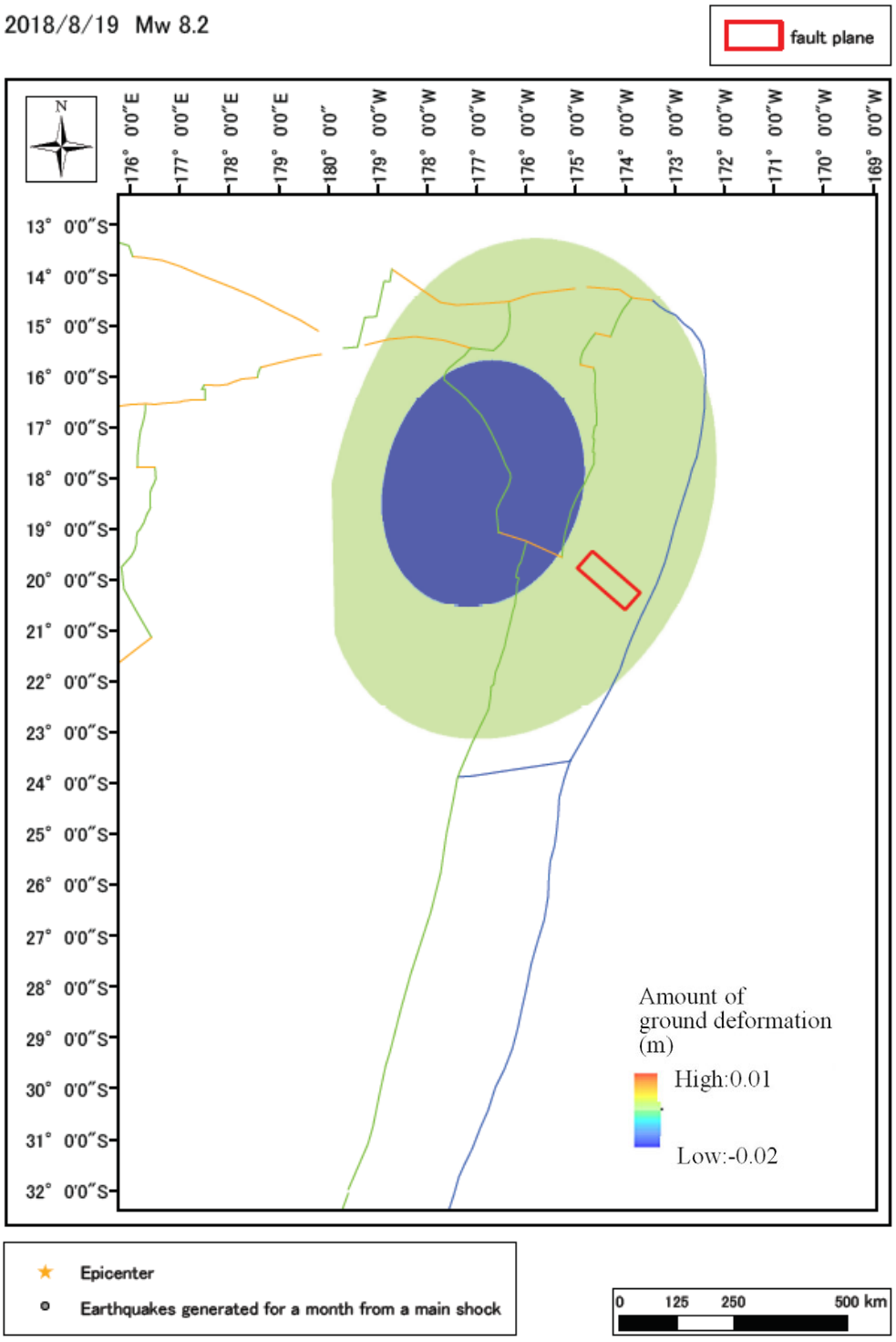

Source: JICA Study Team

Figure 2.7.16 Distribution of Ground Deformation (2018/8/19earthquake)

Table 2.7.9 Fault Parameters (2021/3/4earthquake)

Latitude（°）	Lat	-29.21
Longitude（°）	Long	-176.32
Depth at Top（km）	d	10
Length（km）	L	109.332
Width（km）	W	84.06
Strike（°）	strike	201
Angle of Slope（°）	dip	16
Slide Angle（°）	rake	98
Slip Amount（m）	D	3.87
Moment Magnitude	Mw	8.1

Source: JICA Study Team

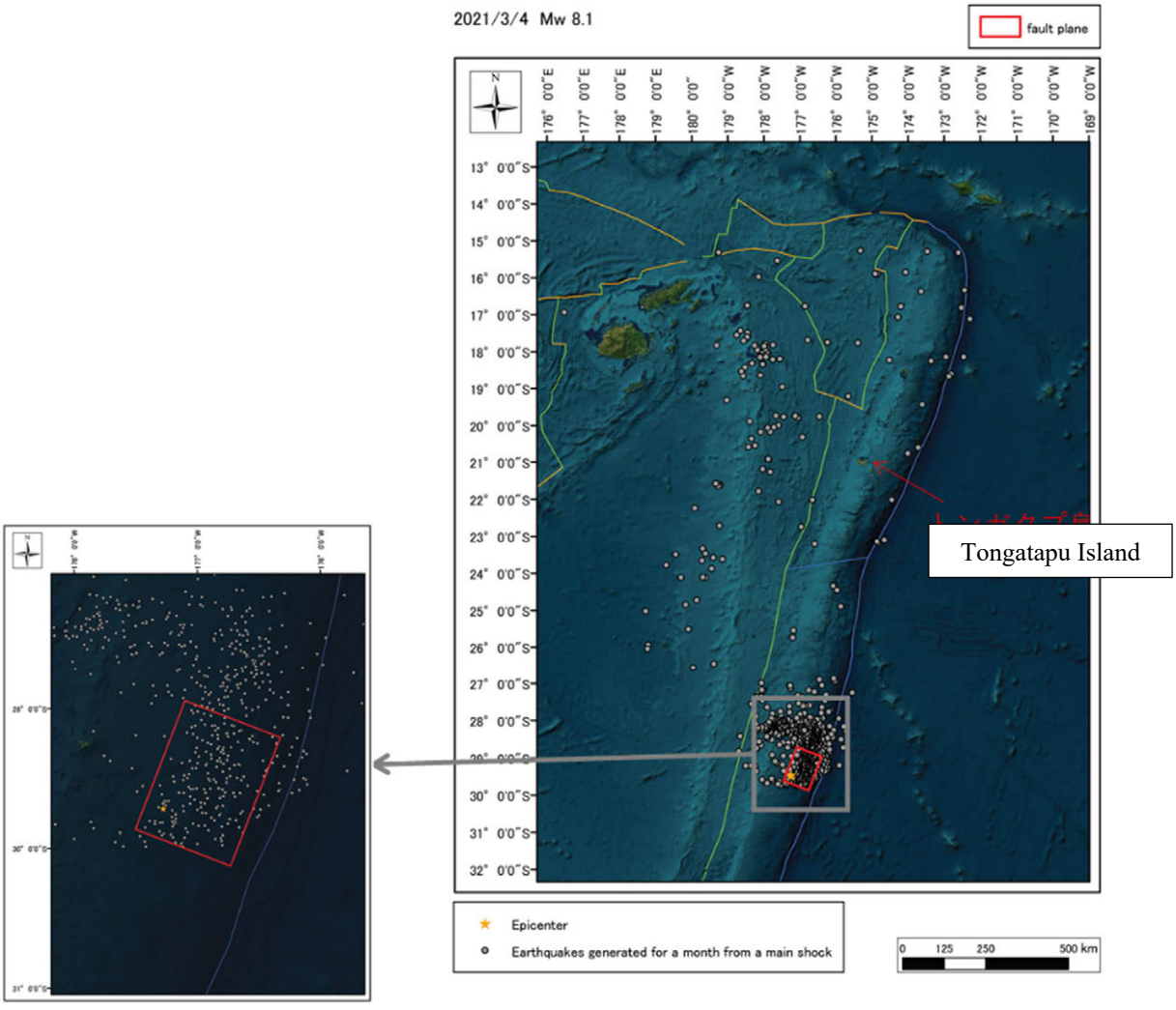

Source: JICA Study Team

Figure 2.7.17 Epicentre Location and Aftershock Distribution of the 4 Mar 2021 earthquake

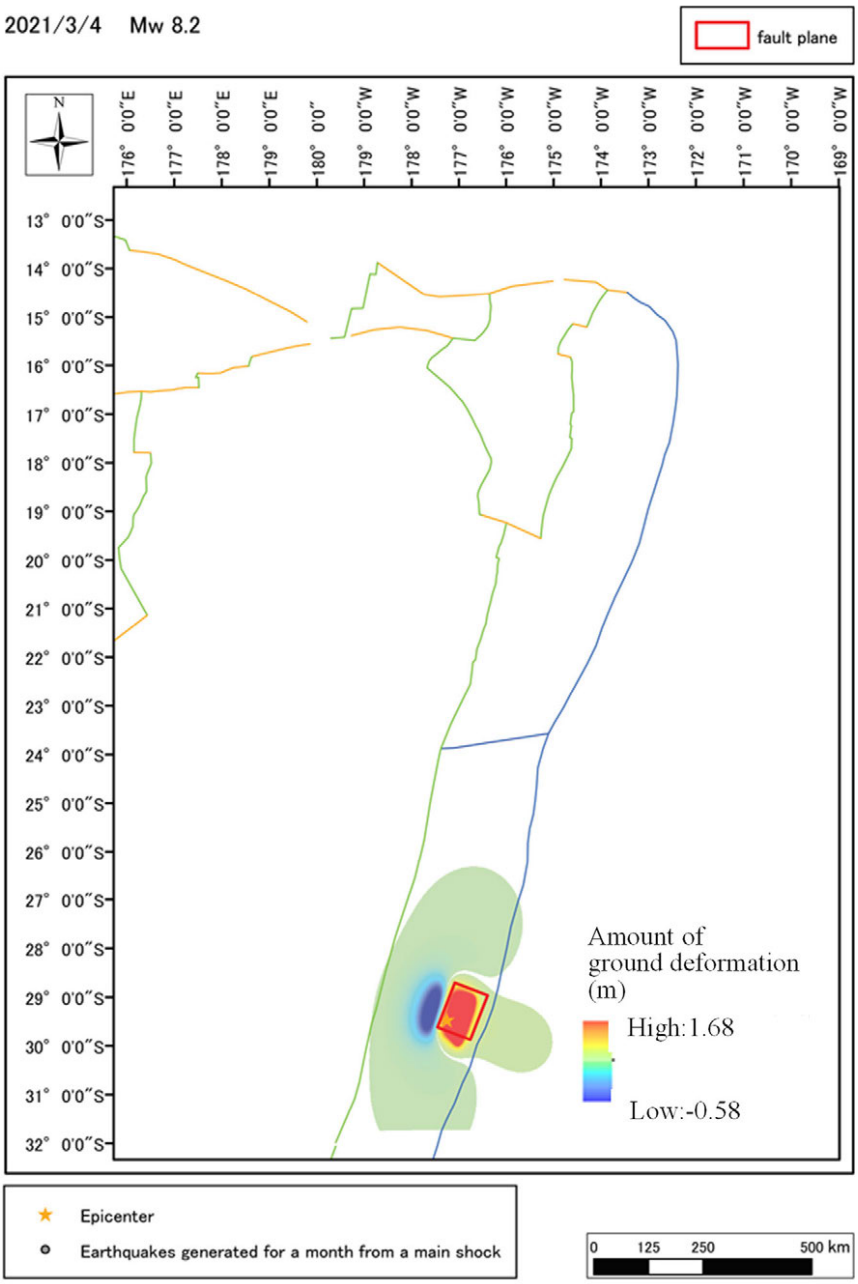

Source: JICA Study Team

Figure 2.7.18 Distribution of Ground Deformation (202 1/3/4earthquake)

(5) Numerical Analysis Cases

The numerical analysis cases are as follows

Table 2.7.10 Numerical Analysis Cases

Source	CASE	Volcano name	Tsunami Source	Structure	Minimum Region
Seismic Tsunami	fault1976-1	1976/1/14 Earthquake	Past Seismic Tsunamis	Exitsting Seawall (Tongatapu Island)	reg4-1(Tongatapu Island 1/3sec grid (10m grid)
	fault2006-1	2006/5/3Earthquake(Model①)			
	fault2006-2	2006/5/3Earthquake(Model②)			
	fault2009-1	2009/9/29 Earthquake			
	fault2018-1	2018/8/19 Earthquake			
	fault2021-1	2021/3/4 Earthquake			
	fault1976-2	1976/1/14 Earthquake		-	reg4-2(Eua Island) 1/3sec grid (10m grid)
	fault2006-1	2006/5/3Earthquake(Model①)			
	fault2006-2	2006/5/3Earthquake(Model②)			
	fault2009-2	2009/9/29 Earthquake			
	fault2018-2	2018/8/19 Earthquake			
	fault2021-2	2021/3/4 Earthquake			

Source: JICA Study Team

(6) Analysis result

1) Max tsunami Water Level Distribution

a. Regional Max Water Level Distribution map including wave sources

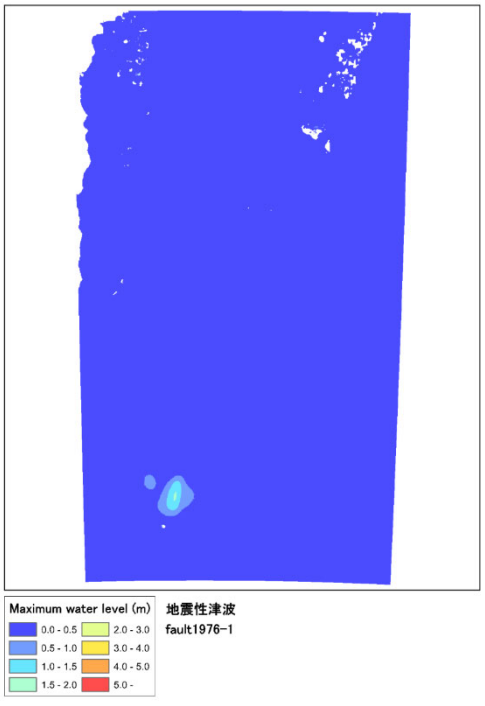

Figure 2.7.19 Max Water Level Distribution (Fault1976)

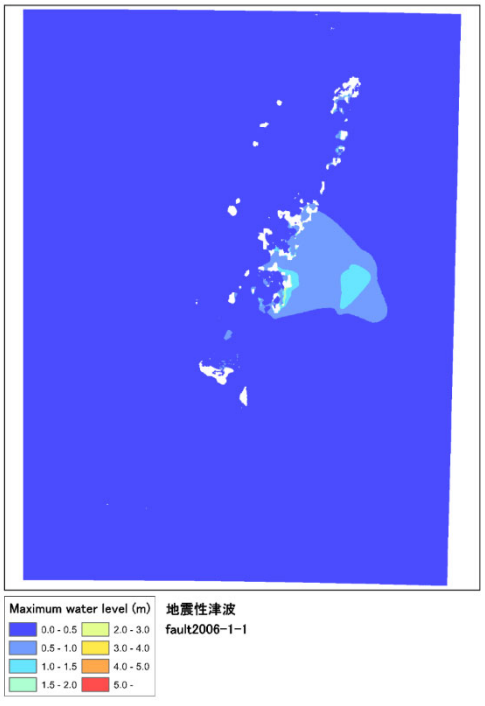

Figure 2.7.20 Max Water Level Distribution (Fault2006-1)

Source: JICA Study Team

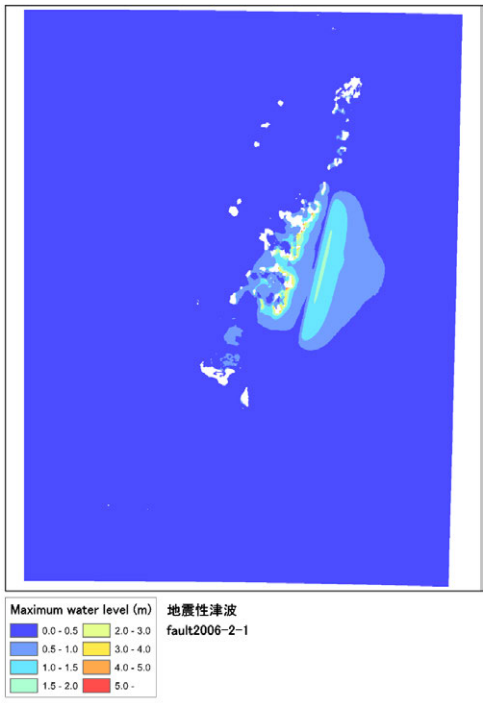

Figure 2.7.21 Max Water Level Distribution (Fault2006-2)

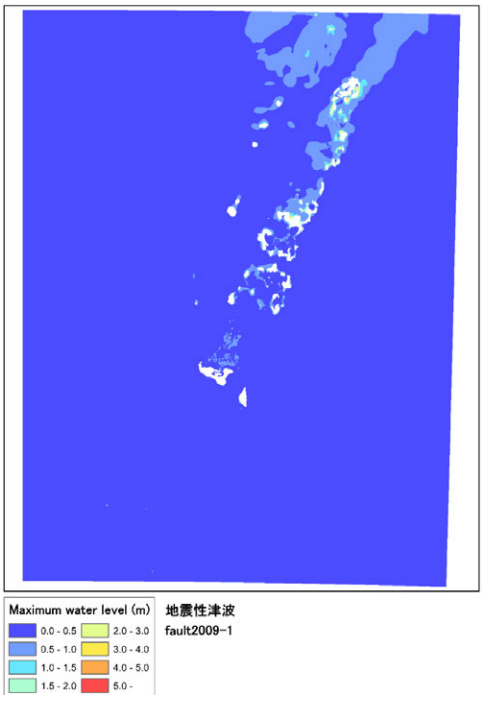

Figure 2.7.22 Max Water Level Distribution (Fault2009)

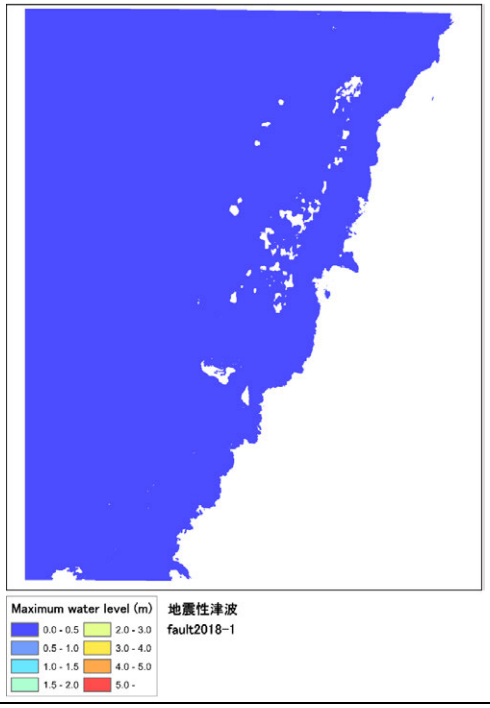

Figure 2.7.23 Max Water Level Distribution (Fault2018)

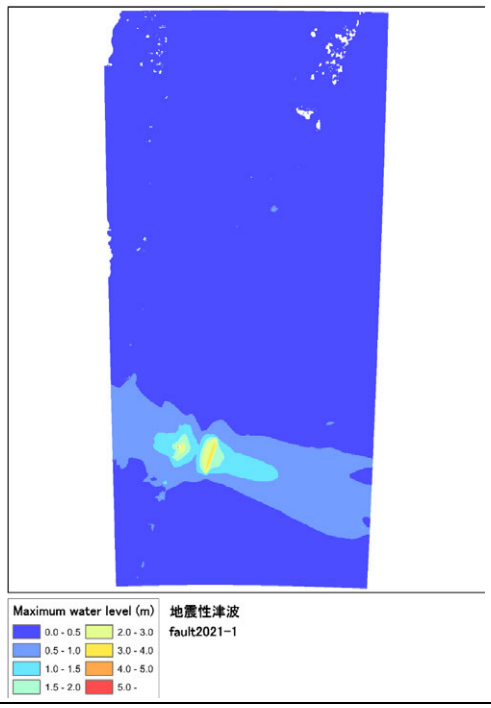

Figure 2.7.24 Max Water Level Distribution (Fault2021)

Source: JICA Study Team

b. Max Water Level Distribution map (Nuku'alofa, Tongatapu Island)

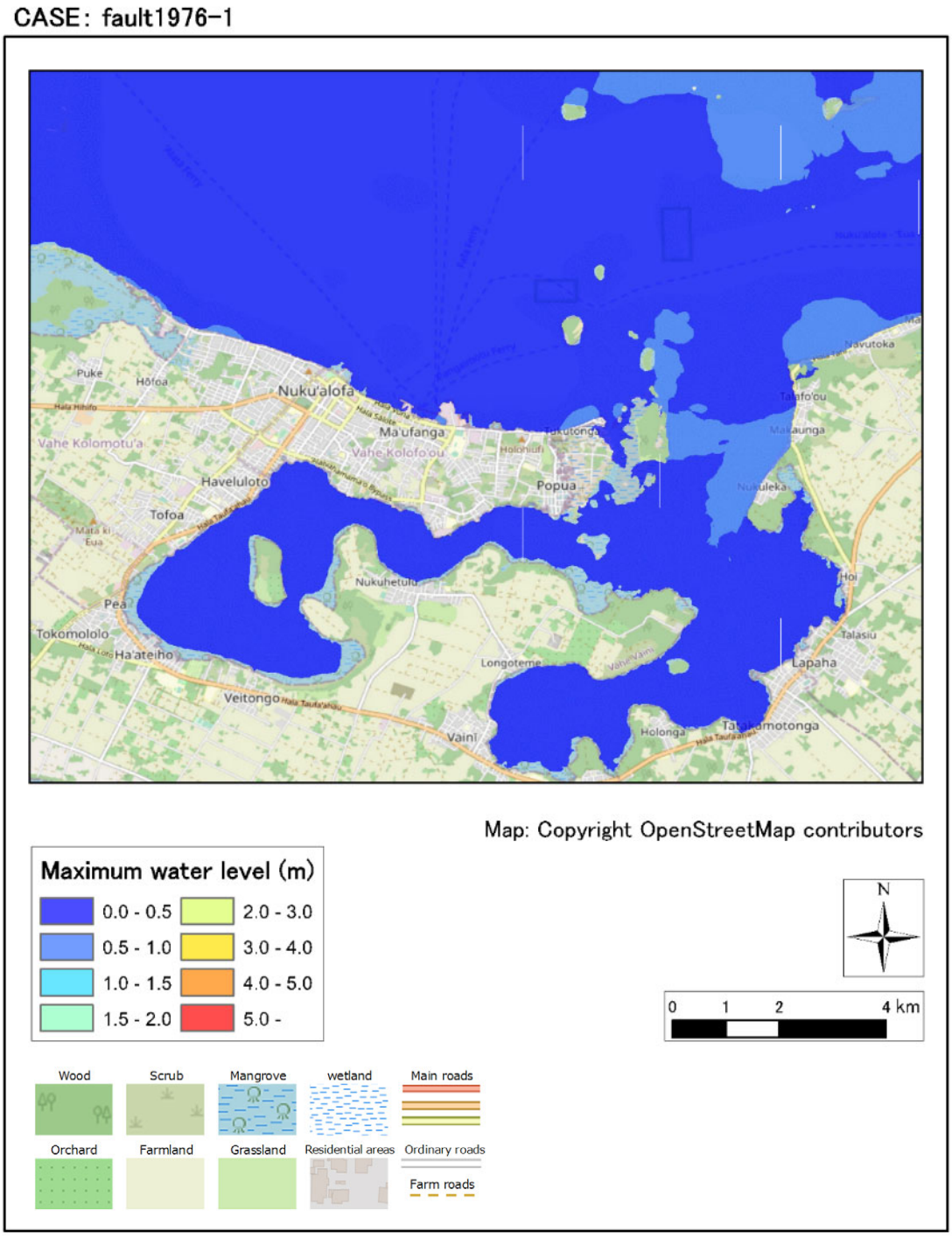

Source: JICA Study Team

Figure 2.7.25 Max Water Level Distribution map (Fault 1976)

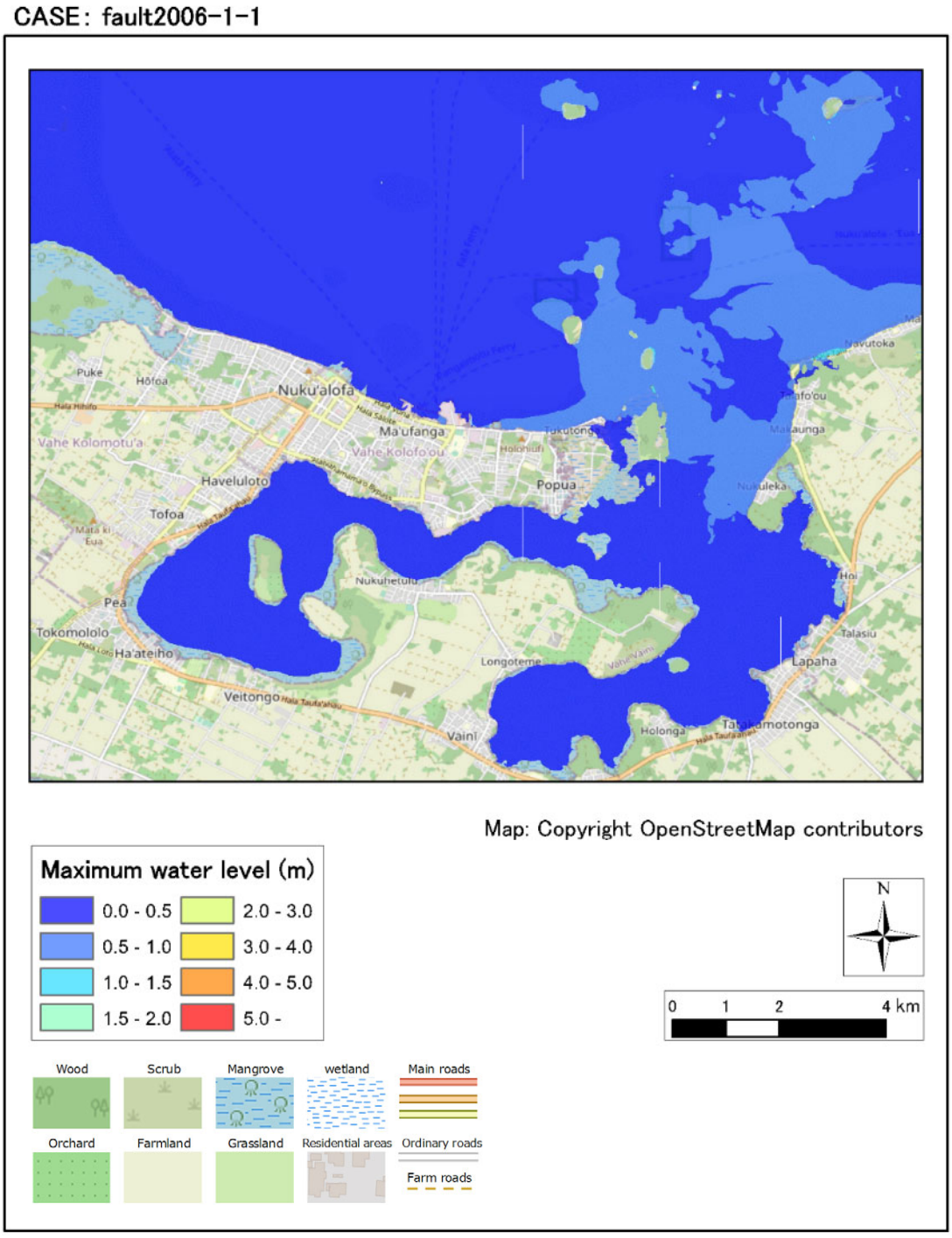

Source: JICA Study Team

Figure 2.7.26 Max Water Level Distribution map (Fault 2006-1)

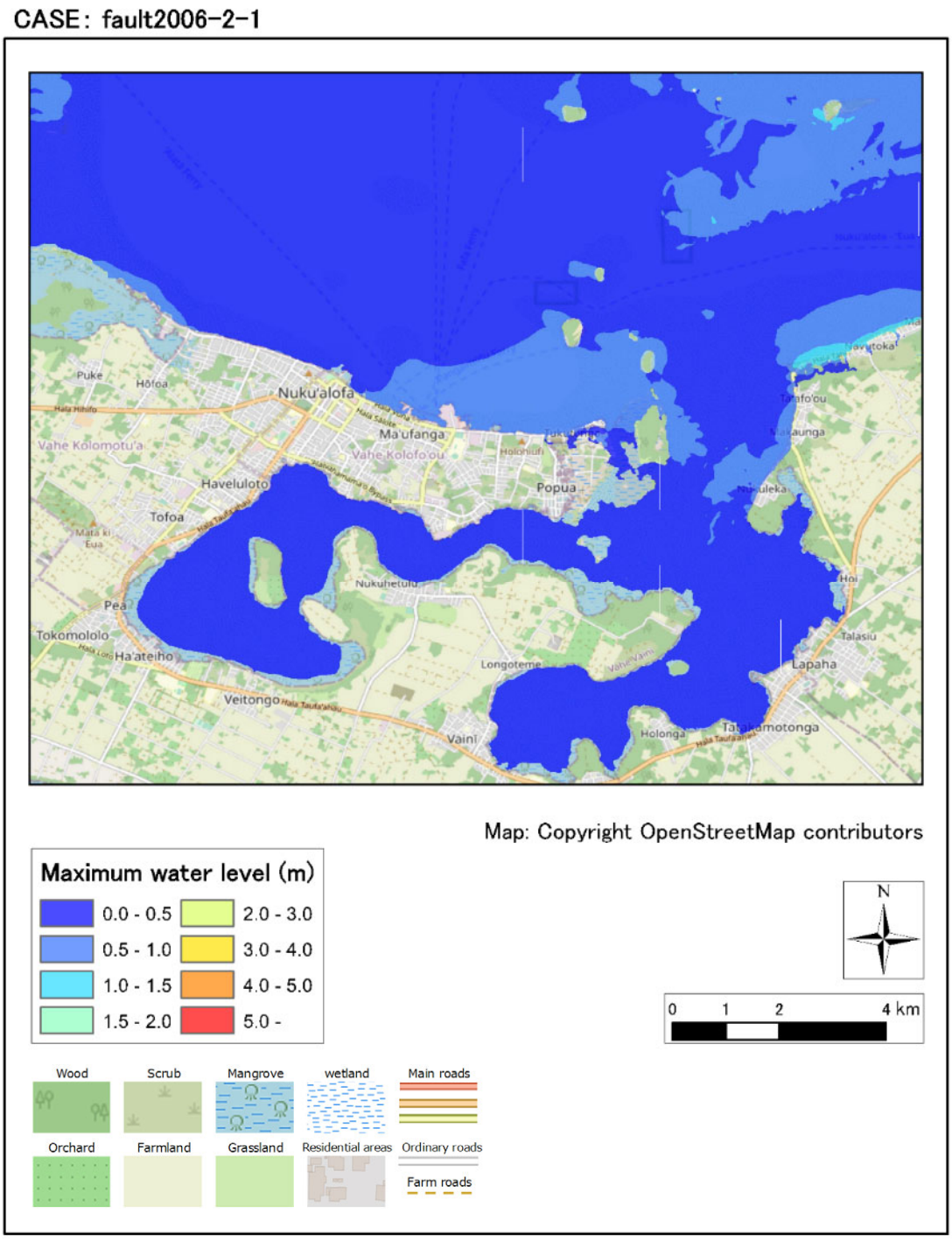

Source: JICA Study Team

Figure 2.7.27 Max Water Level Distribution map (Fault 2006-2)

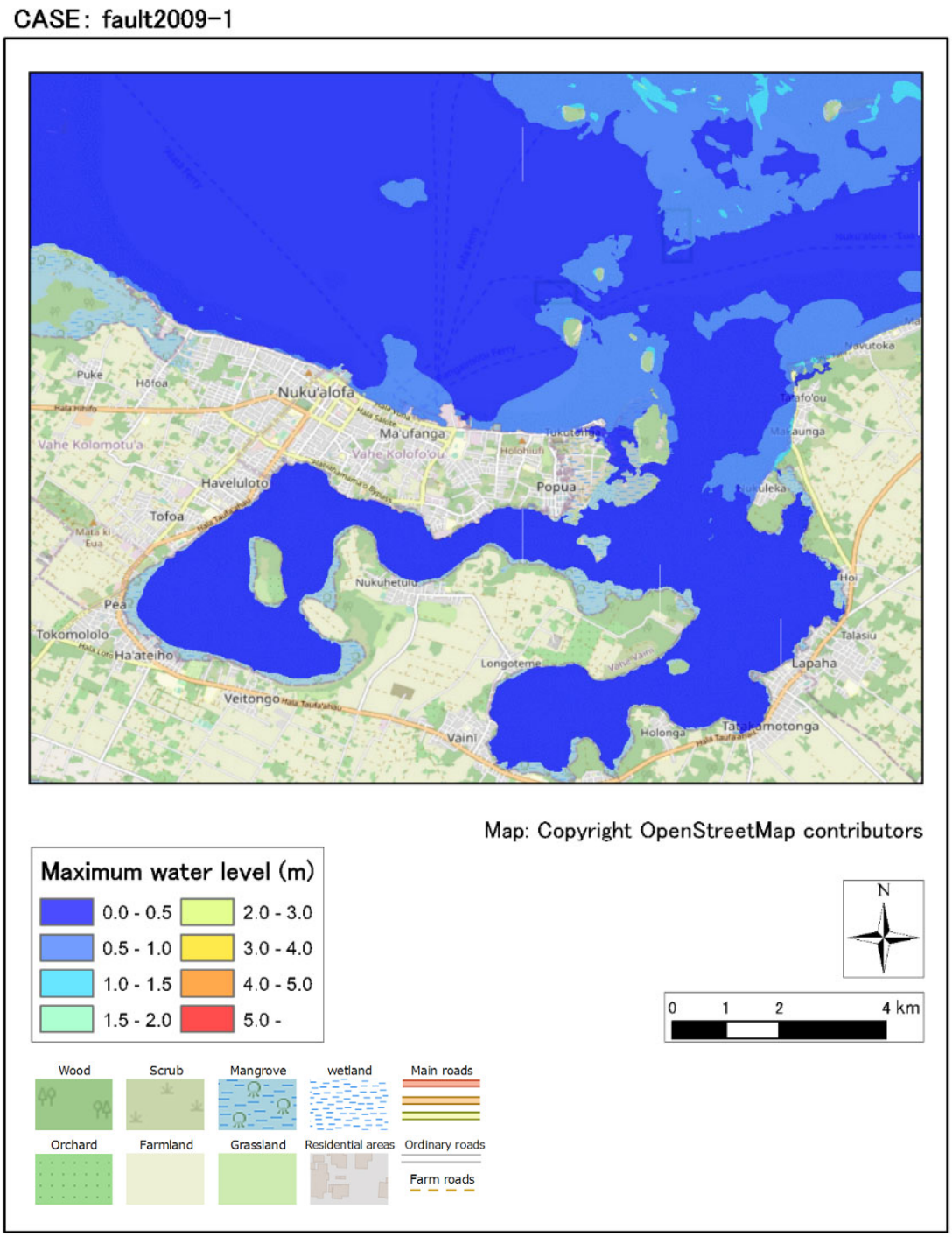

Source: JICA Study Team

Figure 2.7.28 Max Water Level Distribution map (Fault 2009)

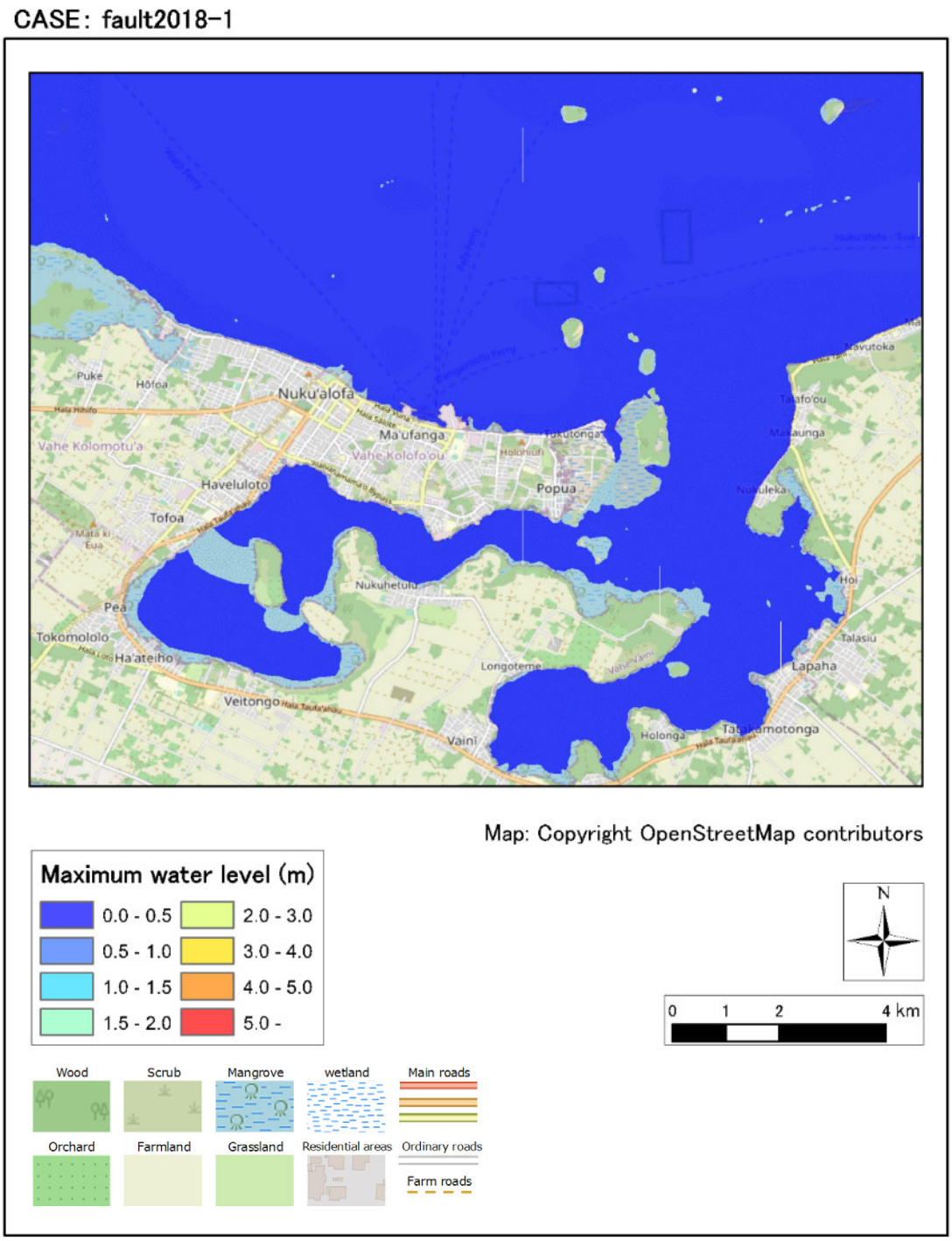

Source: JICA Study Team

Figure 2.7.29 Max Water Level Distribution map (Fault 2018)

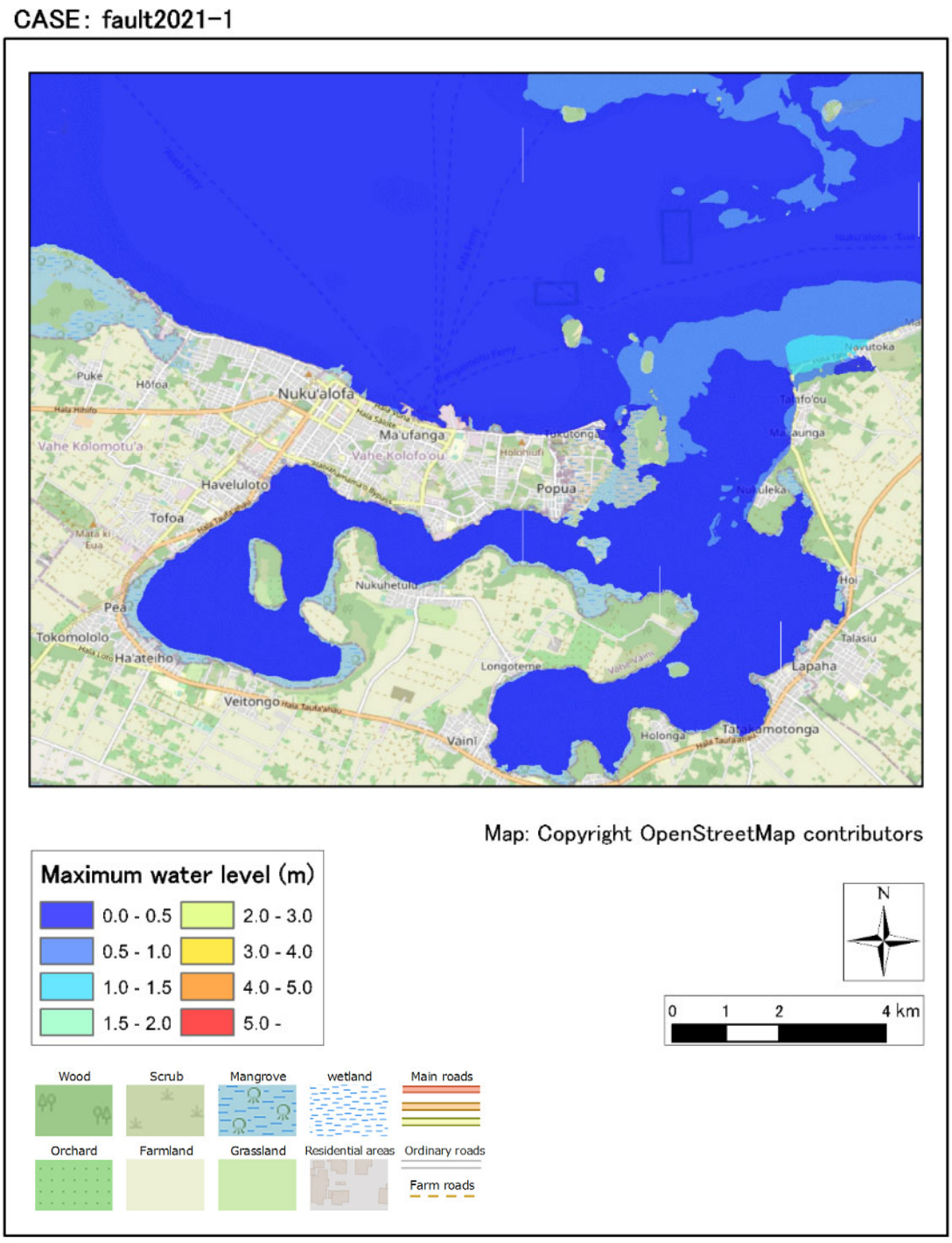

Source: JICA Study Team

Figure 2.7.30 Max Water Level Distribution map (Fault 2021)

2) Max inudation depth distribution(Nuku'alofa, Tongatapu Island)

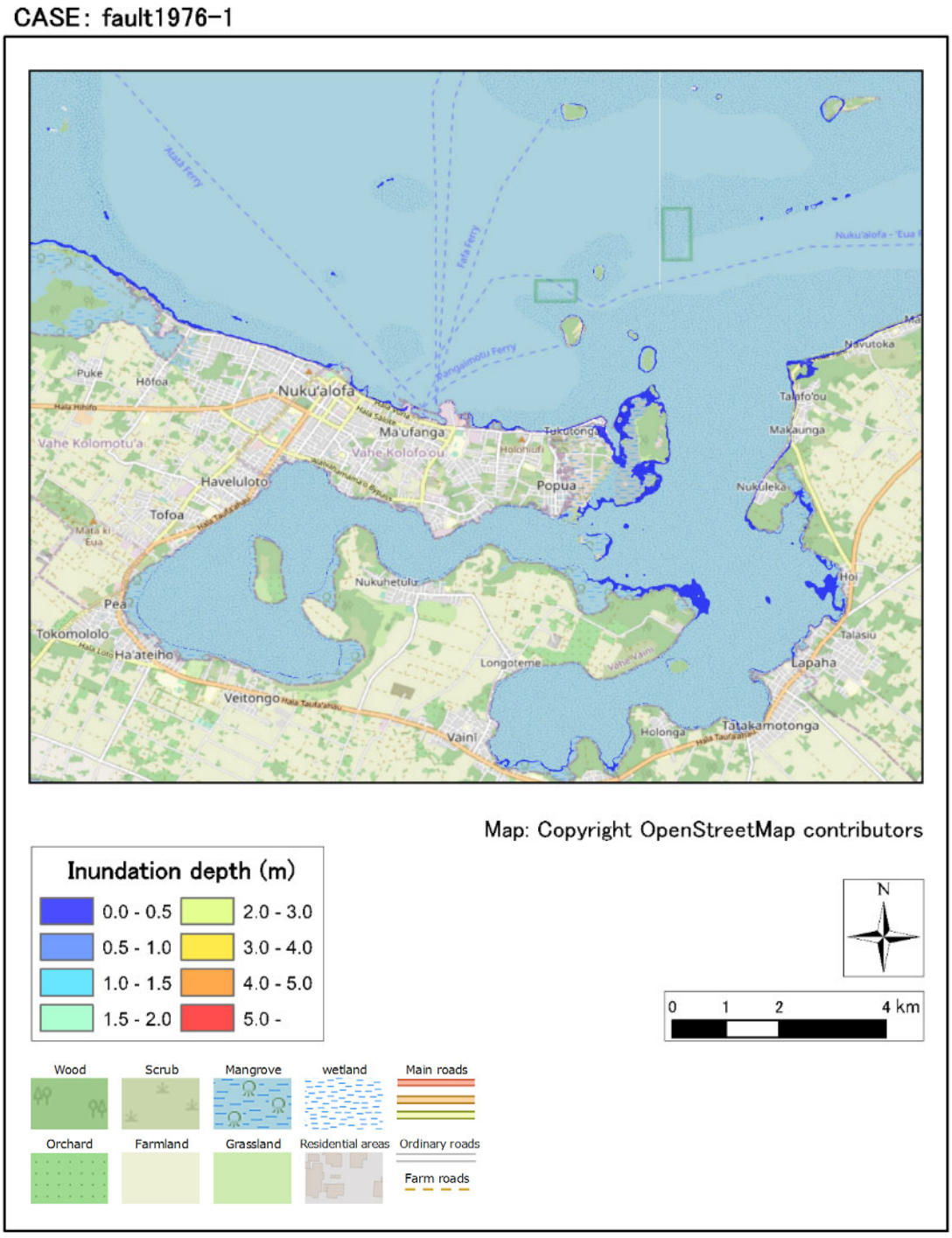

Source: JICA Study Team

Figure 2.7.31 Max inudation depth distribution (Fault 1976)

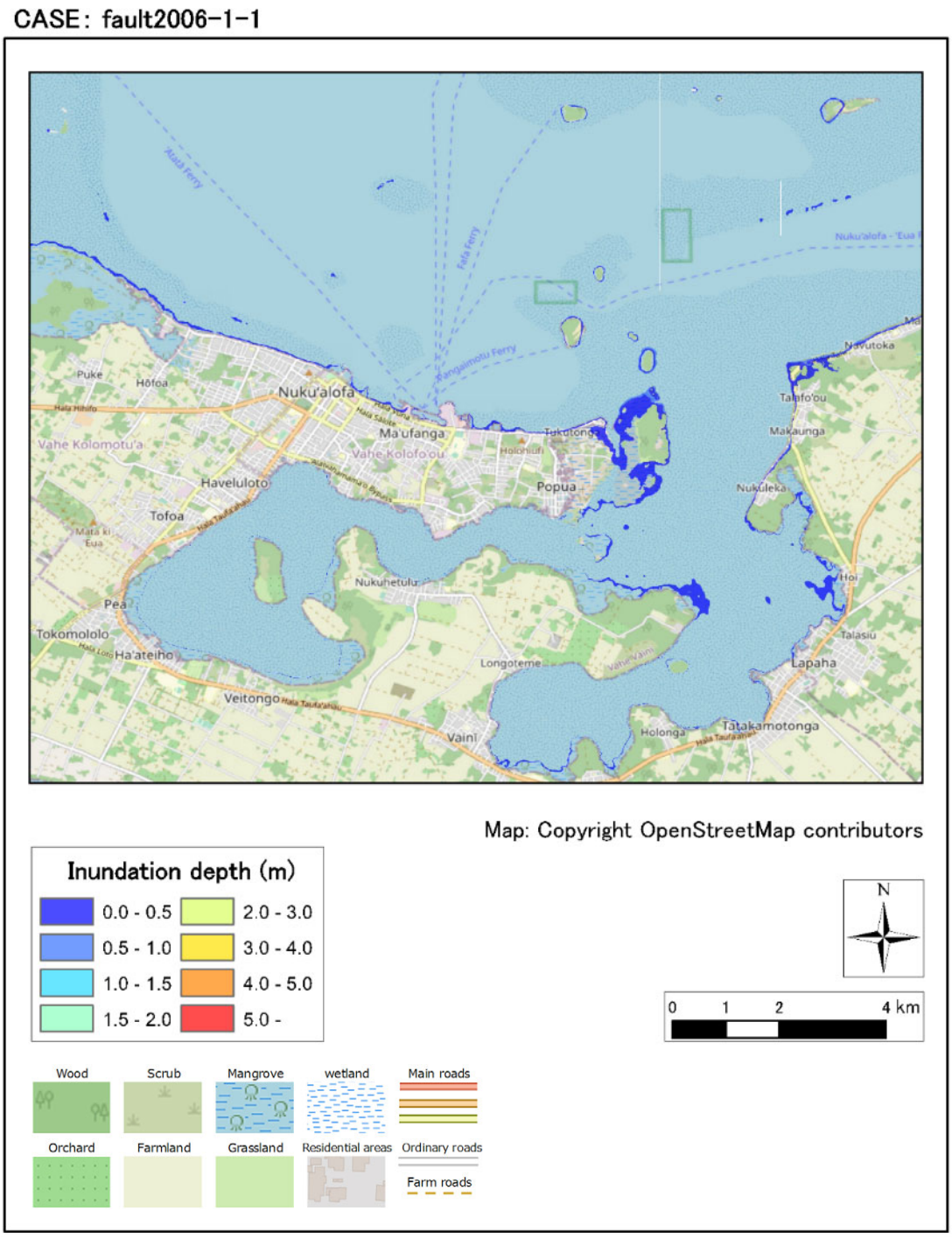

Source: JICA Study Team

Figure 2.7.32 Max inudation depth distribution (Fault 2006-1)

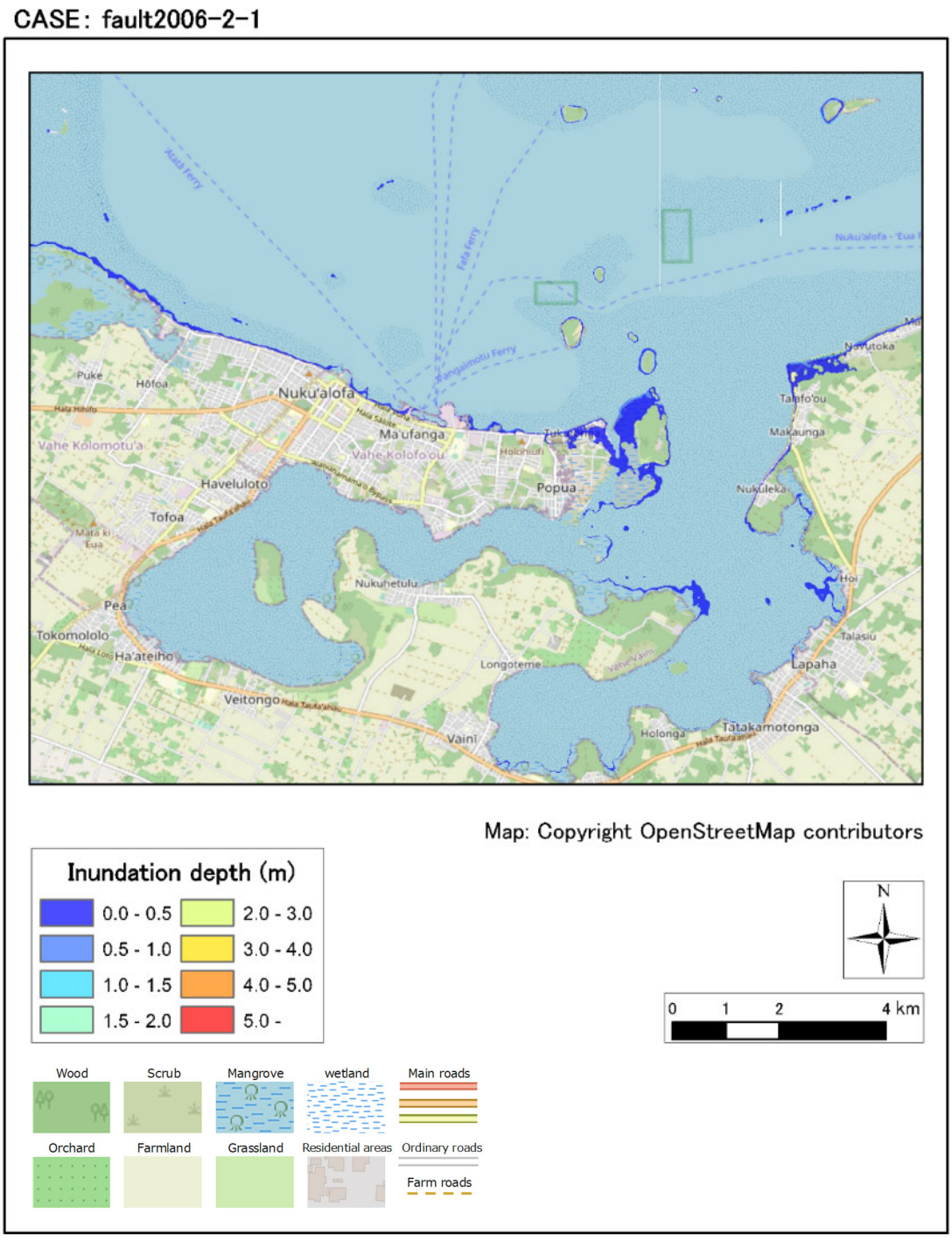

Source: JICA Study Team

Figure 2.7.33 Max inudation depth distribution (Fault 2006-2)

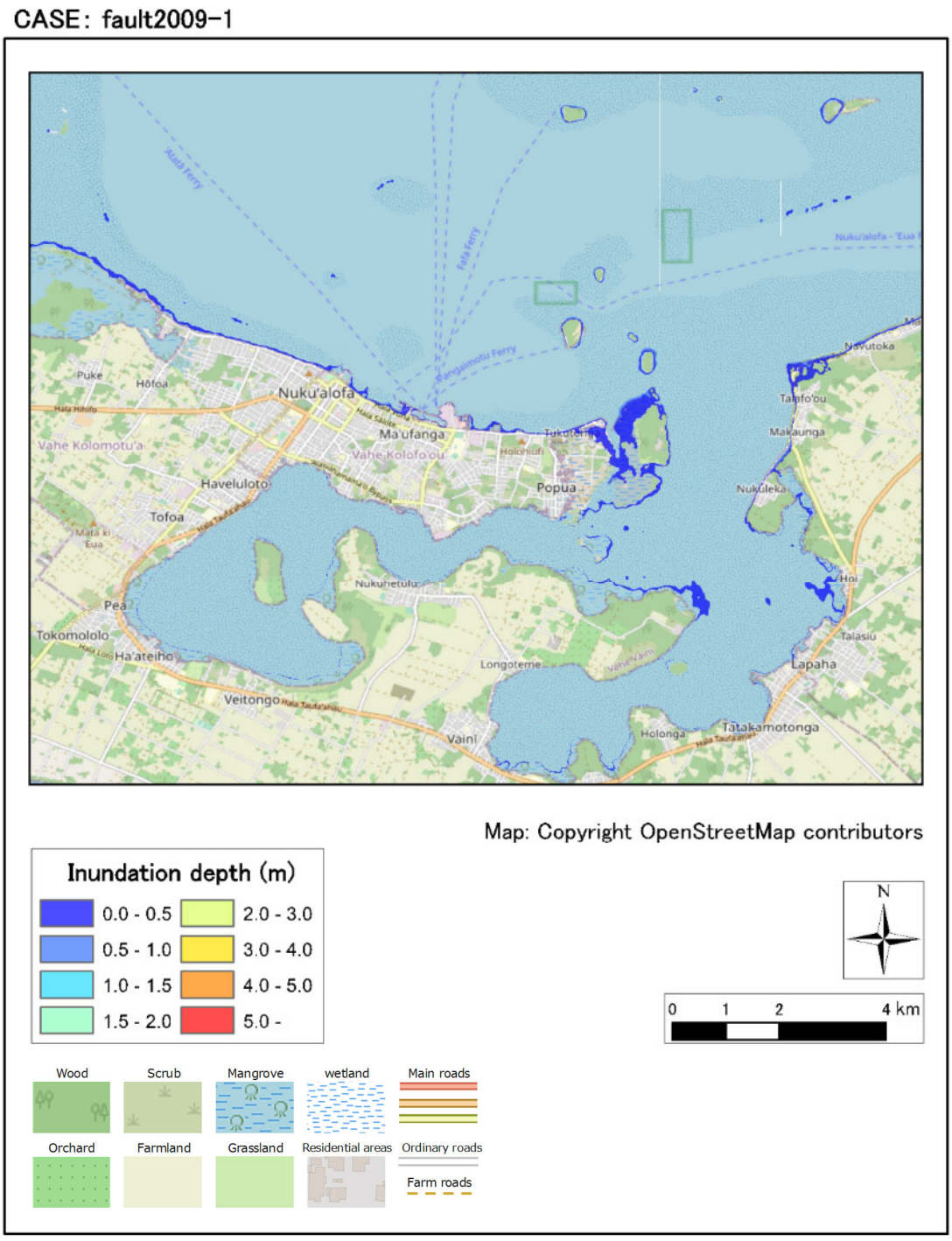

Source: JICA Study Team

Figure 2.7.34 Max inudation depth distribution (Fault 2009)

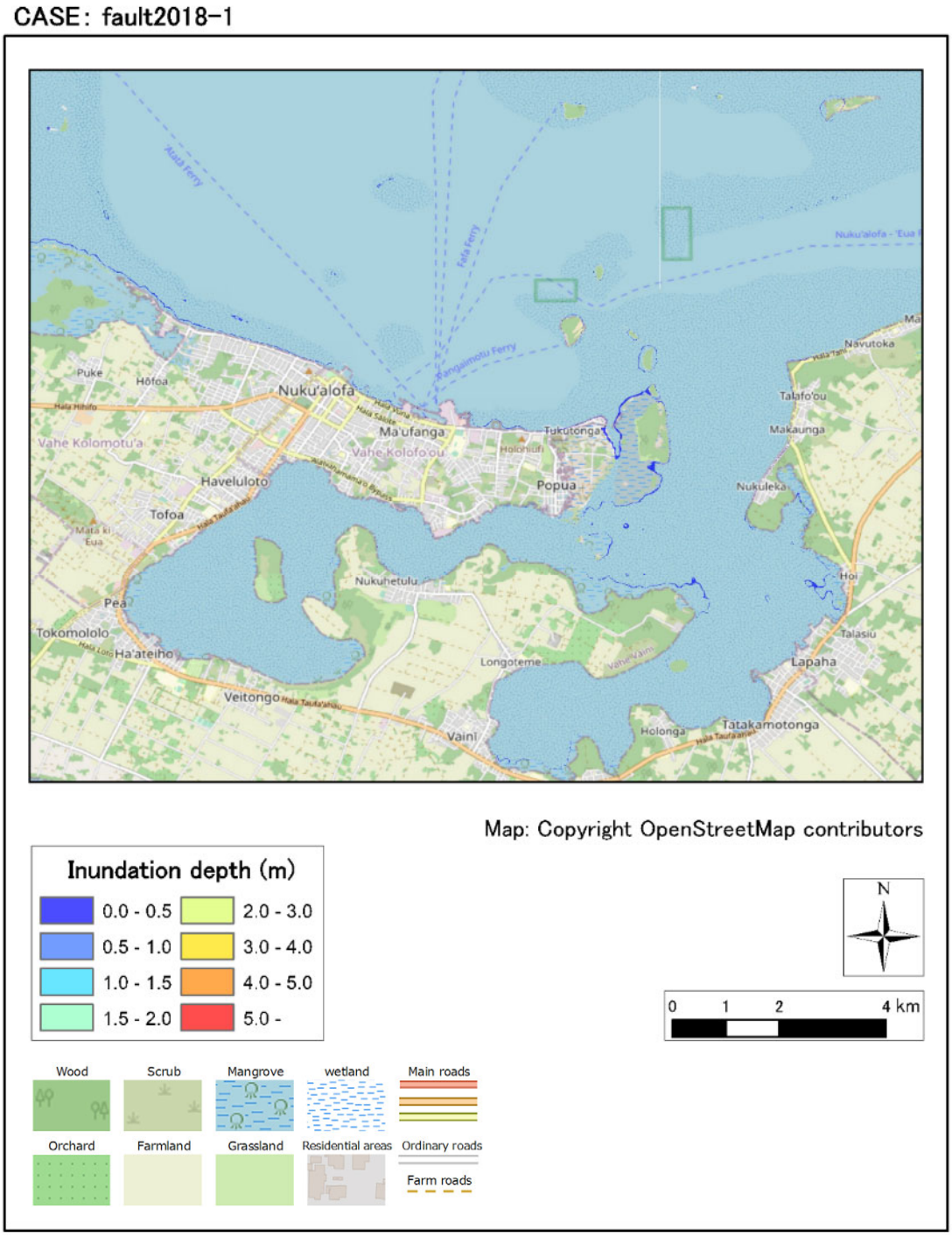

Source: JICA Study Team

Figure 2.7.35 Max inudation depth distribution (Fault 2018)

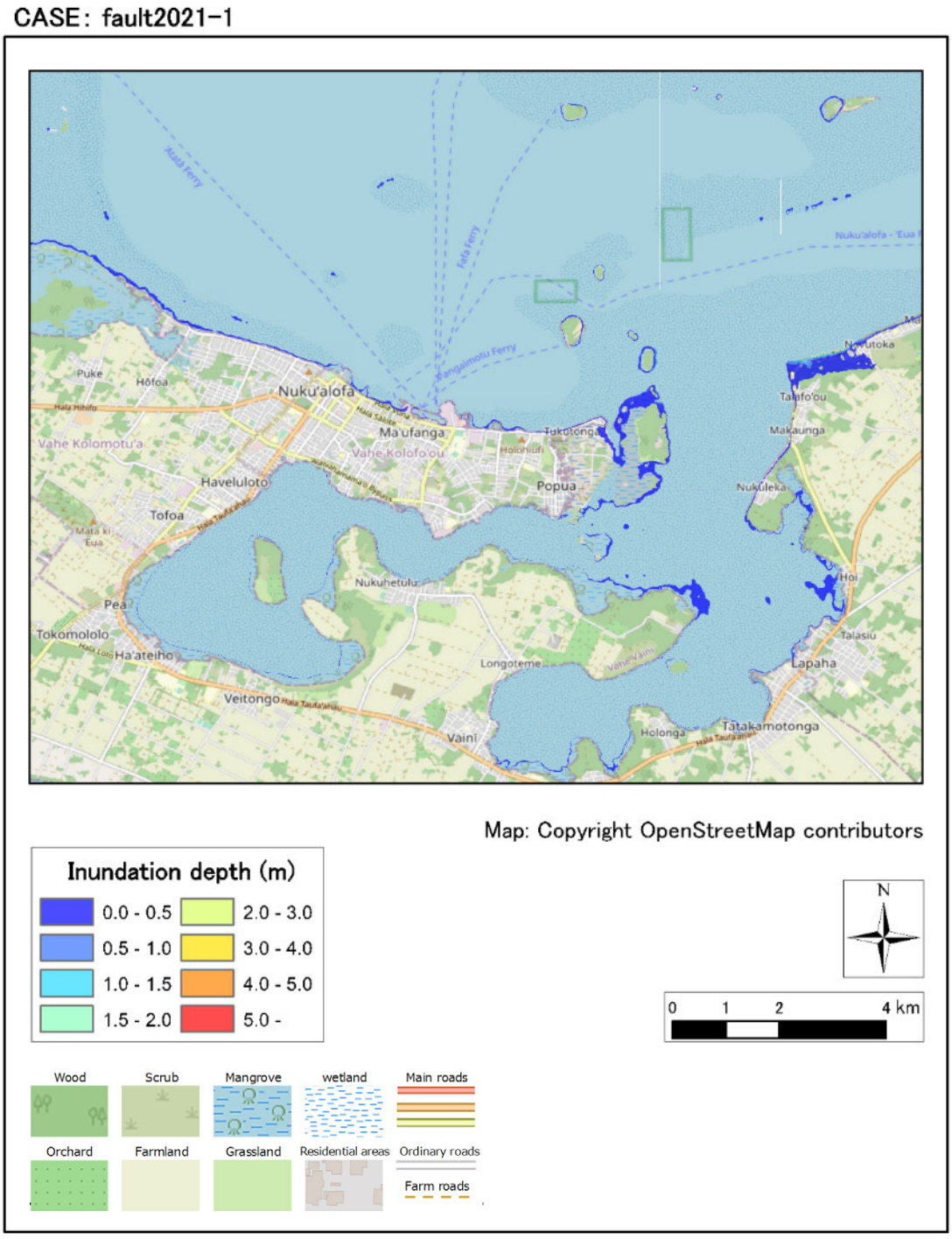

Source: JICA Study Team

Figure 2.7.36 Max inudation depth distribution (Fault 2021)

3) Arrival time map of Tsukuba(Nuku'alofa, Tongatapu Island)

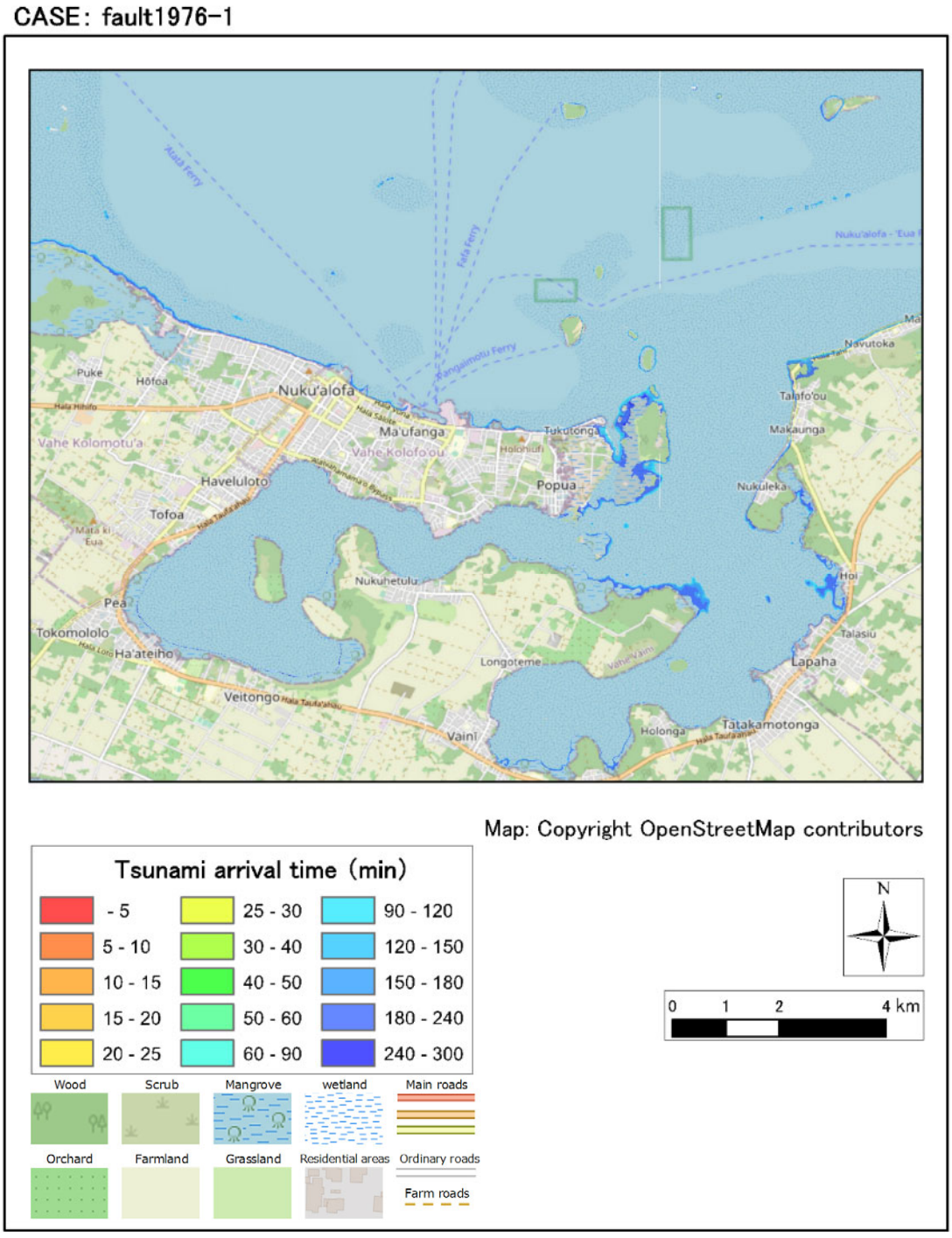

Source: JICA Study Team

Figure 2.7.37 Arrival time map of Tsukuba (Fault 1976)

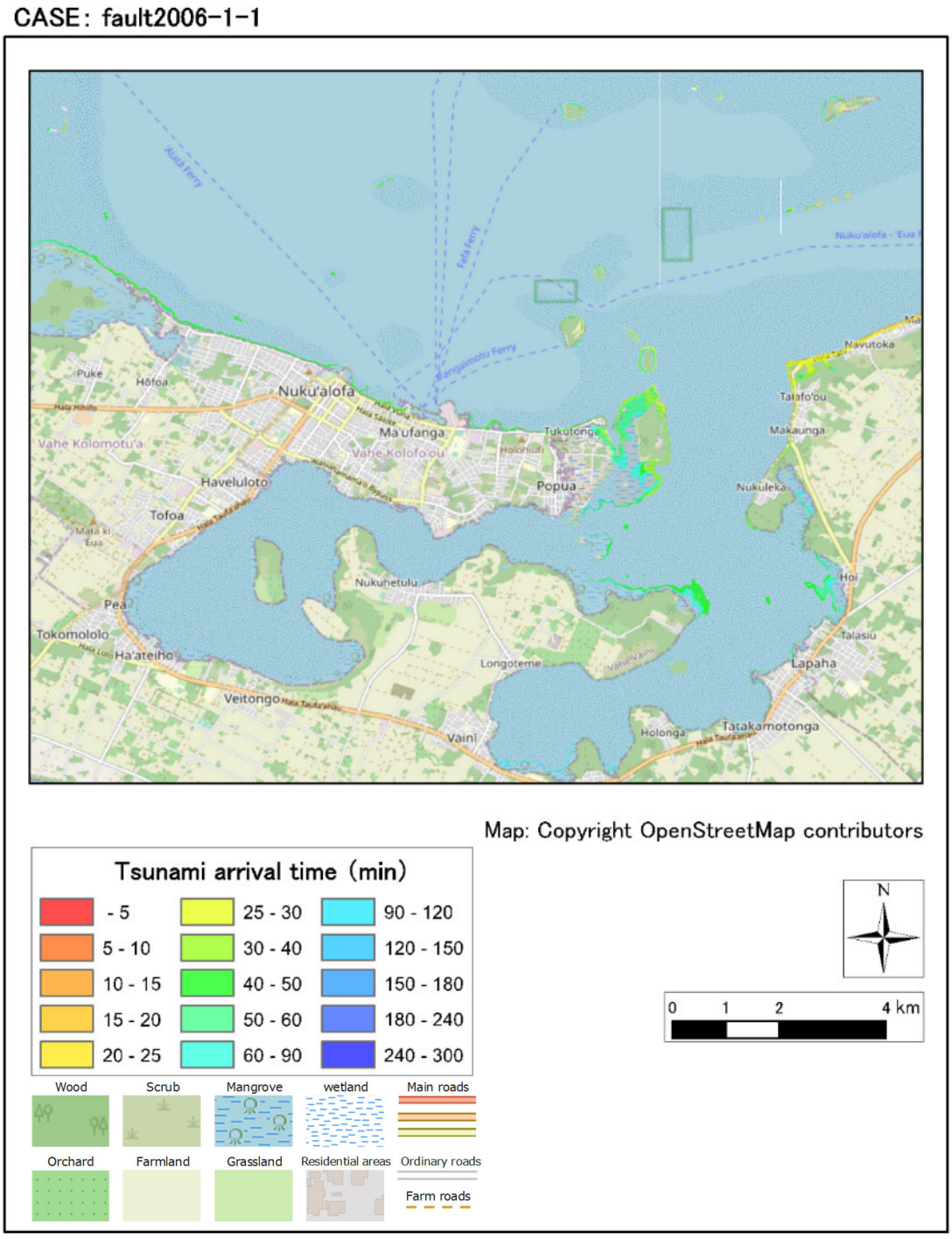

Source: JICA Study Team

Figure 2.7.38 Arrival time map of Tsukuba (Fault 2006-1)

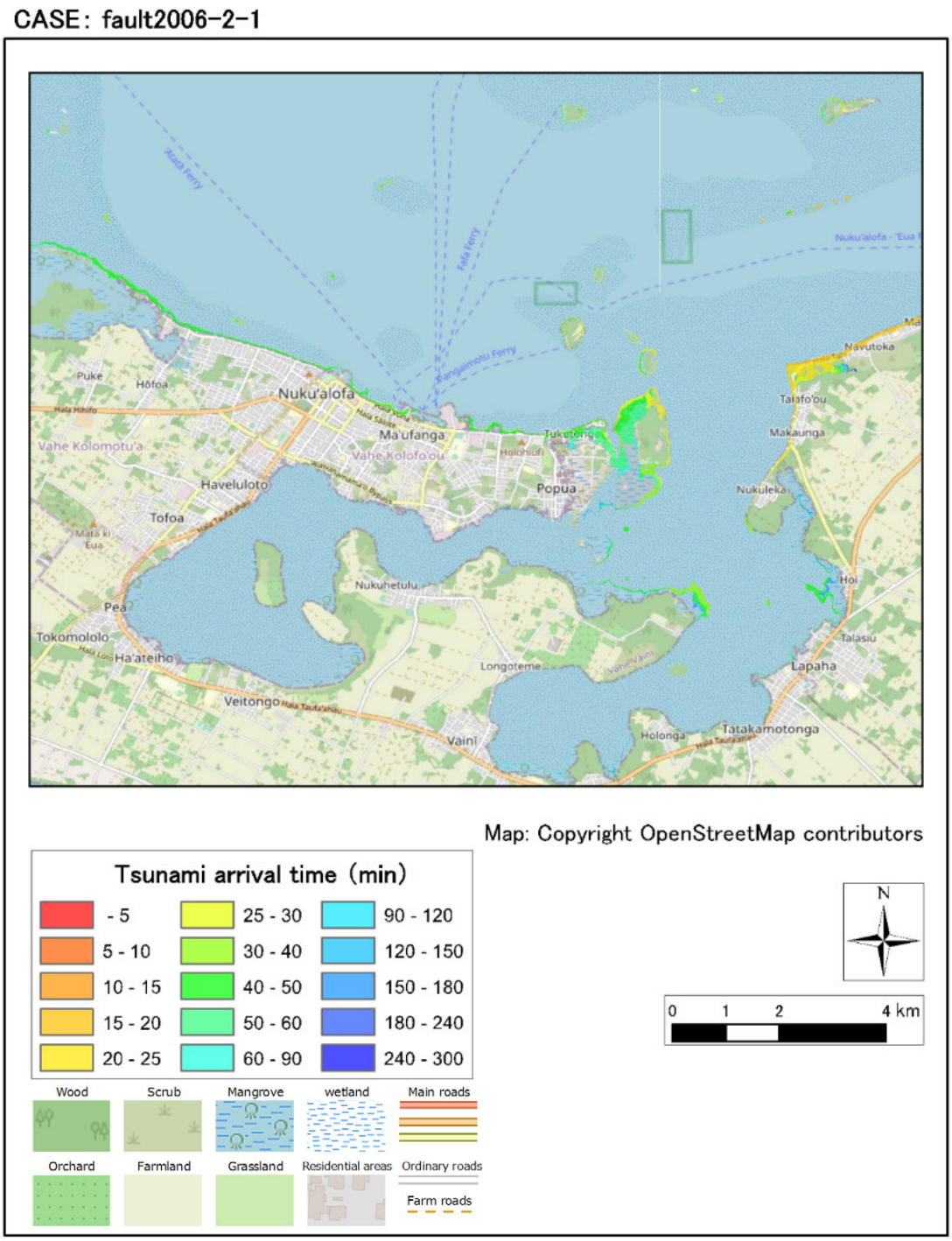

Source: JICA Study Team

Figure 2.7.39 Arrival time map of Tsukuba (Fault 2006-2)

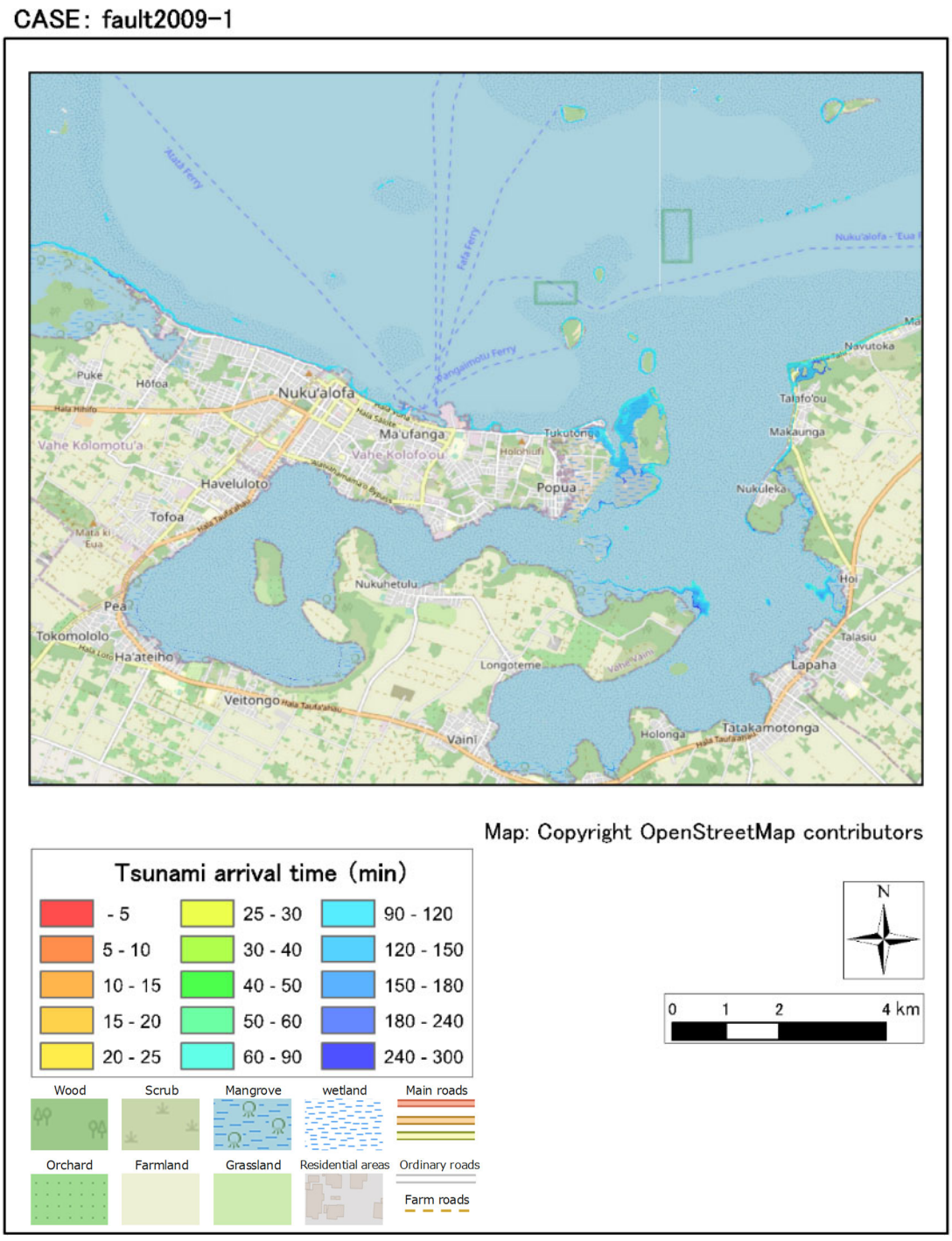

Source: JICA Study Team

Figure 2.7.40 Arrival time map of Tsukuba (Fault 2009)

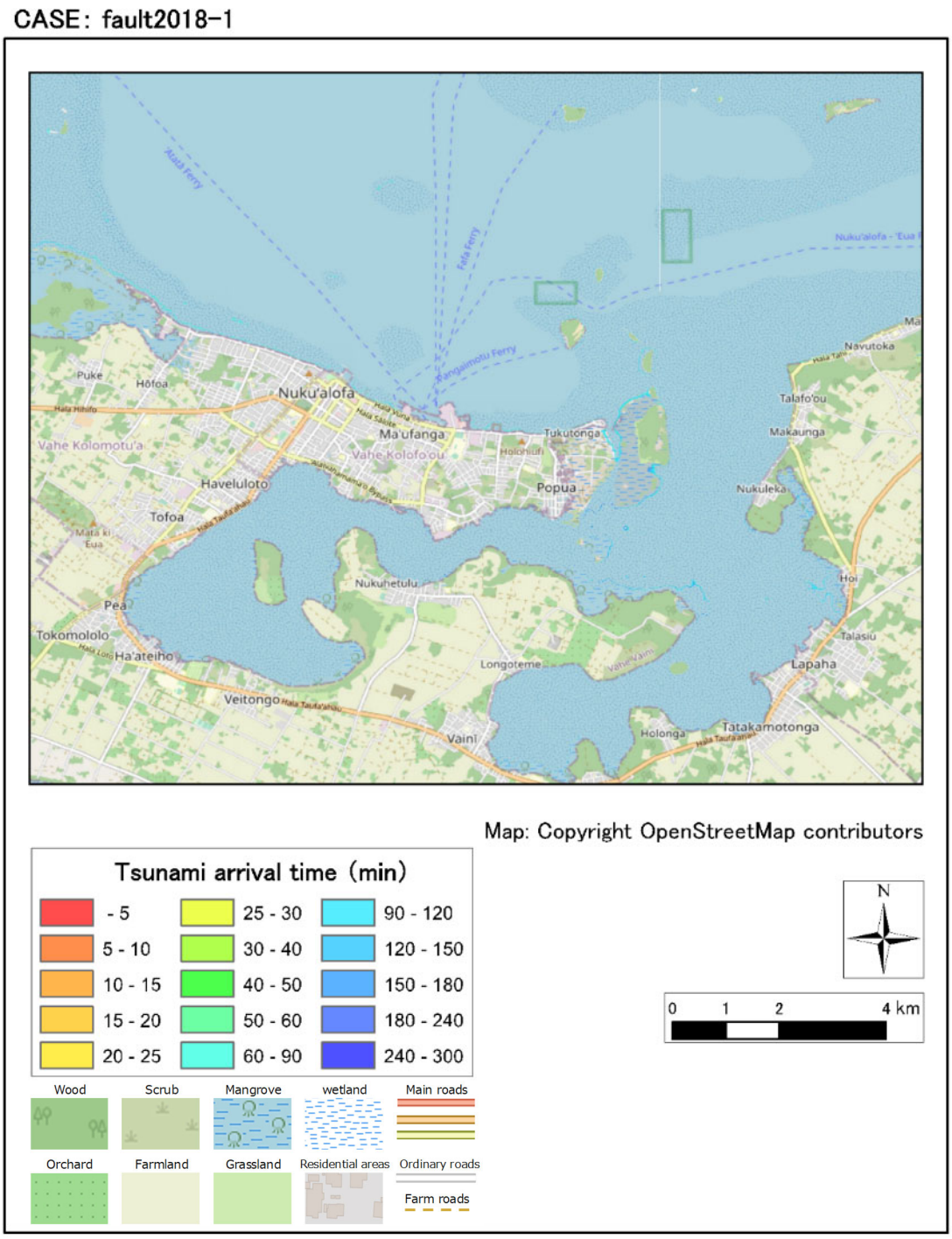

Source: JICA Study Team

Figure 2.7.41 Arrival time map of Tsukuba (Fault 2018)

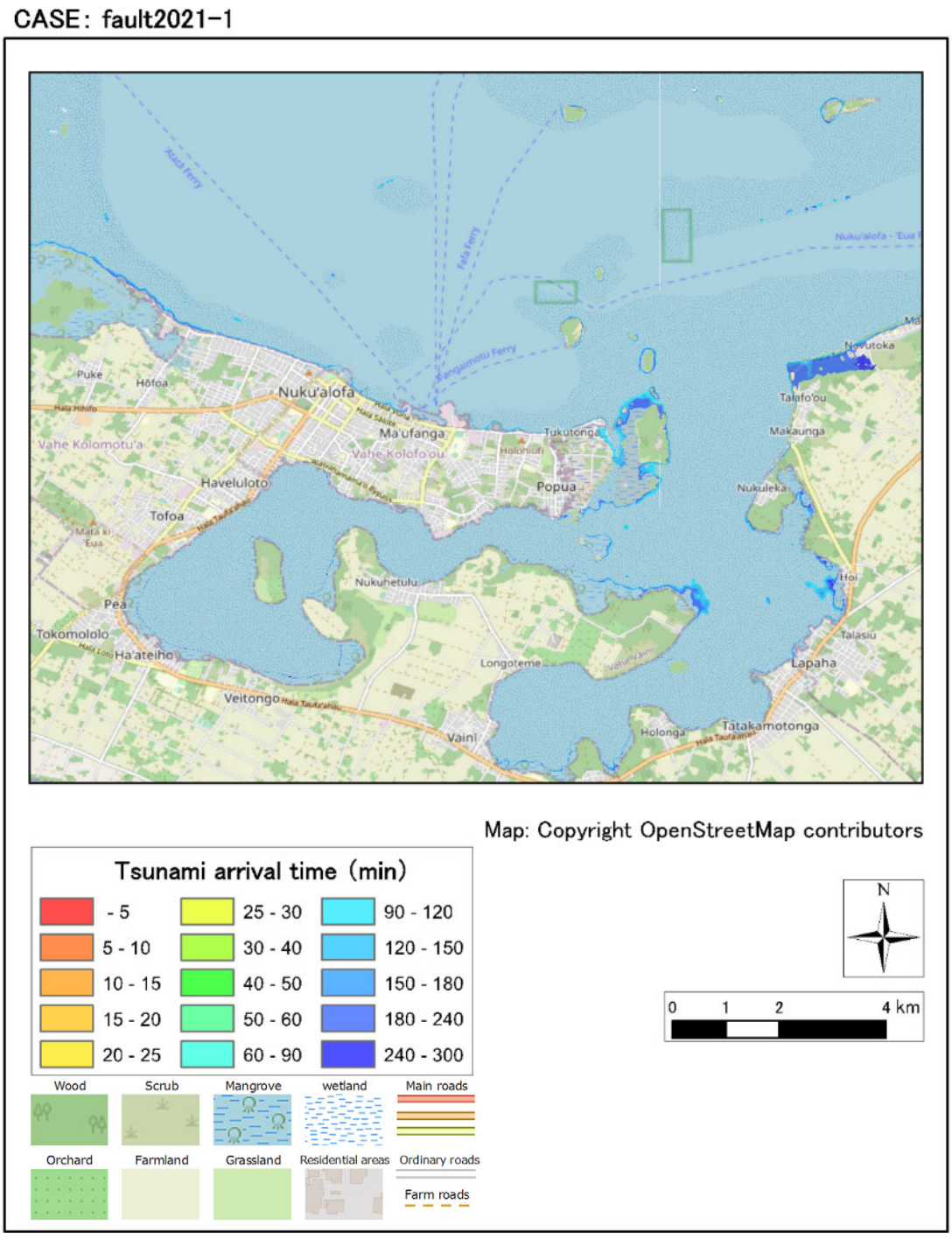

Source: JICA Study Team

Figure 2.7.42 Arrival time map of Tsukuba (Fault 2021)

4) Max Water Level Distribution map(Ohonua, Eua Island).

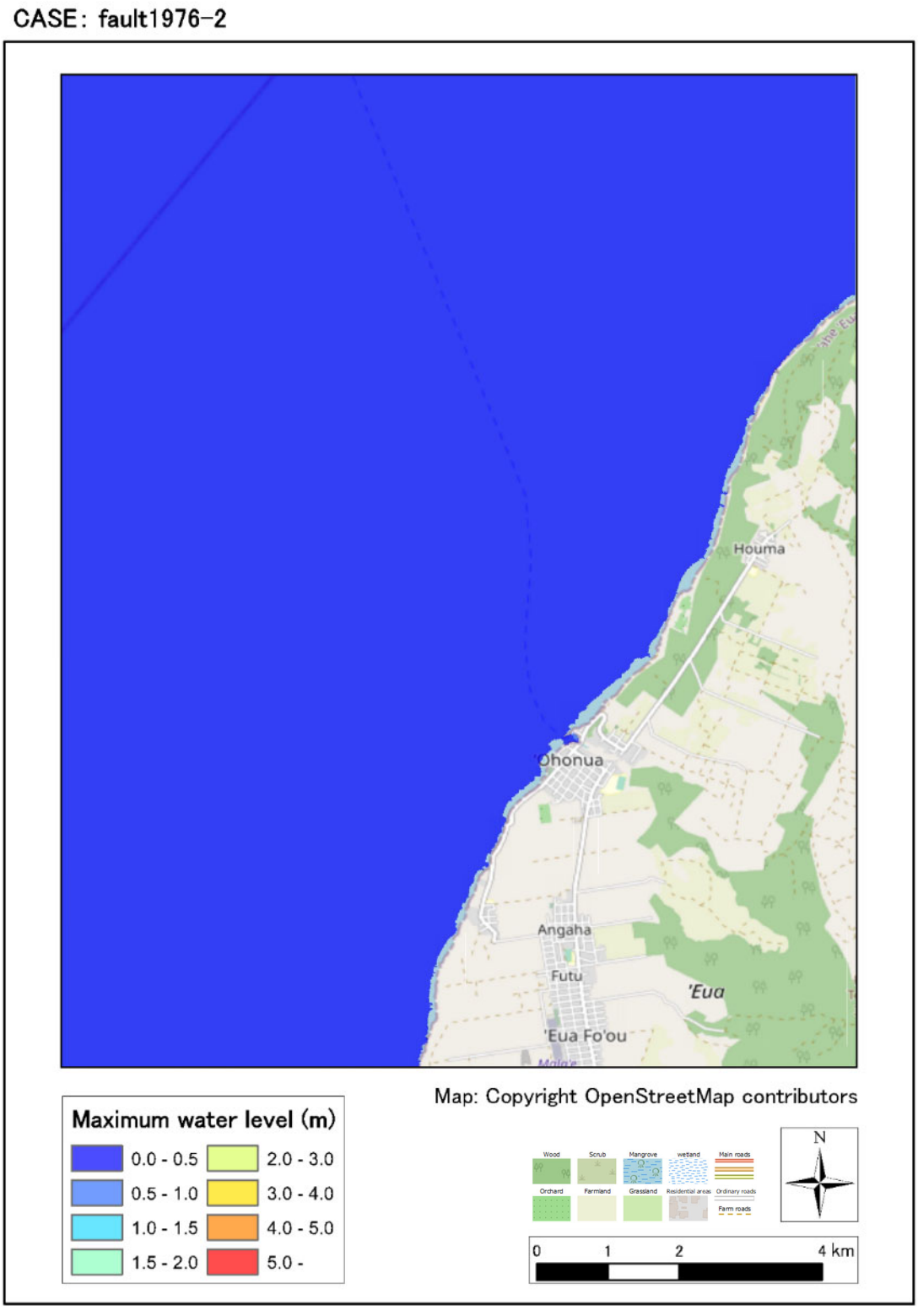

Source: JICA Study Team

Figure 2.7.43 Max Water Level Distribution map (Fault 1976)

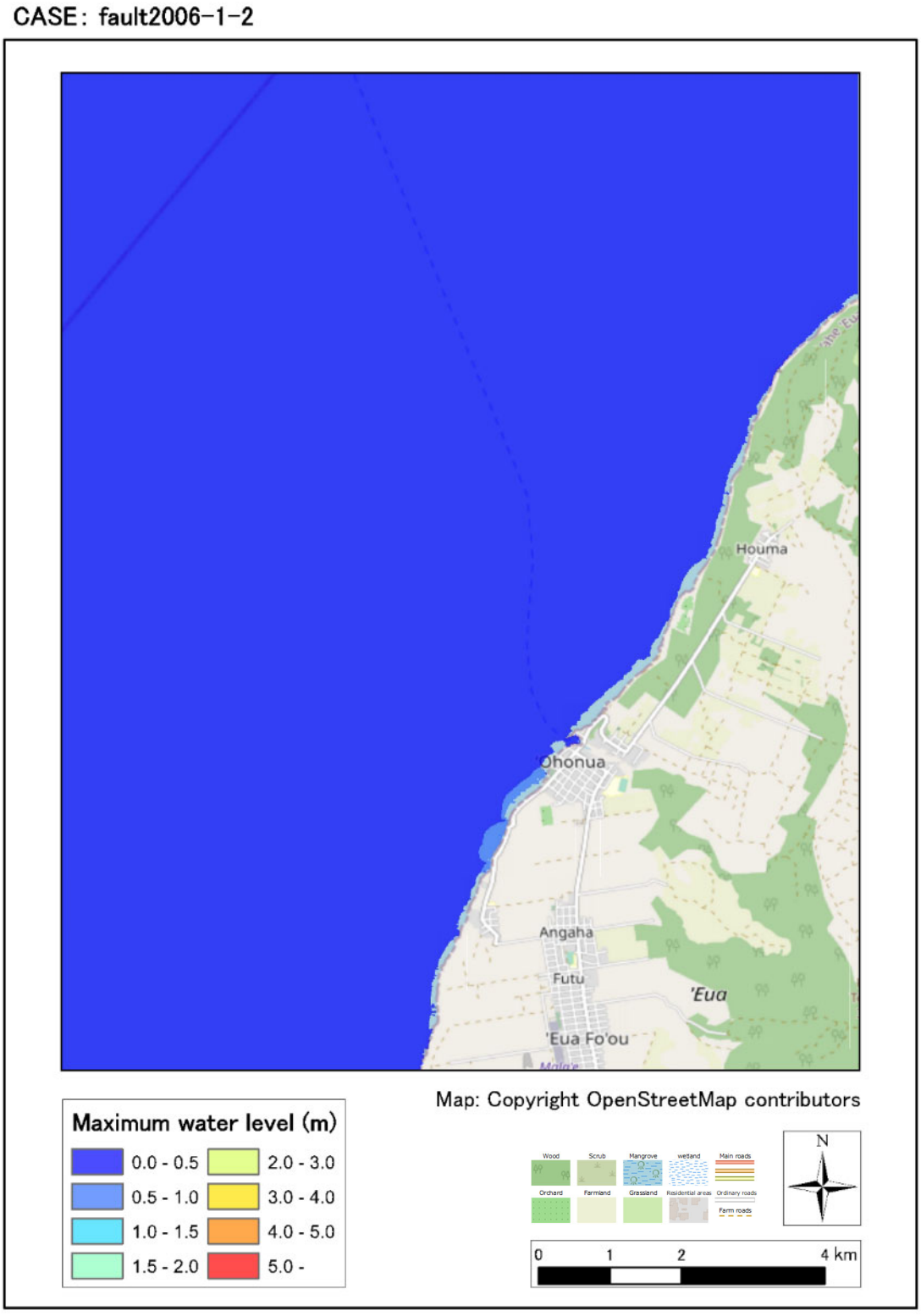

Source: JICA Study Team

Figure 2.7.44 Max Water Level Distribution map (Fault 2006-1)

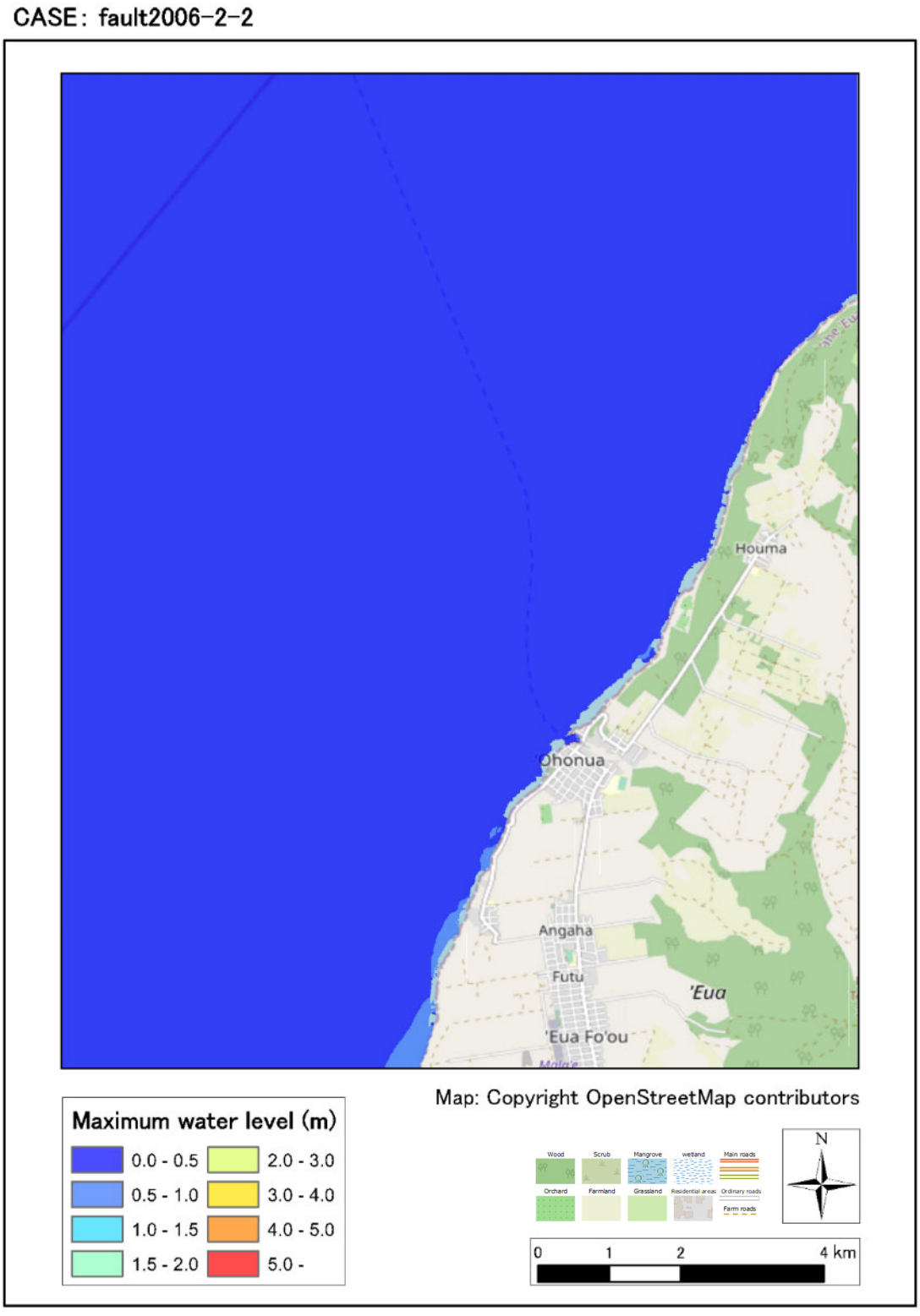

Source: JICA Study Team

Figure 2.7.45 Max Water Level Distribution map (Fault 2006-2)

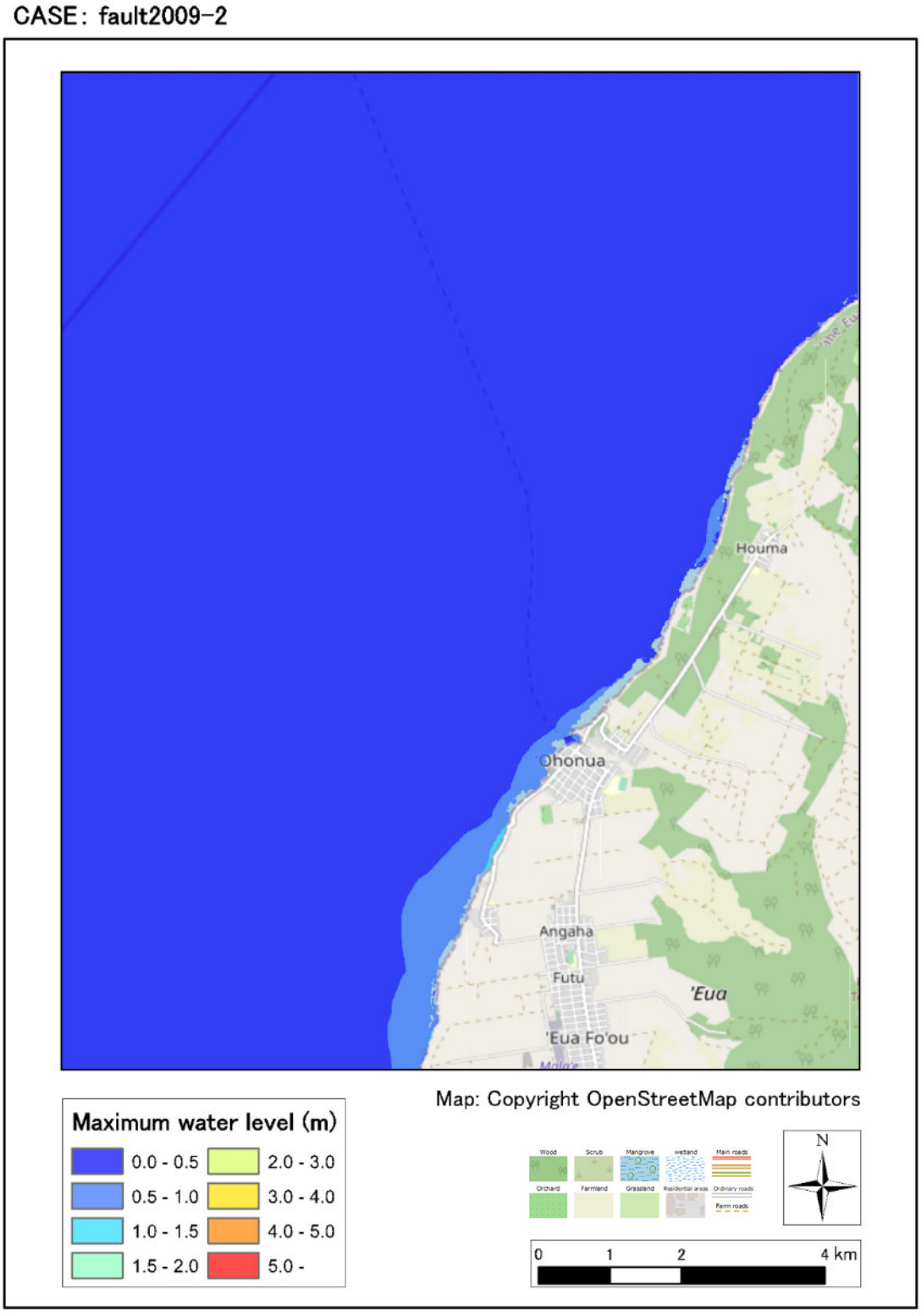

Source: JICA Study Team

Figure 2.7.46 Max Water Level Distribution map (Fault 2009)

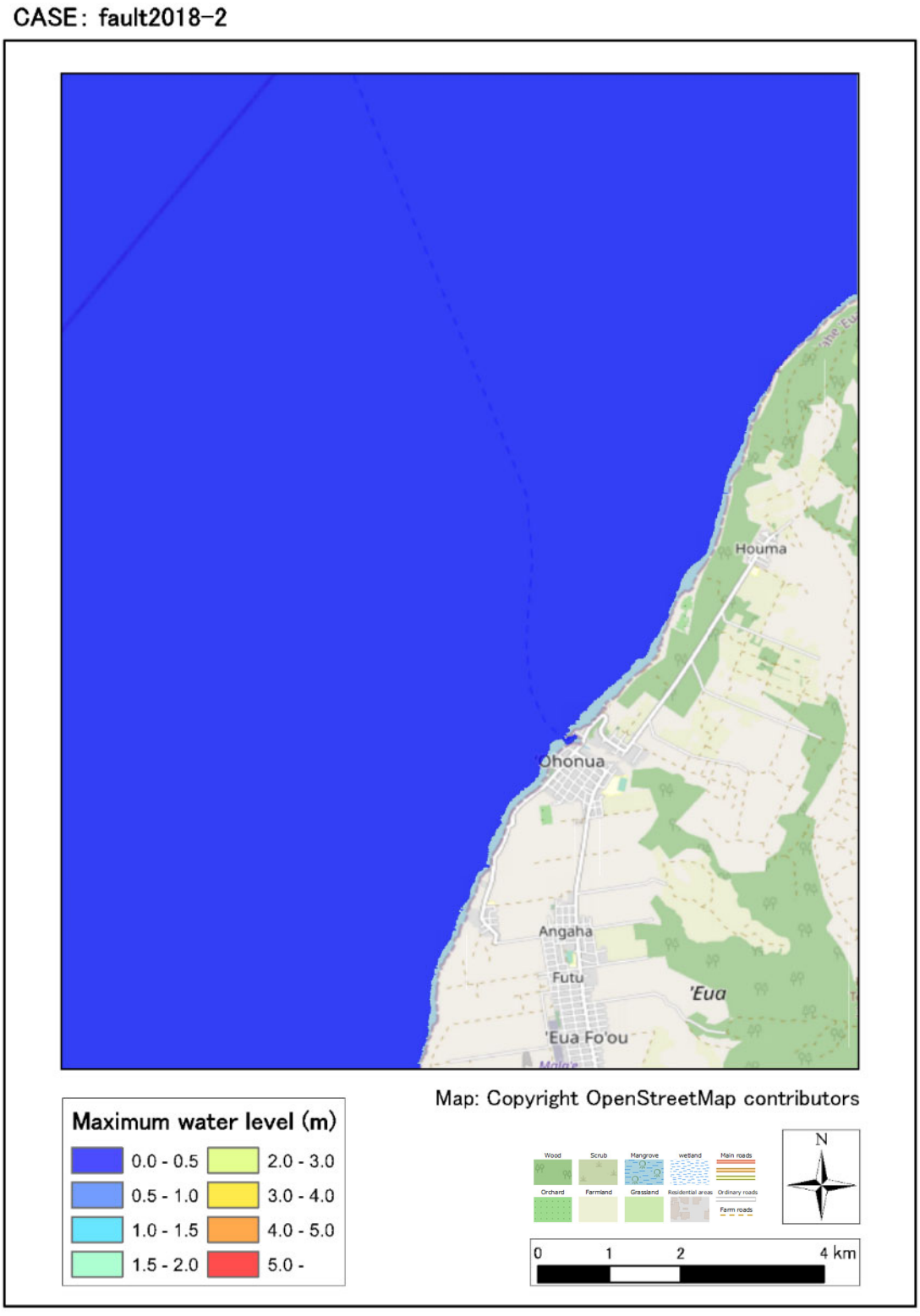

Source: JICA Study Team

Figure 2.7.47 Max Water Level Distribution map (Fault 2018)

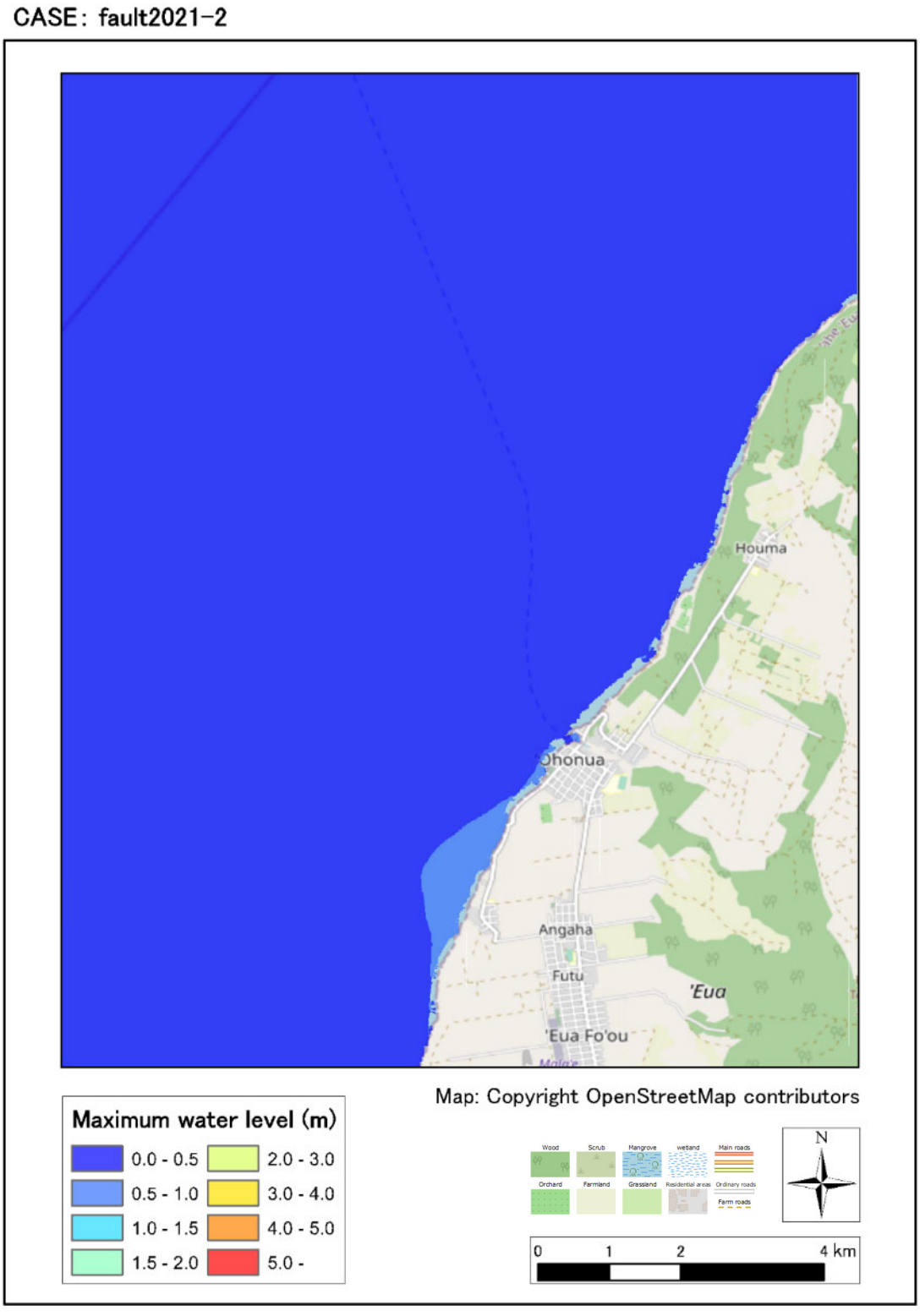

Source: JICA Study Team

Figure 2.7.48 Max Water Level Distribution map (Fault 2021)

5) Max inudation depth distribution(Ohonua, Eua Island).

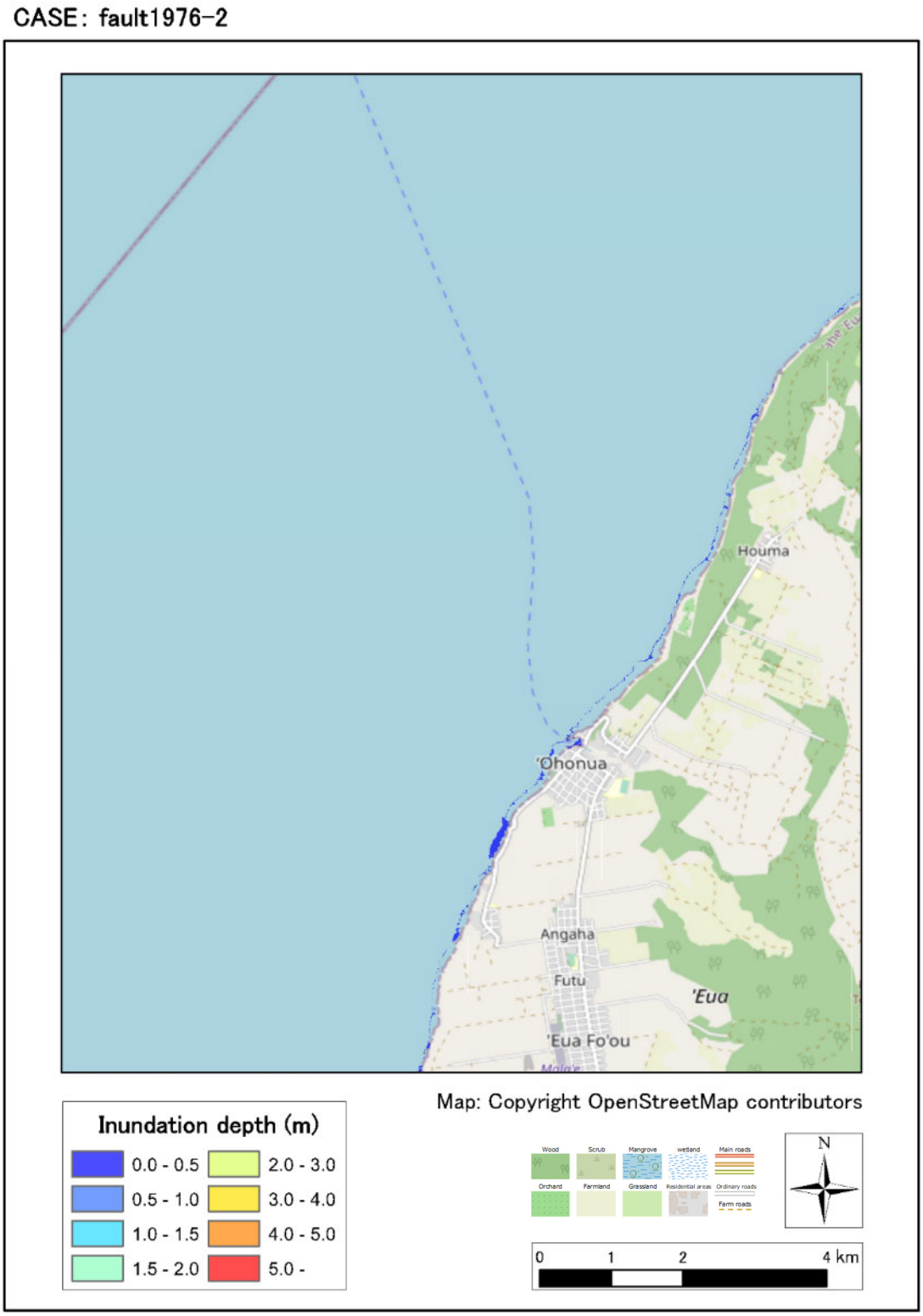

Source: JICA Study Team

Figure 2.7.49 Max inudation depth distribution (Fault 1976)

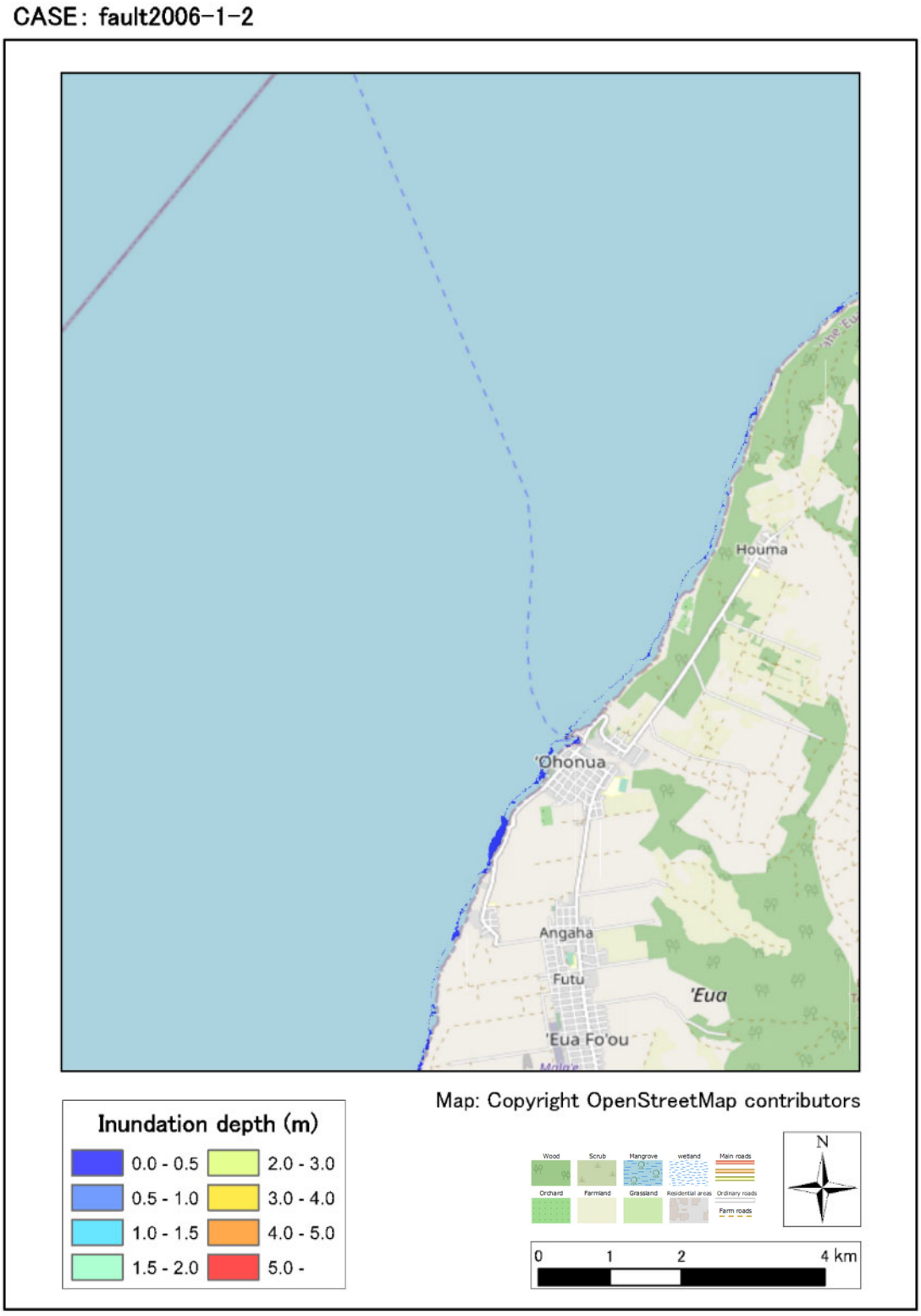

Source: JICA Study Team

Figure 2.7.50 Max inudation depth distribution (Fault 2006-1)

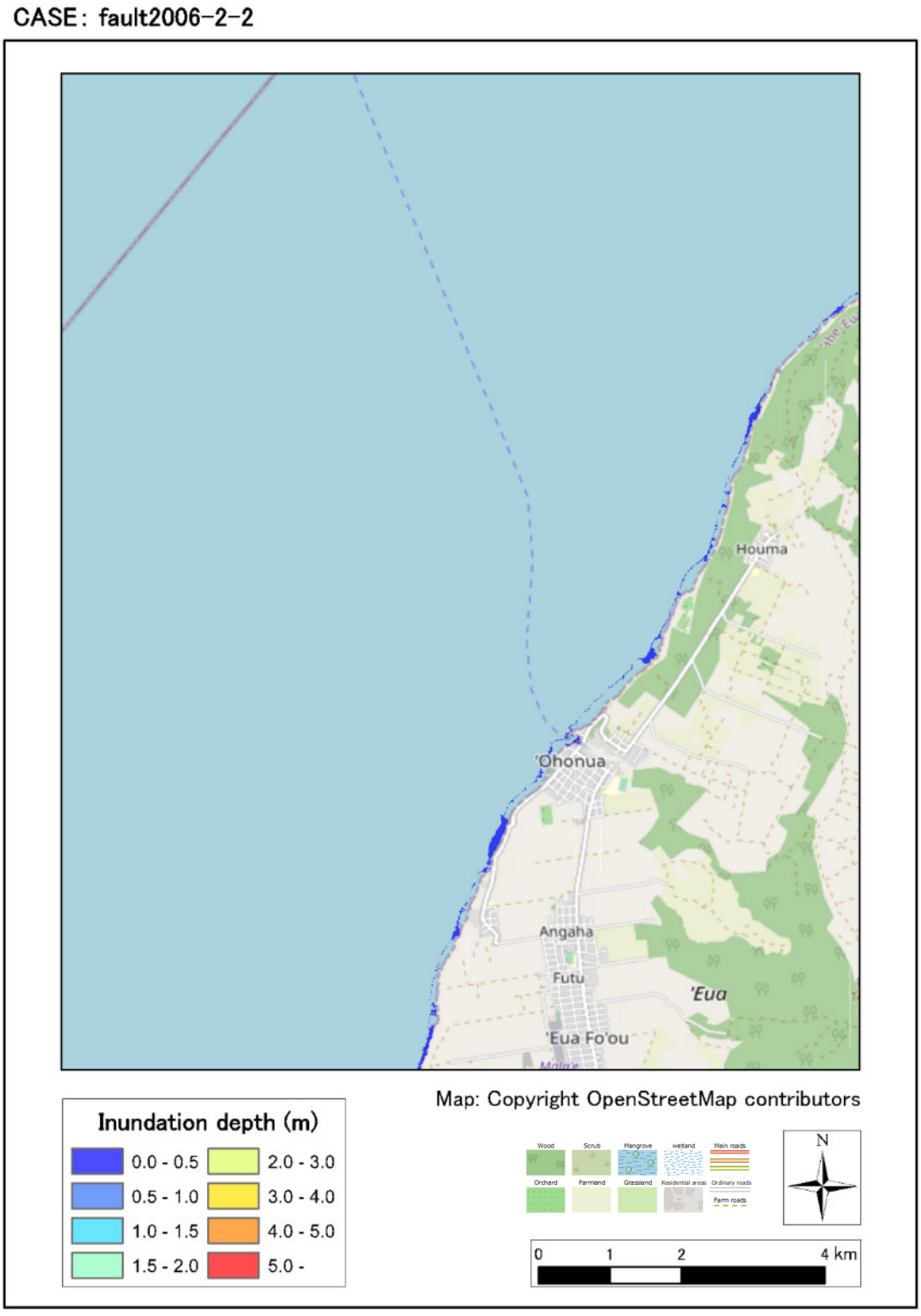

Source: JICA Study Team

Figure 2.7.51 Max inudation depth distribution (Fault 2006-2)

Source: JICA Study Team

Figure 2.7.52 Max inudation depth distribution (Fault 2009)

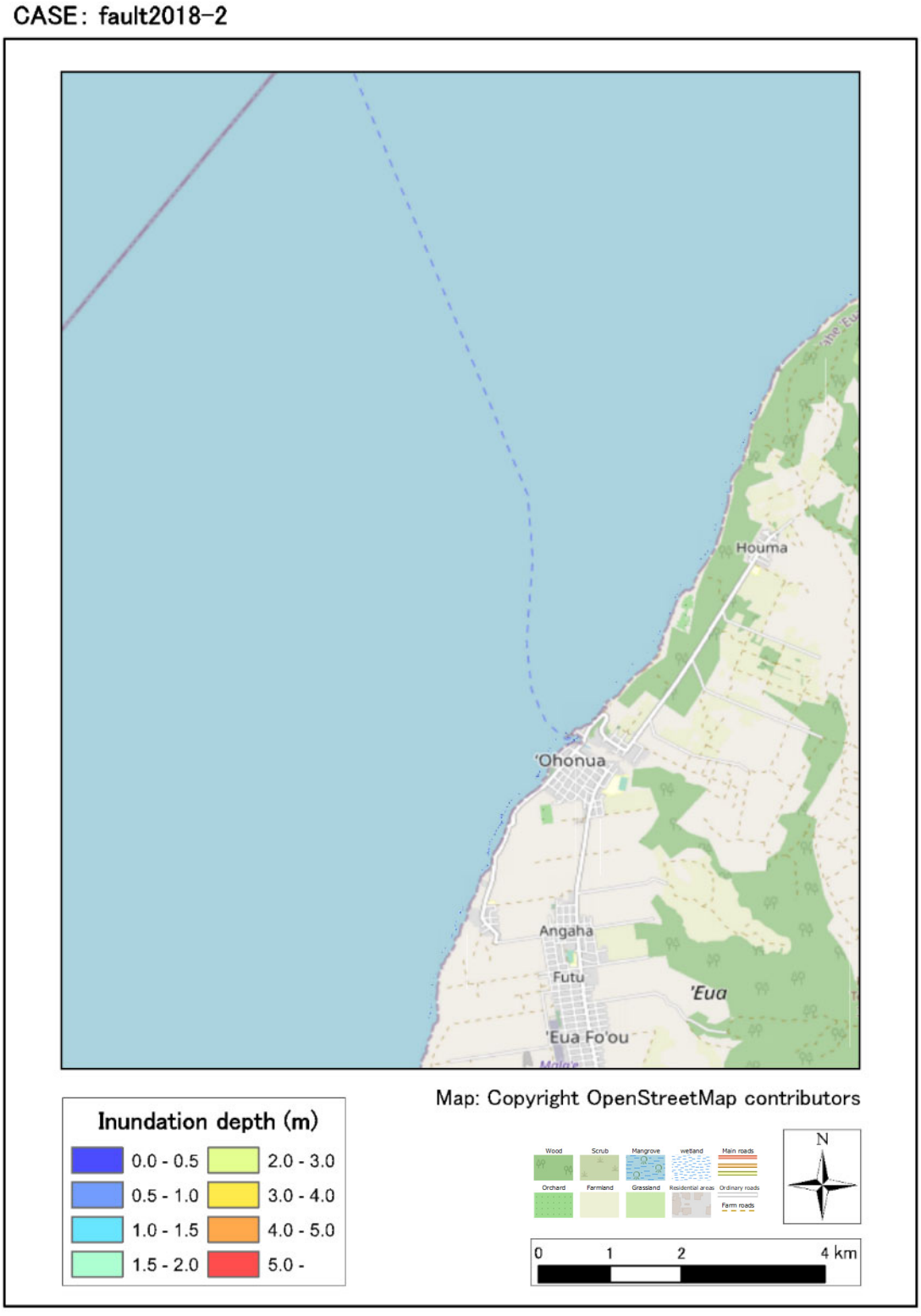

Source: JICA Study Team

Figure 2.7.53 Max inudation depth distribution (Fault 2018)

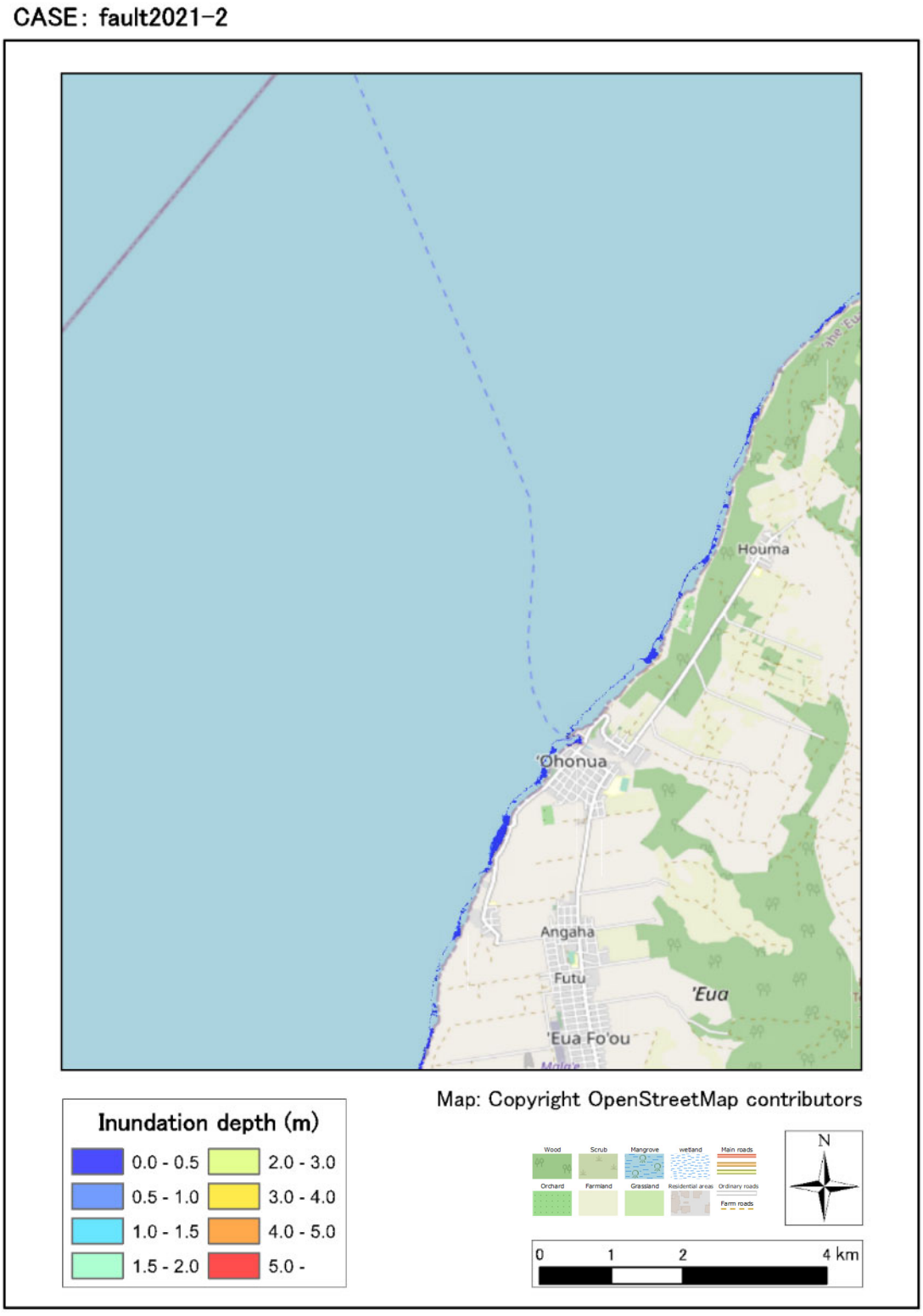

Source: JICA Study Team

Figure 2.7.54 Max inudation depth distribution (Fault 2021)

6) Arrival time map of Tsukuba(Ohonua, Eua Island).

Source: JICA Study Team

Figure 2.7.55 Arrival time map of Tsukuba (Fault 1976)

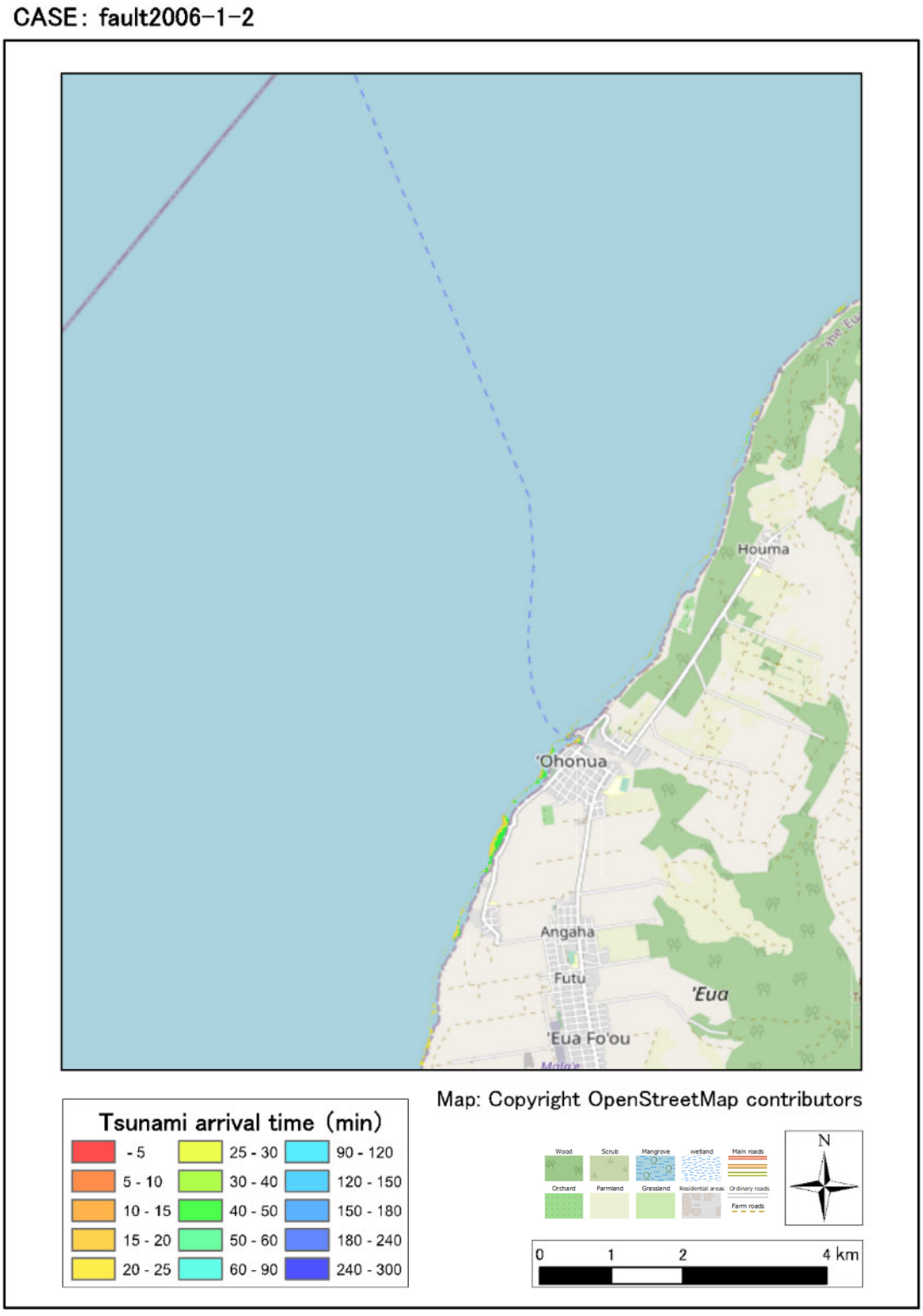

Source: JICA Study Team

Figure 2.7.56 Arrival time map of Tsukuba (Fault 2006-1)

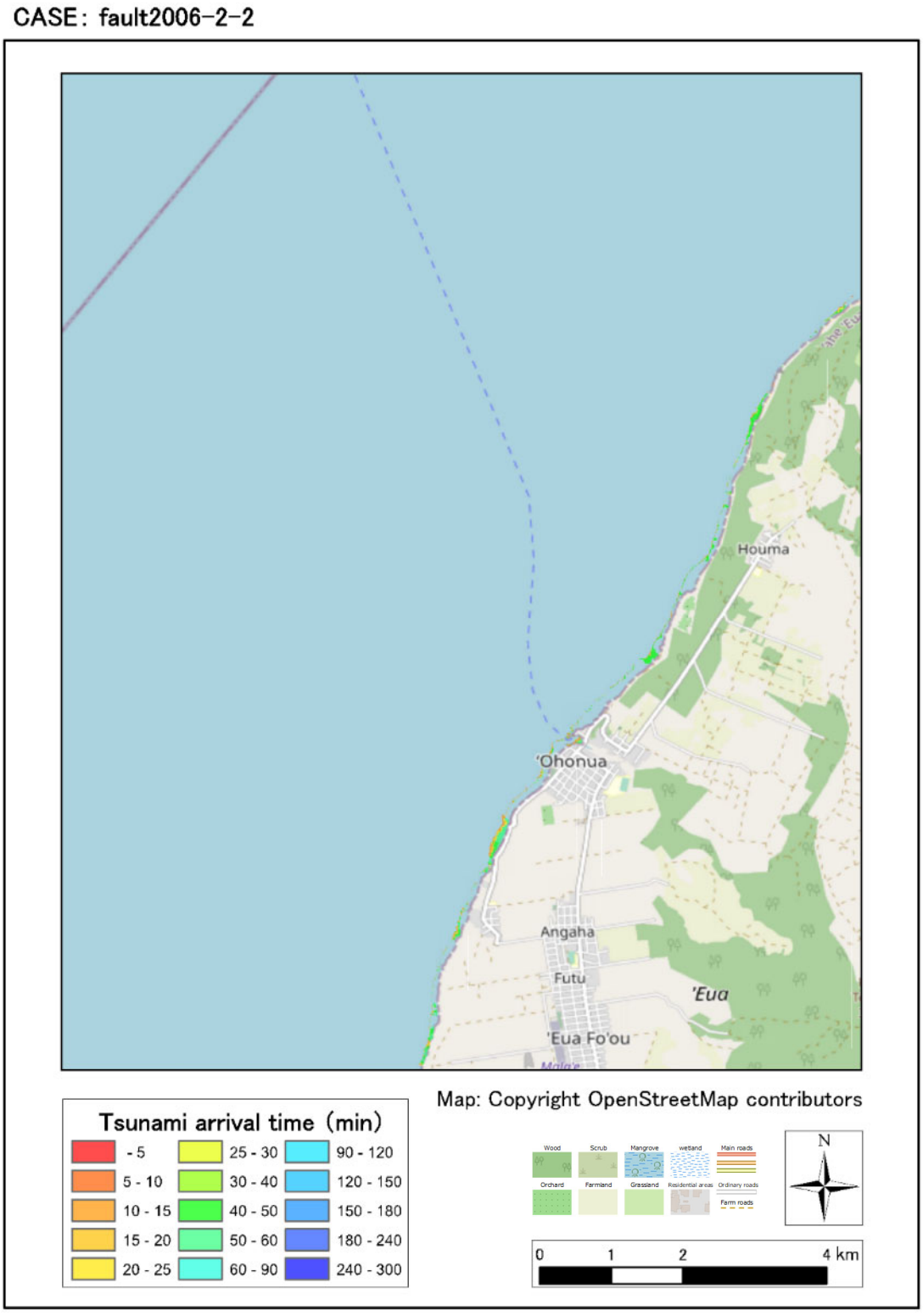

Source: JICA Study Team

Figure 2.7.57 Arrival time map of Tsukuba (Fault 2006-2)

Source: JICA Study Team

Figure 2.7.58 Arrival time map of Tsukuba (Fault 2009)

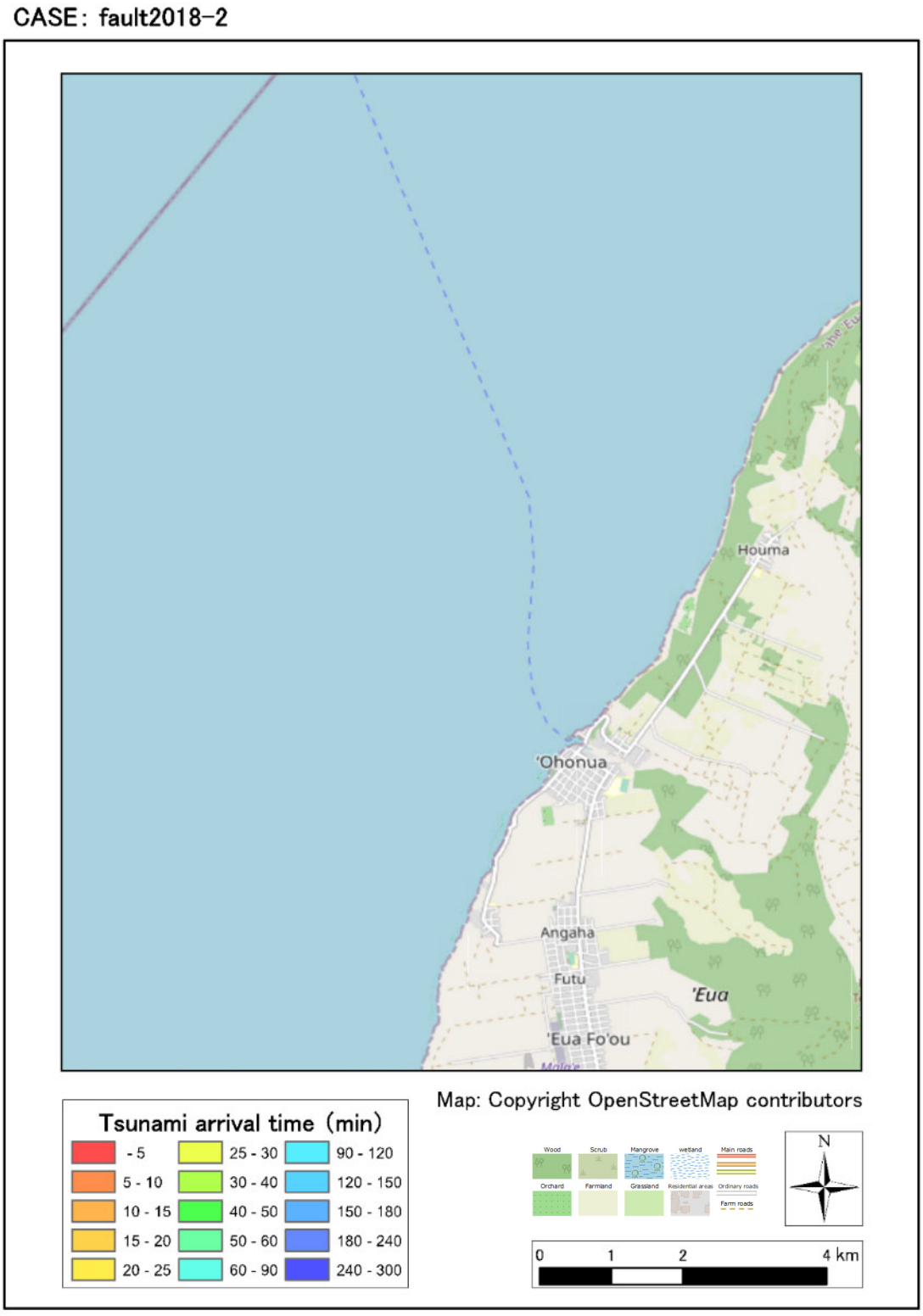

Source: JICA Study Team

Figure 2.7.59 Arrival time map of Tsukuba (Fault 2018)

Source: JICA Study Team

Figure 2.7.60 Arrival time map of Tsukuba (Fault 2021)

7) Comparison of tsunami water levels

A comparison of seismic tsunami water levels is shown in the figure below.

The tsunami water levels are all less than 1 m, indicating that the water levels of seismic tsunamis that have occurred in the last 100 years are low.

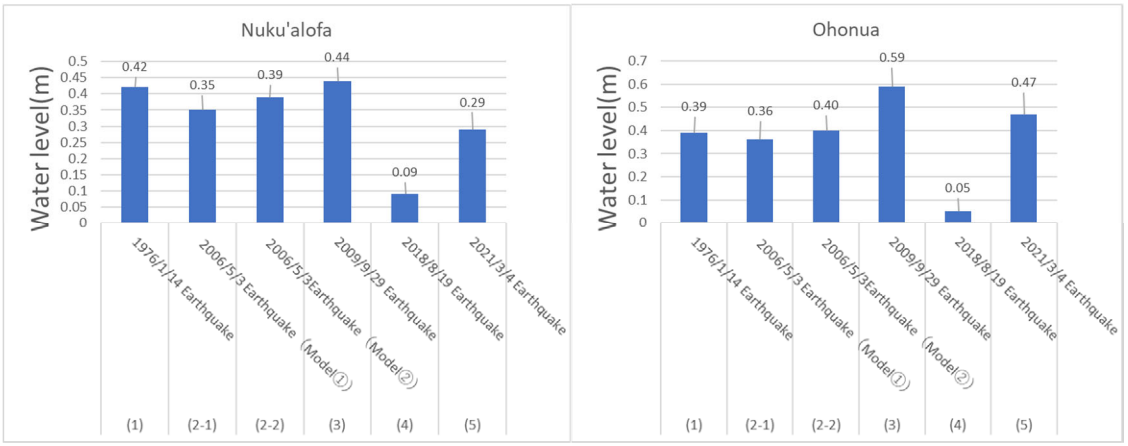

Source: JICA Study Team

Figure 2.7.61 Comparison of seismic tsunami water levels

2.7.2 Analysis for seawalls

For seismic tsunamis, the water level is generally below 1 m, and is not expected to exceed the current seawall height in Nuku'alofa. Therefore, for seismic tsunamis, the need to raise the seawall height is low.

2.8 Examination of hazard levels

2.8.1 Examination of hazard levels based on tsunami analysis results

Based on the tsunami analysis results, two hazard levels, Level 1 and Level 2, are considered as hazard levels for disaster mamagement planning and disaster management measures. The definition of each hazard level is given in Table 2.8.1.

Table 2.8.1 Intensity and frequency of each hazard level and measures

Hazard level	Hazard intensity and frequency	Countermeasures
Level 1 (L1)	**High frequency hazard** Hazard that causes serious damage despite a low hazard intensity with a higher frequency of occurrence than the largest class of hazards. l **Period of occurrence of the hazard: several tens to several hundreds of years**	Structure measures are implemented to protect human lives, their property and the local economy.
Level 2 (L2)	**Largest class of hazard** Hazard that occurs infrequently but causes extensive damage once it occurs. **Period of hazard occurrence: hundreds to thousands of years**	Comprehensive measures should be taken to evacuate the population by combining all soft and Structure measures, with lifesaving as the first priority.

Source: JICA Study Team

(1) Tsunami hazard levels

The results of the tsunami analysis in Nukualofa for both volcanic and seismic tsunamis are plotted in a time series in Figure 2.8.1.

The height of past seismic tsunamis in Nukualofa is about 1-2 m at H.W.L., and they have occurred several times in about 100 years. Therefore, past seismic tsunamis can be considered as Hazard Level 1 tsunamis to be dealt with by hard countermeasures.

On the other hand, the height of volcanic tsunamis expected in Nukualofa in the future when a volcano of the same size as the 2022 Hunga tonga-Hunga haapai volcano occurs elsewhere is 1.5-4.2 m at H.W.L. Tsunamis exceeding 3 m, including the tsunami caused by the 2022 Hunga tonga-Hunga haapai volcano, are not expected in the 100 years, and it is unlikely that a volcano of the same size as the Hungatonga-Hungaahaapai volcano will occur again in about a hundred years. Therefore, volcanic tsunamis of the same size as the Hungatonga-Hungaahaapai volcano are classified as Hazard Level 2 tsunamis (the largest class of tsunamis) for which evacuation measures and other measures should be taken.

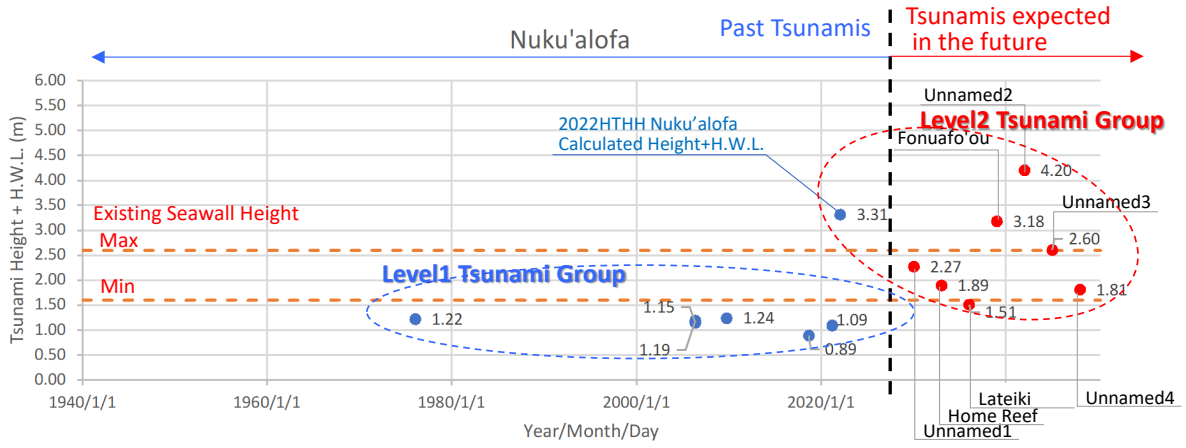

Source: JICA Study Team

Figure 2.8.1 Classification of tsunami hazard levels in Nuku'alofa

Past seismic tsunamis in Ohonua, Eua Island, have also been 1-2 m high at H.W.L. and have occurred several times in about 100 years. Therefore, past seismic tsunamis can be considered as Hazard Level 1 tsunamis to be dealt with by hard countermeasures.

On the other hand, the height of future volcanic tsunamis expected at Ohonua, Eua Island, in the event of a volcano of the same size as the HTHH in January 2022 occurring elsewhere, is 2.7-12 m at H.W.L. No tsunamis exceeding 3 m have occurred in Ohonua in the past 100 years, including the tsunami caused by the HTHH in 2022, and it is unlikely that a volcano of the same size as the HTHH will occur repeatedly in about a hundred years. Therefore, volcanic tsunamis of the same size as the Hungatonga-Hungaahaapai volcano are classified as Hazard Level 2 tsunamis (the largest class of tsunamis) for which evacuation measures and other measures should be taken.

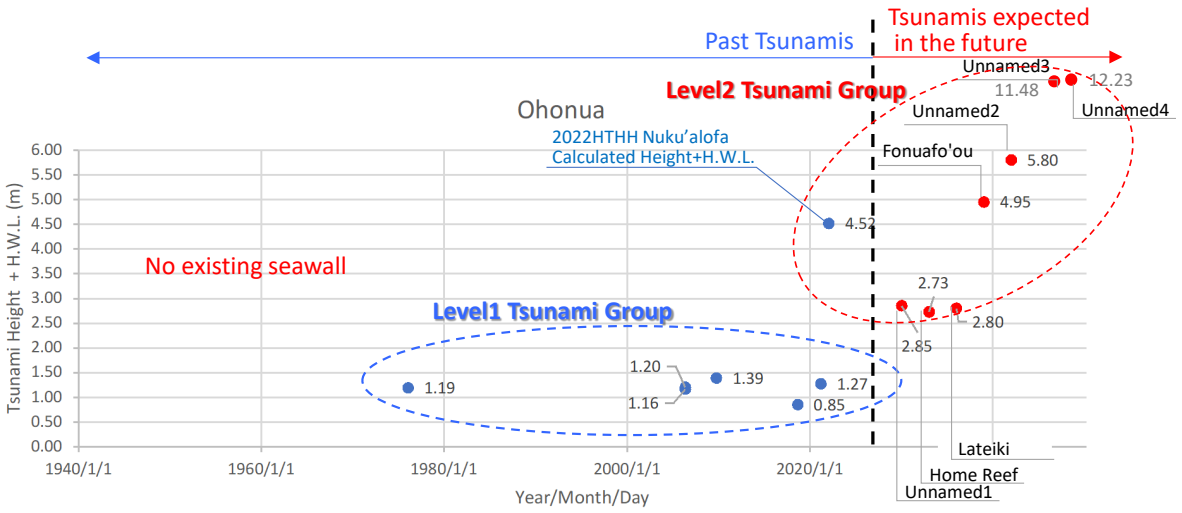

Source: JICA Study Team

Figure 2.8.2 Classification of tsunami hazard levels in Ohonua

It should be noted that although this study considered volcanic tsunamis of the same size as the HTHH, tsunamis caused by volcanoes smaller than the HTHH may occur several times during a 100-year period.

2.9 Analysis of Hazard Level 2 tsunamis

(1) Tsunami analysis for Hazard Level 2 (volcanic tsunamis)

Based on the results of the studies up to the previous section, tsunamis caused by volcanoes of the same magnitude as the January 2022 HTHH were classified as Hazard Level 2 tsunamis if they were generated by other submarine volcanoes. Among these cases, the cases with the greatest impact on Tongatapu and Eua islands are discussed. The results of the study are shown in Table 2.9.1 and Figure 2.9.1.

For the volcanoes shown in Table 2.9.3, the inundation area is calculated with the tide level as H.W.L. (M.S.L. + 0.8 m) as the adverse condition and the Max extent of the envelope is the inundation area of Hazard Level 2. The results of the inundation area calculations are shown in Figures 2.9.1 and Figure 2.9.2.

Table 2.9.1 Cases with predominant inundation extent and depths on Tongatapu and Eua islands (names of submarine volcanoes)

Tongatapu Island	Eua Island
Unnamed1 (H=90m)	Unnamed2 (H=90m)
Unnamed2 (H=90m)	Unnamed3 (H=90m)
Unnamed3 (H=90m)	Unnamed4 (H=90m)
Unnamed4 (H=90m)	–

Source: JICA Study Team

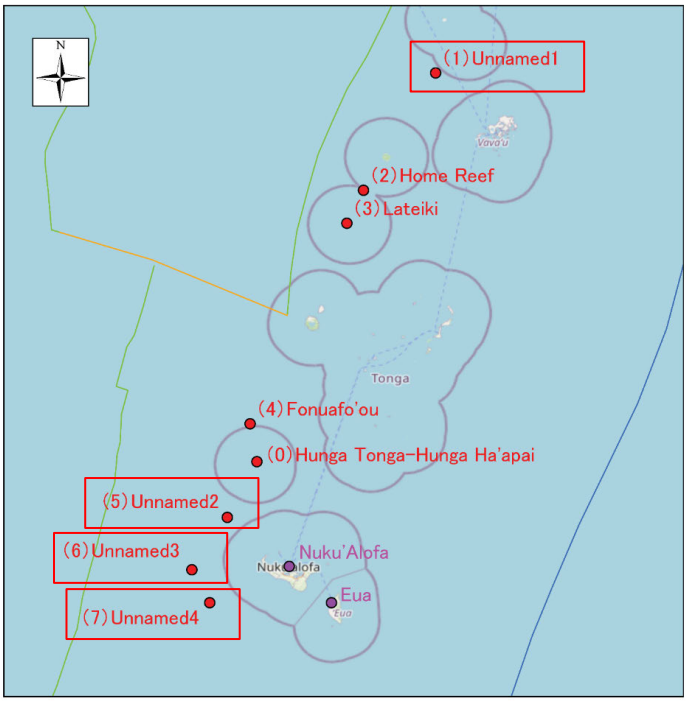

Source: JICA Study Team

Figure 2.9.1 Volcanoes with significant impact on Tongatapu and Eua Island.

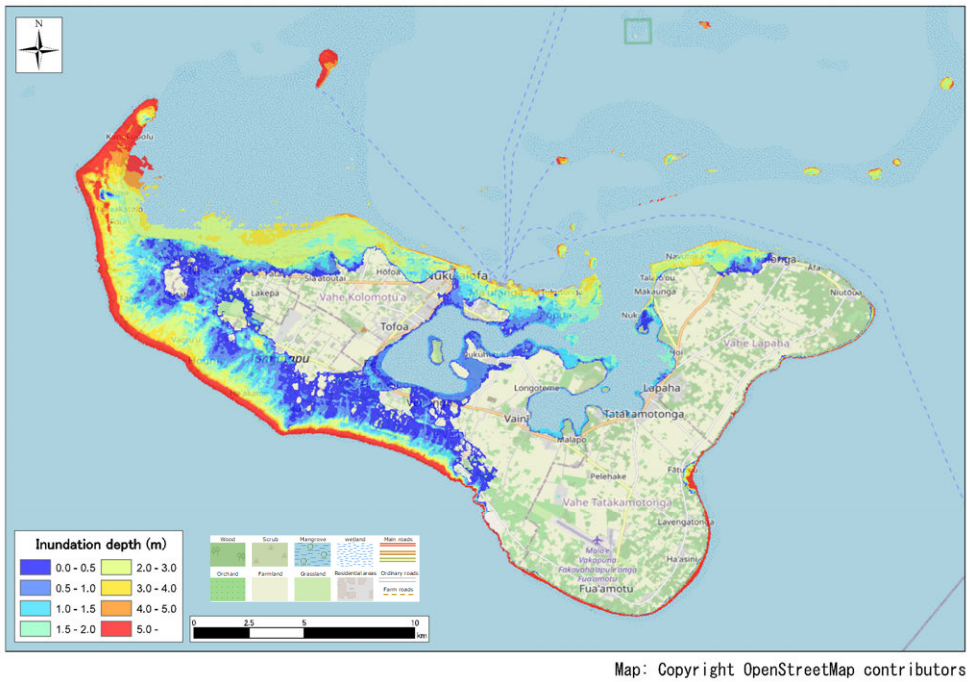

Source: JICA Study Team

Figure 2.9.2 Tongatapu Island Flooding Map (Volcanic Tsunami Hazard Level 2)

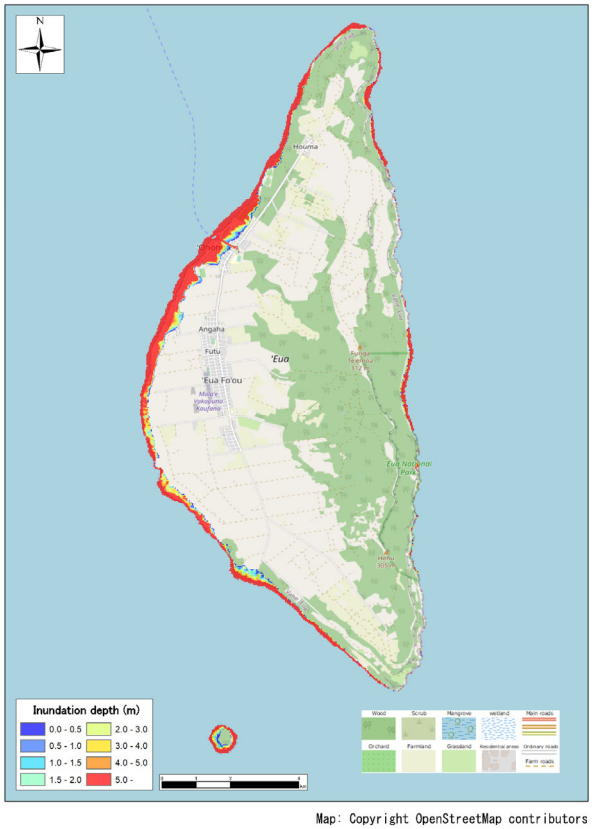

Source: JICA Study Team

Figure 2.9.3 Eua Island Inundation Assumption Map (Volcanic Tsunami Hazard Level 2)

(2) Tsunami analysis for Hazard Level 2 (seismic tsunami)

For tsunami hazard maps, the Southwest Pacific Tsunami Risk Assessment Capacity Enhancement (Phase 3) Tsunami Simulation Map was prepared in 2012 by the SOPAC project. The "case of an M8.7 earthquake in the central Tonga Trench (east of Tongatapu Island)" adopted in this study is discussed.

As there is no clear information on Fault Parameters for the SOPAC earthquake fault model, the initial Water Level Distribution is reproduced and used as the input wave for the tsunami. The initial Water Level Distribution is shown in Figure2.9.6.

Using this initial Water Level Distribution as the wave source, inundation calculations were carried out with the tide level as H.W.L. (M.S.L. + 0.8 m) as the adverse condition. The seawall condition was the existing seawall. The results of the inundation calculations are shown in Figures 2.9.7 and 2.9.8.

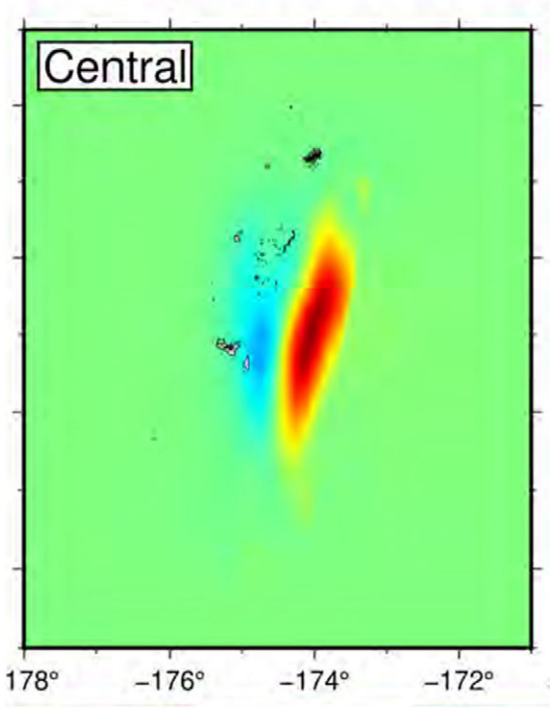

Source: Multi-Hazard Risk Assessment Tongatapu Interim Hazard Assessment Report – Tsunami, Asian Development Bank

Figure 2.9.4 Initial Water Level Distribution (SOPAC M8.7 earthquake: central Tonga Trench (east of Tongatapu Island))

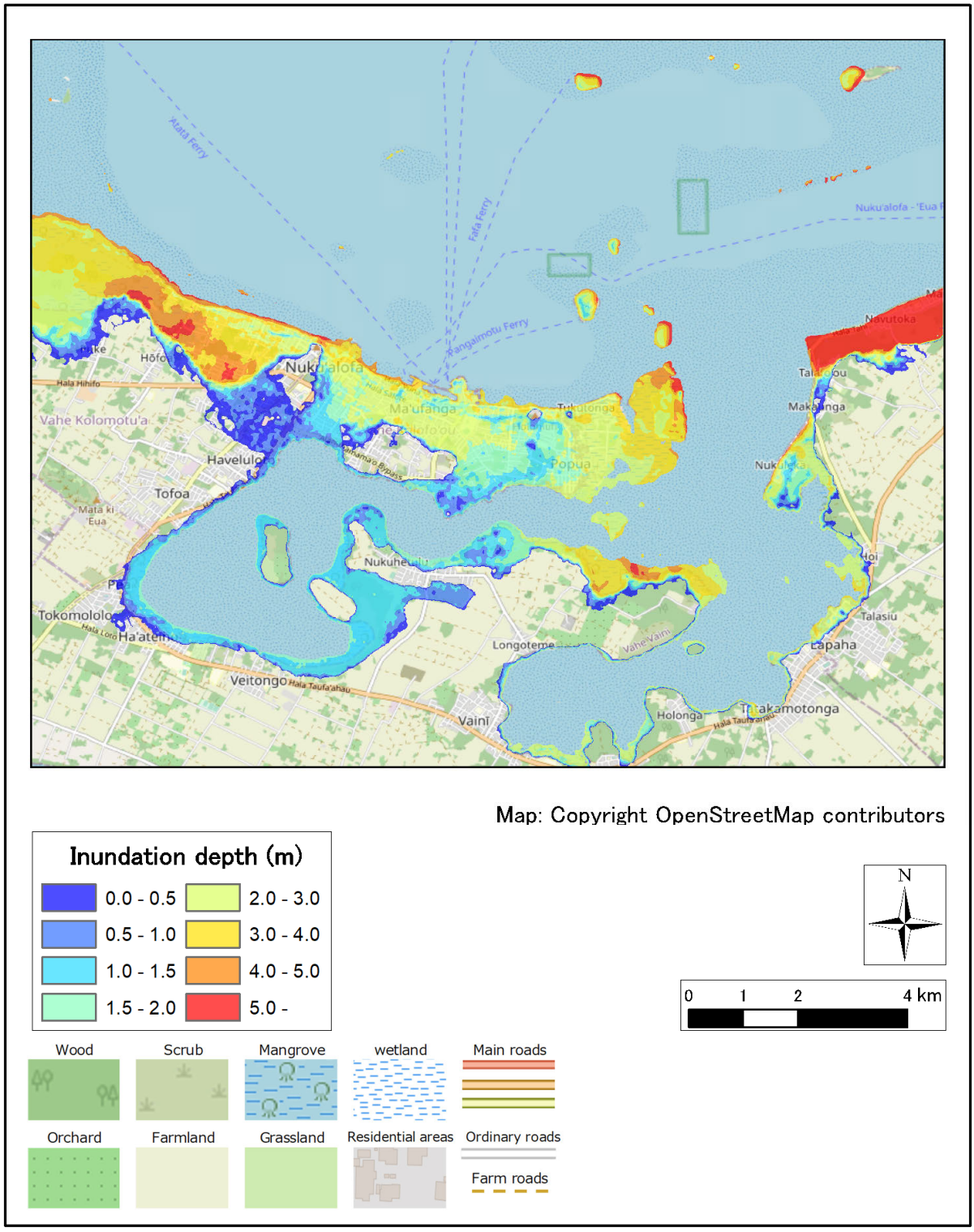

Source: JICA Study Team

Figure 2.9.5 Tongatapu Island inundation scenario (Seismic Tsunami Hazard Level 2)

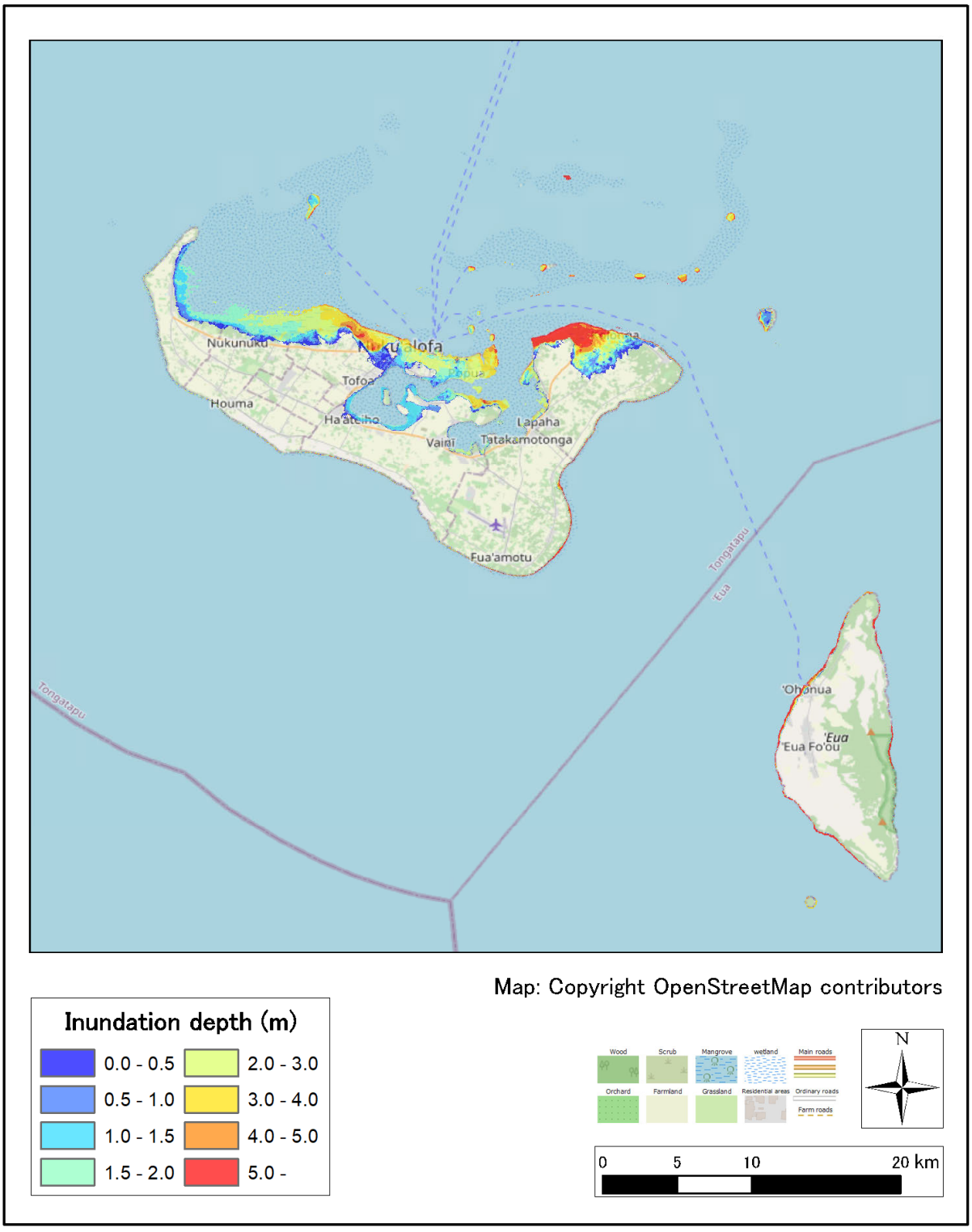

Source: JICA Study Team

Figure 2.9.6 Tongatapu Eua Island Inundation Hazard Map (Seismic Tsunami Hazard Level 2)

3. storm surge analysis

3.1 Study flow

The flow of the storm surge analysis is shown in Figure 3.1.1.

In this work, cyclones that have had a significant impact on Tongatapu Island in the past are extracted, and reproduction calculations and probability storm surge anomalies are calculated. The largest class of cyclones will then be considered.

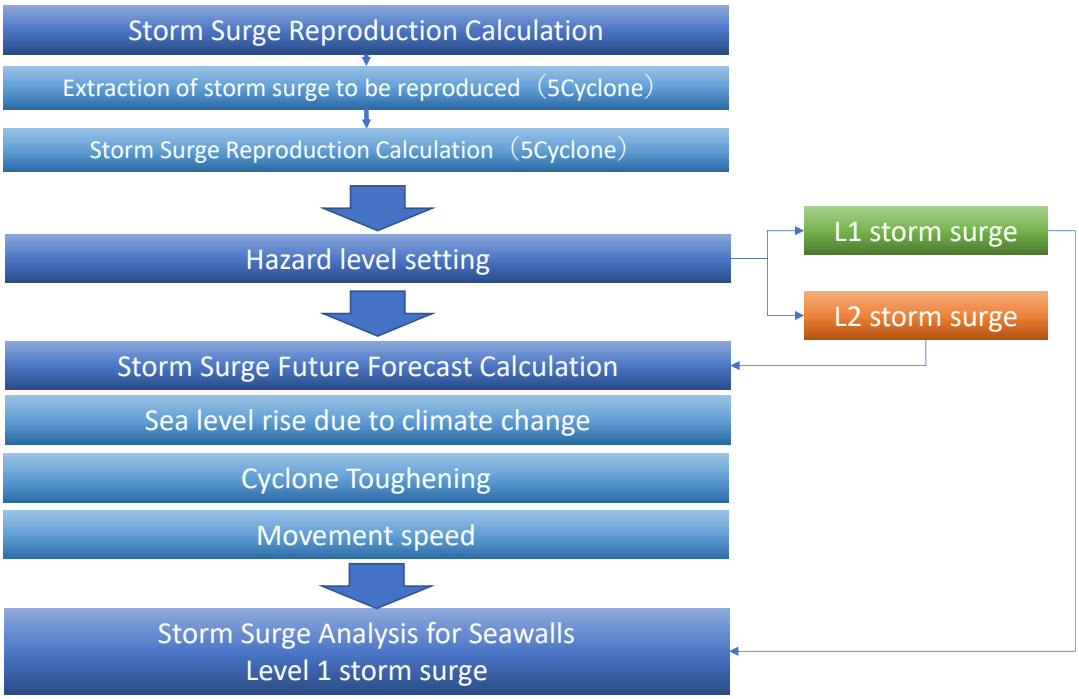

Source: JICA Study Team

Figure 3.1.1 Storm surge analysis flow

Table 3.1.1 Numerical analysis cases

Item	Cyclone	Sea Level	Structure	Minimun Region
Reproduction Calculation	2018 GITA	M.S.L.+0.00m	Existing Sea Wall	10m Tongatapu Island
	2020 Harold			
	2010 Lene			
	2009 Lin			
	1982 Isaac			
Examination of Probable Storm Surge Anomaly	1989 Gina	M.S.L.+0.00m	—	4050m
	1985 Drena			
	1982 Isaac			
	1981 Not named 86			
	1981 Not named 47			
	1981 Betsy			
	1979 Leslie			
	1977 Pat			
	1975 Betty			
	1973 Elenore			
	1972 Helen			
	1970 Gillian100			
	1970 Gillian98			
Future Forecast Calculation	Isaac Course Maximum swing radius course Aire Pressure: 930Hpa Constant Max Speed	M.S.L.+0.8m	Existing Sea Wall	10m Tongatapu Island
		M.S.L.+0.99m		
		M.S.L.+1.12m		
		M.S.L.+1.24m		
	Isaac Course Direct course Aire Pressure: 930Hpa Constant Max Speed	M.S.L.+0.8m	Existing Sea Wall	10m Tongatapu Island
		M.S.L.+0.99m		
		M.S.L.+1.12m		
		M.S.L.+1.24m		
Confirmation of seawall	1982 Isaac	M.S.L.+0.8m	Existing Sea Wall	10m Tongatapu Island
			Raised Sea Wall M.S.L.+3.0m	
		M.S.L.+1.12m	Existing Sea Wall	
			Raised Sea Wall M.S.L.+3.0m	

3.2 Storm surge reconstruction calculations

3.2.1 Analysis of tidal surge anomalies

At Nuku'alofa, tide level observation has been conducted since 1991. Therefore, it can be calculated the astronomical tide by performing harmonic decomposition on the tide level observation data from 1991 to 2021 and calculating the harmonic constant. In addition, the astronomical tide was subtracted from the measured tide level to calculate the storm surge tide level deviation. Figure 3.2.1. shows the calculated storm surge level deviation. Table 3.2.1. shows storm surge anomalies by climate change.

Among the cyclones hit Tonga from 1991 to 2021, Cyclone Gita hit February 2018 had the largest tidal anomalies.

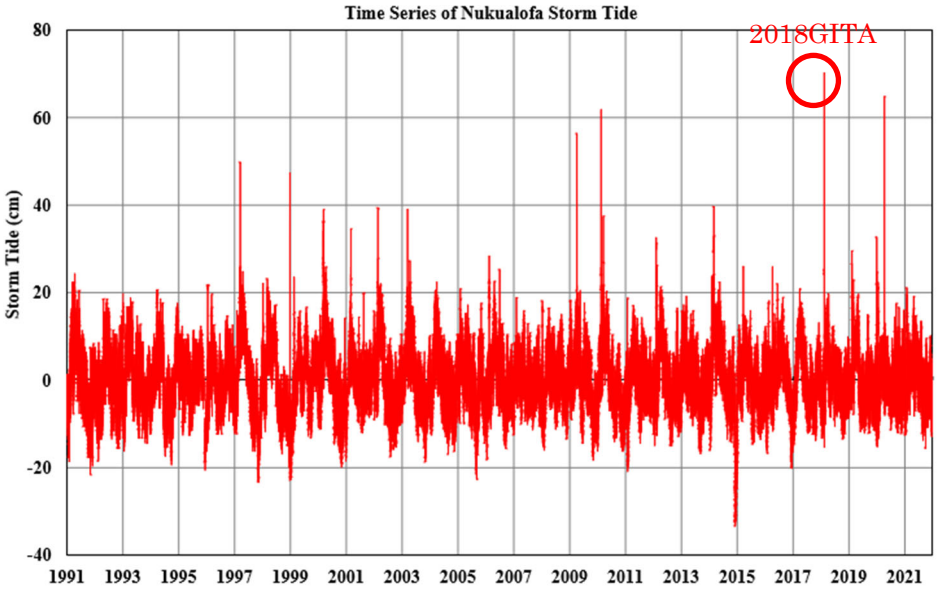

Source: JICA Study Team

Figure 3.2.1 Storm surge tide level deviations, Nuku'alofa, 1991-2021

Table 3.2.1 List of tide level anomalies by meteorological disturbance

Year	Month	Day	Hour	Storm surge deviation:cm	Rank
1997	3	8	15	25.78	
1997	3	10	4	25.78	
1997	3	14	9	25.78	
1997	3	16	8	49.78	5
1998	12	26	2	47.15	6
2000	3	9	9	39.00	10
2000	4	7	21	25.90	
2001	3	2	12	34.59	
2002	2	19	1	39.20	8
2002	2	20	14	27.80	
2003	3	13	5	39.03	9
2003	4	14	14	27.23	
2006	2	13	11	28.36	
2006	6	30	1	25.26	
2009	4	4	23	56.31	4
2010	2	15	9	61.70	3
2010	3	16	20	37.50	
2012	2	5	15	32.42	
2012	2	14	5	26.22	
2014	3	1	15	39.68	7
2015	3	21	18	25.97	
2016	4	5	14	25.93	
2018	2	12	11	70.19	1
2019	2	8	11	29.56	
2019	12	30	18	32.66	
2020	4	8	18	64.82	2

2018 GITA

Note:Ranked in descending order of tidal level anomaly, with the first three ranks coloured yellow.
Source: JICA Study Team

3.2.2 Analysis method

(1) Objective Cyclone for calculation

Table 3.2.2 shows the selection results of the cyclones selected for the reproducible calculation based on the analysis results of the storm surge level. Basically, those with large tide level deviations were selected from Table 3.2.1. Cyclone Isaac in 1982 was selected because of the serious damage caused by Tonga. IBTrACS[5] was used for basic information of the course of the cyclone used for numerical calculation.

Table 3.2.2 Selection of objective cyclone

Year	Month	Day	Hour	Storm Surge Deviation (cm)	Rank	Cyclone NAME	Reasons for Selection
2018	2	12	11	70.2	1	Gita	High storm surge deviation
2020	4	8	18	64.8	2	Harold	ditto
2010	2	15	9	61.7	3	Rene	ditto
2009	4	4	23	56.3	4	Lin	ditto
1982	3	3	-	No DATA	–	Isaac	Most Severe Damage

Source: JICA Study Team

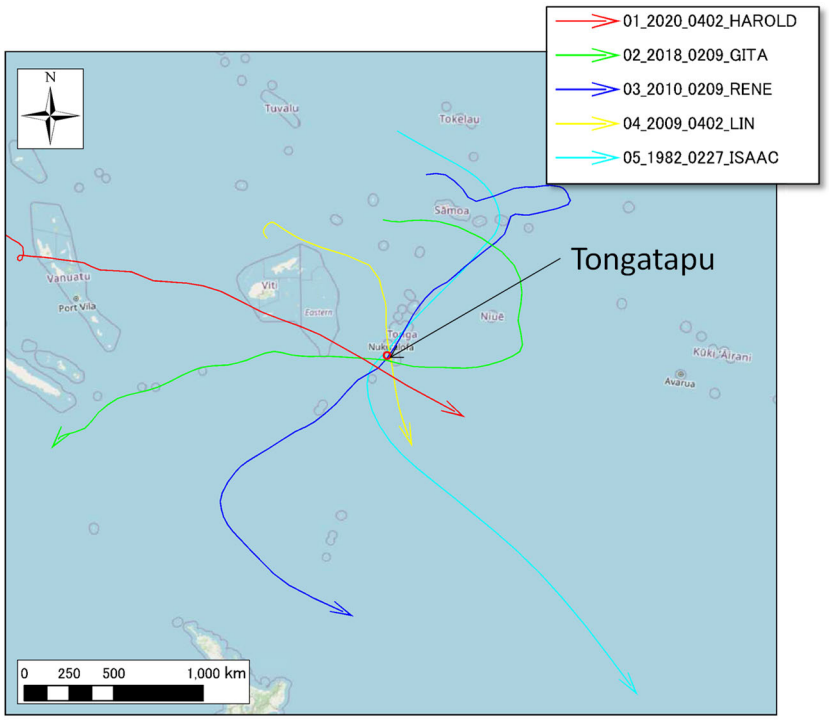

Source: JICA Study Team

Figure 3.2.2 Calculation Course of Cyclone

[5] IBTrACS(https://www.ncei.noaa.gov/products/international-best-track-archive)

(2) Numerical analysis method

The analysis method used for storm surge analysis was also STOC, as for tsunami analysis. Outline of STOC is shown in Figure 3.2.3.

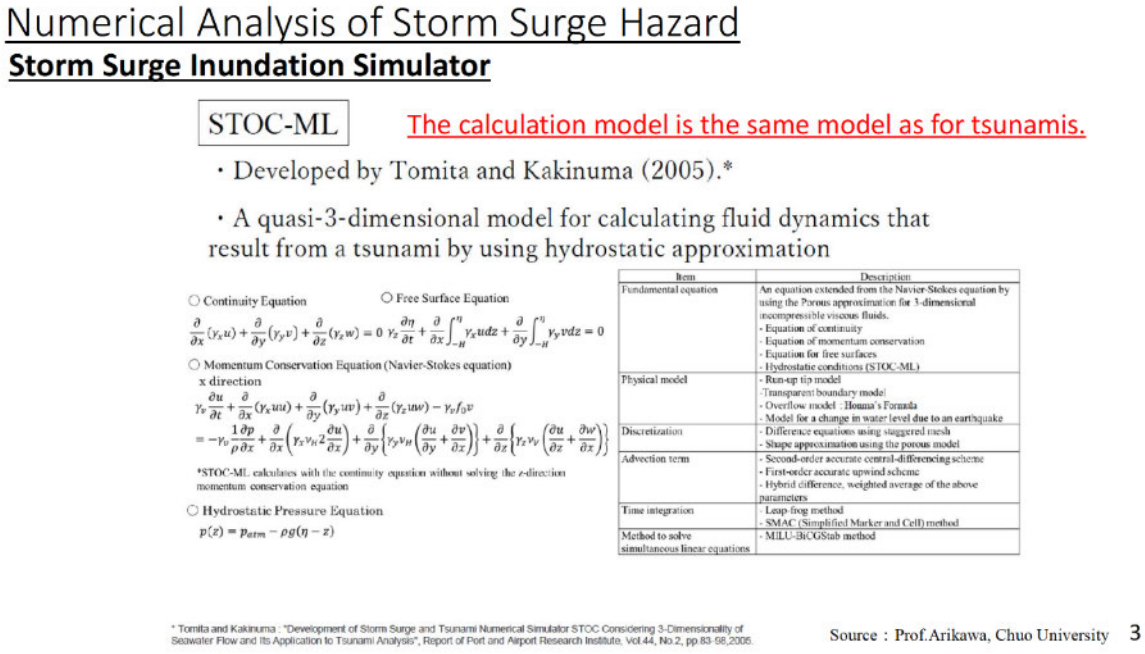

Source: Domestic Support Committee

Figure 3.2.3 Outline of STOC

(3) Numerical analysis conditions

A list of calculation conditions is shown in Table 3.2.3. In order to include the cyclone course in the calculation, the calculation was expanded from the tsunami. Figure 3.2.4 shows the topographic model used for storm surge calculation.

Table 3.2.3 Calculation conditions (storm surge)

Items	Calculation conditions
Composition of mesh	Region1(135sec (around4050m)mesh) : Cyclone development range
	Region2(45sec (around 1350m)mesh) : Cyclone development range
	Region3(15sec (around 450m)mesh) : Cyclone development range
	Region4(3sec (around 90m)mesh) : Tongatapu island
	Region5(1sec (around 30m)mesh) : Tongatapu island
	Region6(1/3sec (10m)mesh) : Tongtapu island
Analytical Method	STOC-ML(Tomita and Kakinuma, 2005)
Objective Cyclone	2018 Gita, 2020 Halord, 2010 Rene, 2009 Lin, 1982 Isac
Cyclone model	Cyclone central pressure・Cyclone cource: IBTrACS Cyclone pressure:Myers (1954)[6] Cyclone radius: Kato(2005)[7]

[6] Myers, V.A.(1954): Characteristics of U.S. hurricanes pertinent to levee design for lake Okeechabee, Fla., Hydrometeological. Rep., No. 32, Weather Bureau, U. S. Dept. Commerce, Wash D. C. 106p.

[7] Kato, F (2005); Study on Risk Assessment on Storm Surge Flood, TECHNICAL NOTE of National Institute for Land and Infrastructure Management, No.275

Items	Calculation conditions
Geological Conditions	Based on topographic data from Tohoku University
Tide level	M.S.L.0m
Calculation Time	Calculated according to the start and end times of each cyclone
	Time resolution：min0.01sec
Others	Structure measures：Existing level

Source: JICA Study Team

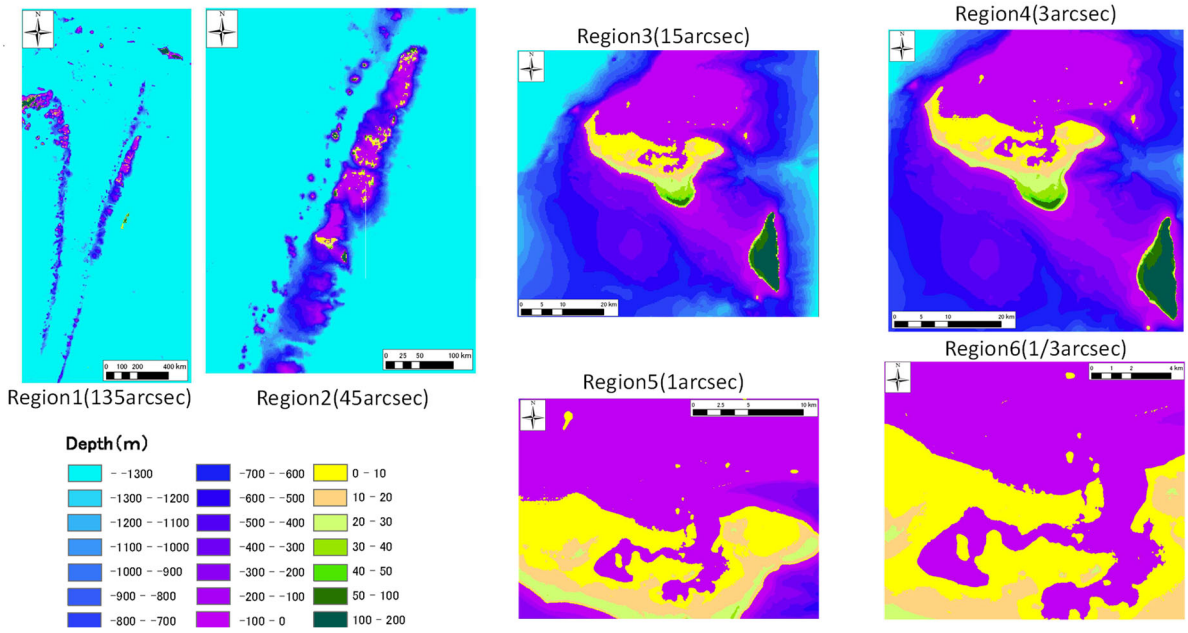

Source: JICA Study Team

Figure 3.2.4 Calculation results (storm surge)

(4) Numerical analysis cases

Analytical case is shown below.

Table 3.2.4 Numerical Analysis

Year	Name	Calculation period	
		Start	End
2018	Gita	2018/02/11 18:00	2018/02/12 18:00
2020	Harold	2020/04/08 00:00	2020/04/09 00:00
2010	Renee	2010/02/14 18:00	2010/02/15 18:00
2009	Lin	2009/04/04 06:00	2009/04/05 06:00
1982	Isaac	1982/03/02 09:00	1982/03/03 09:00

Source: JICA Study Team

3.2.3 Analysis results

(1) Reproduced Calculation Results for each cyclone

A summary of the analysis results for each cyclone is shown in Figure 3.2.5 to Figure 3.2.9

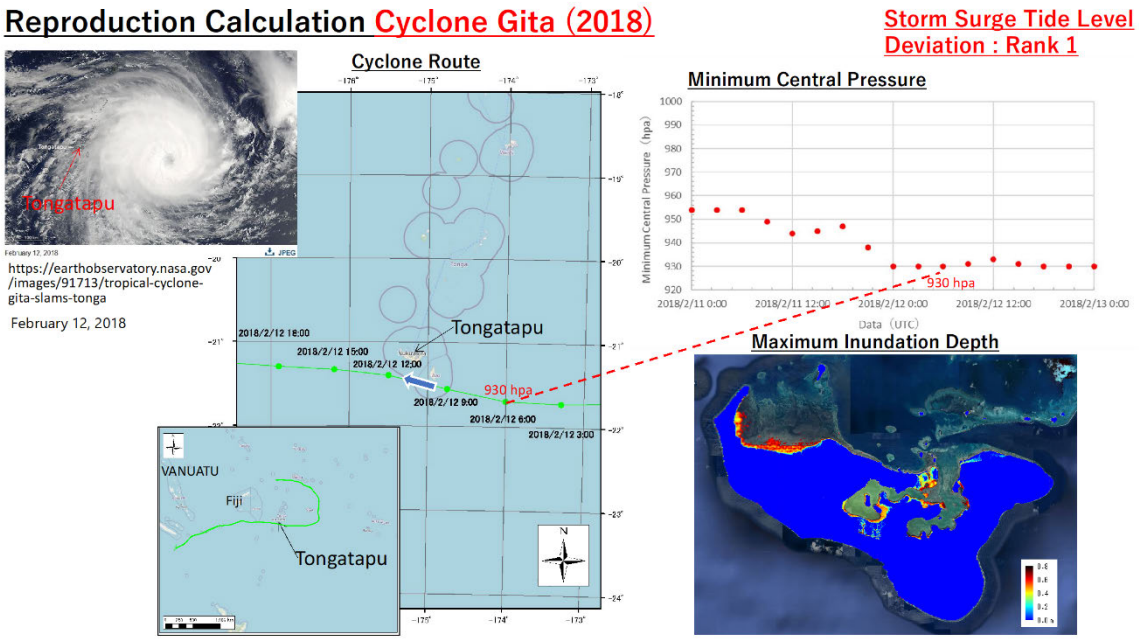

Source: JICA Study Team

Figure 3.2.5 Reproduced Calculation Results for Cyclone Gita (2018)

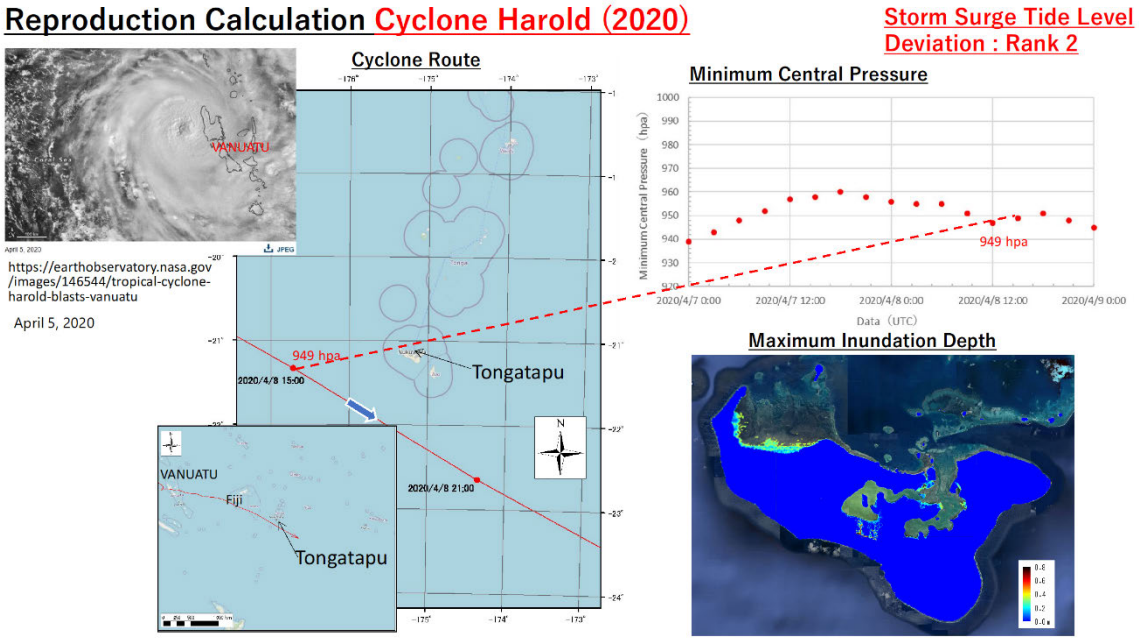

Source: JICA Study Team

Figure 3.2.6 Reproduction calculation of Cyclone Harold (2020)

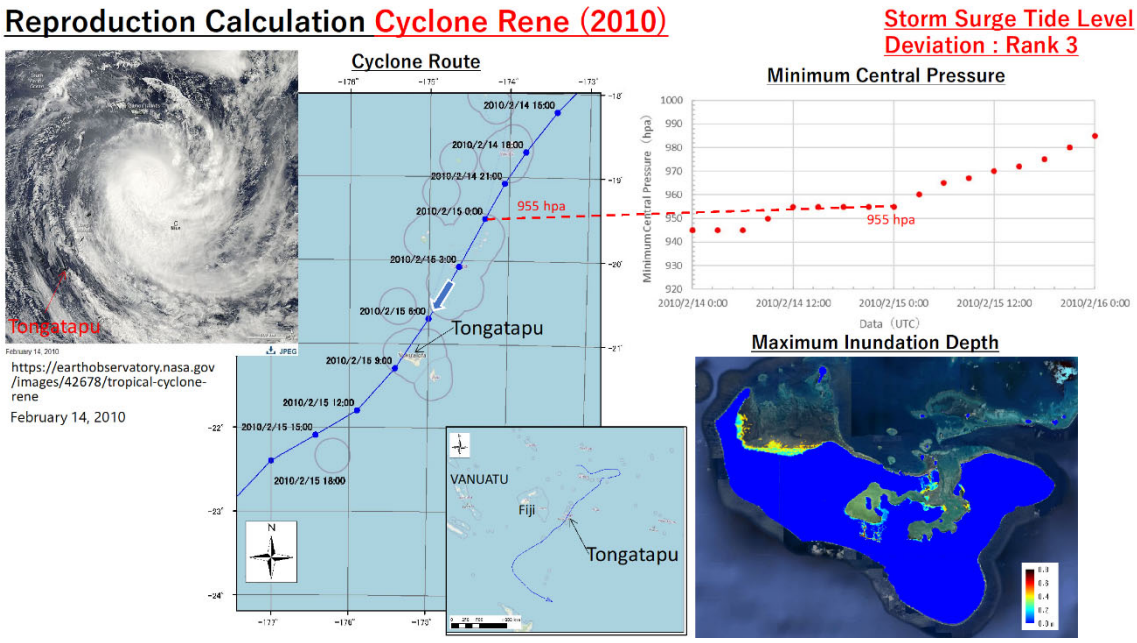

Source: JICA Study Team

Figure 3.2.7 Reproduction calculation of Cyclone Rene (2010)

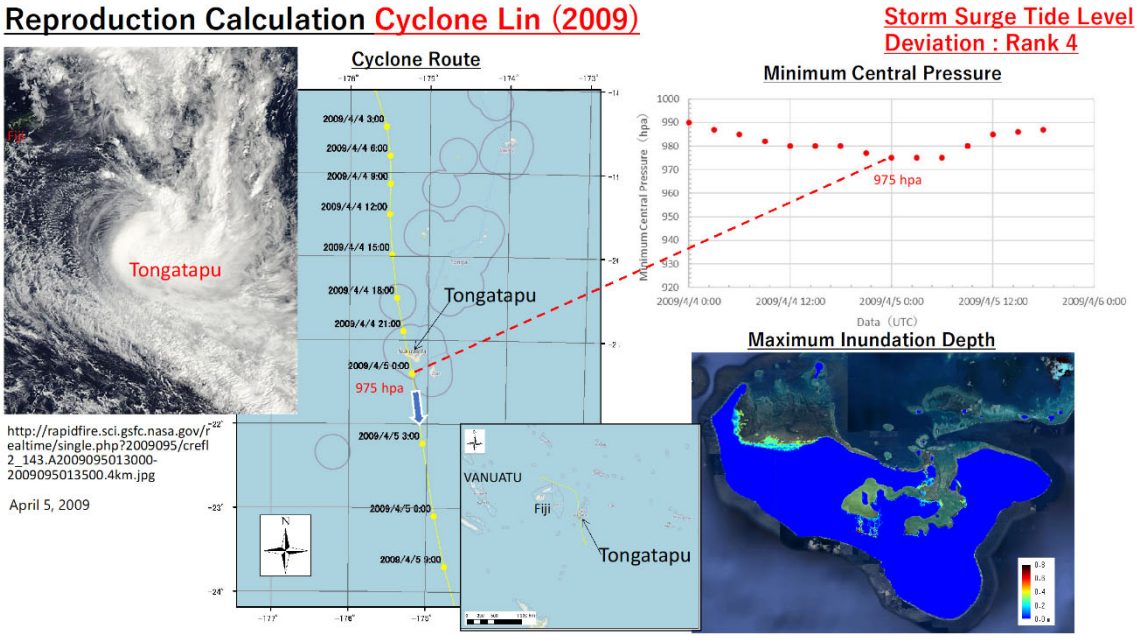

Source: JICA Study Team

Figure 3.2.8 Reproduction results for Cyclone Lin (2009)

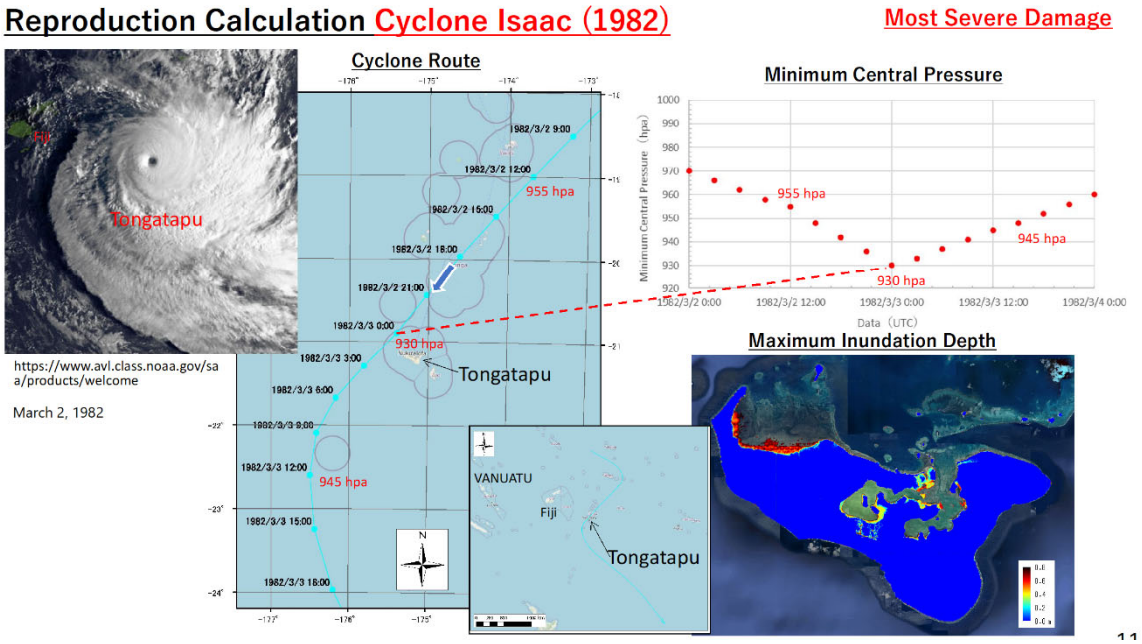

Source: JICA Study Team

Figure 3.2.9 Reproducibility Calculation Results for Cyclone Isaac (1982)

3.3 Assessment of reproducibility

3.3.1 Examination of reproducibility

(1) Gita

There are three types of cyclone path information for Gita: WMO, USA and NADI, and calculations using NADI showed good agreement with observed values without modification.

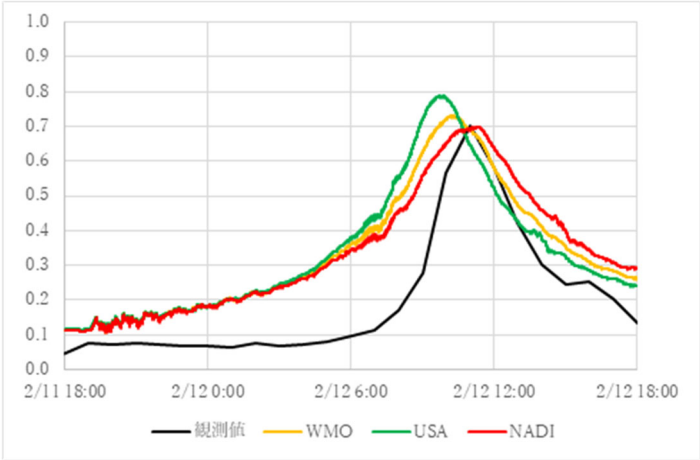

Source: JICA Study Team

Figure 3.3.1 Reproduced Calculation Results for Cyclone Gita (2018)

(2) Harold

As Harold passes away from the study point, the tidal deviation was increased by moving the route closer to the study point. Good agreement was obtained by changing the route to 80 km closer to the study point.

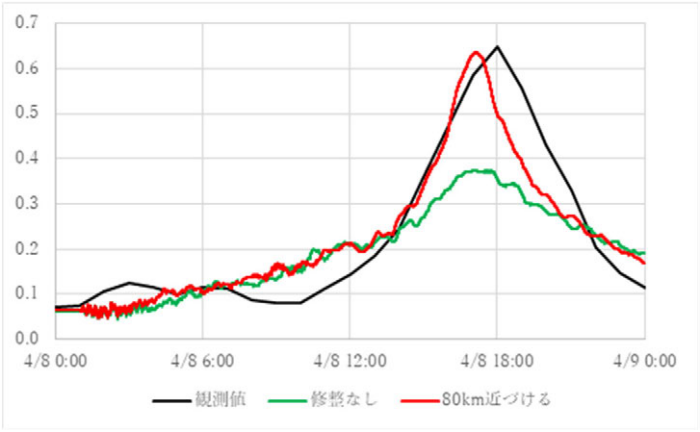

Source: JICA Study Team

Figure 3.3.2 Reproduced Calculation Results for Cyclone Harold (2020)

(3) Renai

As Renee passed near the study point, changing its path did not increase the tidal anomaly, and increasing the barometric depth brought it closer to the observed value. A good agreement was obtained by increasing the barometric depth by a factor of 1.31.

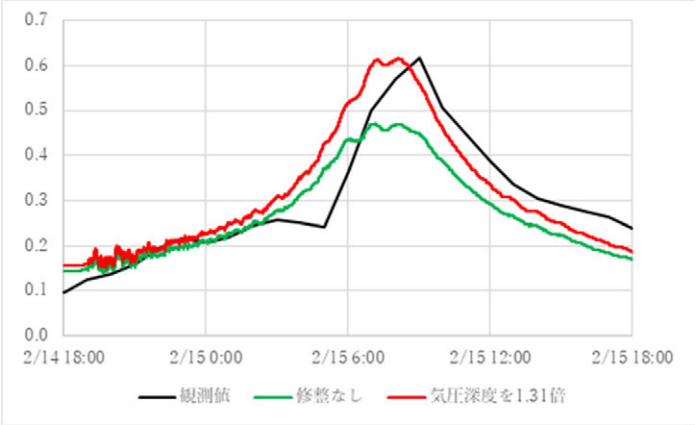

Source: JICA Study Team

Figure 3.3.3 Reproduced Cyclone Renee (2010) calculation results

(4) Lin.

As Lynn passes near the study point, changing its path did not increase the tidal anomaly, and increasing the barometric depth brought it closer to the observed value. A good agreement was obtained by increasing the barometric depth by a factor of 1.55.

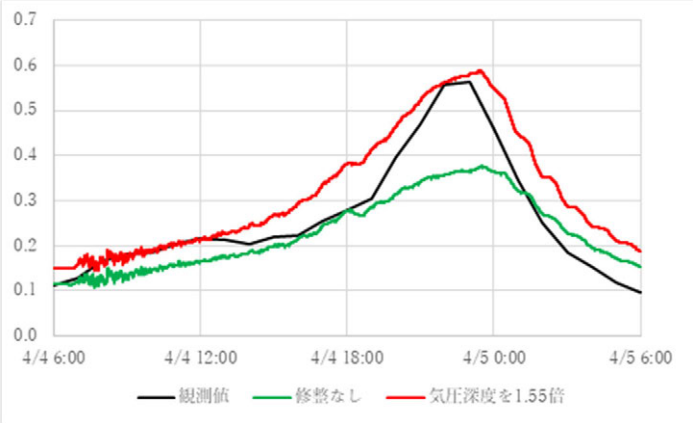

Source: JICA Study Team

Figure 3.3.4 Cyclone Lynn (2009) reconstructed calculation results.

(5) Isaacs

As Isaac has no observed tidal level anomalies.Max inundation depth distribution diagram was prepared and compared with the B.Max inundation depth distribution diagram of Domestic Support Committee. For this calculation only, the tide level was assumed to be 0.8 m.

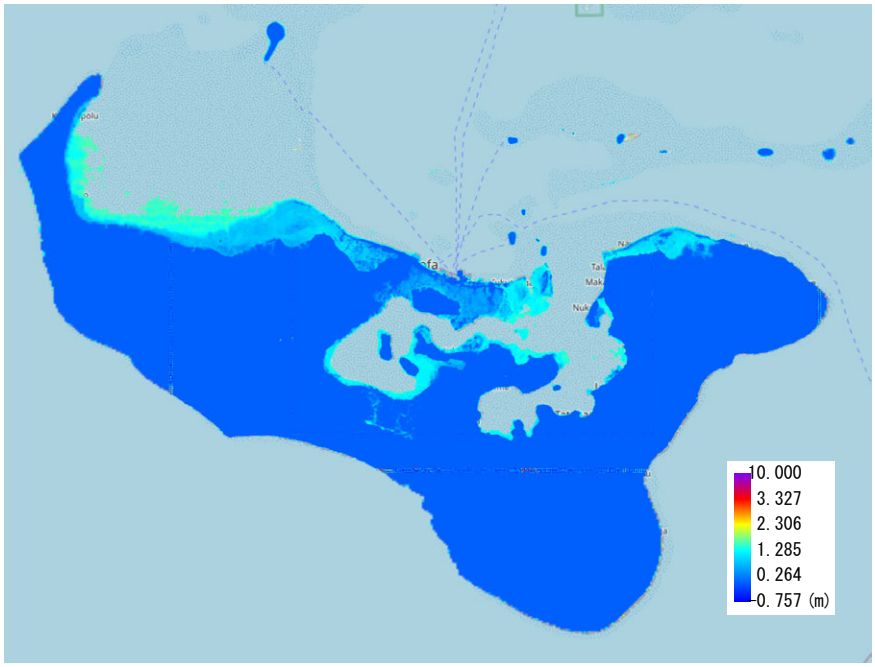

Source: JICA Study Team

Figure 3.3.5 Results of the Cyclone Isaac (1982) reconstruction calculations.

3.3.2 Characteristics of cyclones caused severe conditions in Nuku'alofa.

Figure 3.3.6. shows a comparison of the courses of cyclones that have caused large storm surges in Nuku'alofa. The cyclones generate large storm surges in Nuku'alofa are listed below.

In general, storm surges are high when a cyclone passes near Tongatapu Island. The wind in the same direction as the cyclone will be strong, so if Tongatapu Island is located on the left side of the cyclone, the wind is strong and the storm surge is high.

Each cyclone has caused a remarkable storm surge in passes directly above or very close to Tongatapu Island. Tongatapu Island is located on the left side of the cyclone's direction of travel (4 cyclones out of 5 reproduced cyclones).

However, Cyclone Gita (2018) has a different course from other cyclones with large storm surges, and Tongatapu Island is located on the right side of the direction of travel. Because the cyclone was huge (minimum atmospheric pressure of 930 hPa), and that the cyclone passed slowly over the south side of Tongatapu Island, and strong winds blew from the north side of Tongatapu Island to the south side for a long time.

As another example, Cyclone Harold is the wind became stronger and the storm surge became higher because Cyclone Harold moved faster.

Taking all of the above into consideration, Cyclone Isaac (1982), which caused enormous damage, is considered to be the typical example of the worst course for Tongatapu Island (Nuku'alofa).

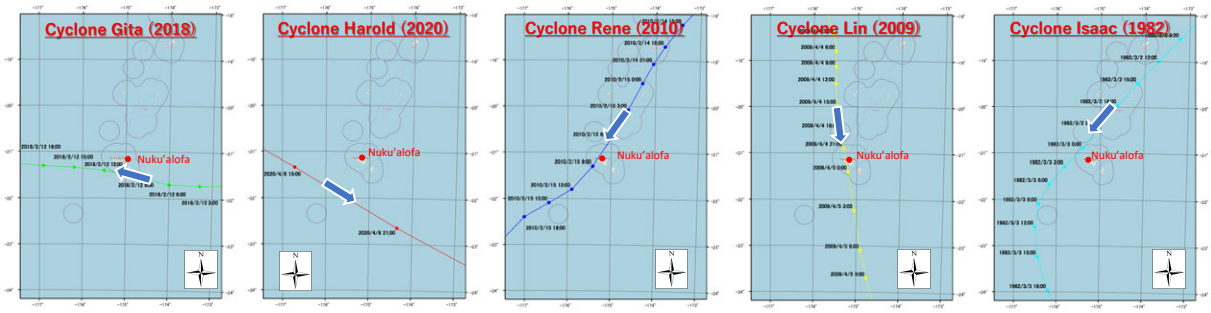

Source: JICA Study Team

Figure 3.3.6 Comparison of the Courses of the Cyclones

3.4 Simplified Storm Surge Calculations and Probable Storm Surge Anomalies

3.4.1 Examination of Probable Storm Surge Anomaly Setting Target cCyclones

The tide level observation period on Tongatapu Island (Nuku'alofa) has been 30 years since 1991. It is rather short as a statistical period for calculating probable tide level anomalies. Therefore, cyclones are affected Tongatapu Island before 1991 will be extracted, and the data for statistical analysis will be supplemented by calculating the anomalies of storm surge levels.

As for the extraction method, IBTrACS is used to extract cyclones within a 500 km radius on Nuku'alofa on Tongatapu Island. Tide level observations were not conducted in Tonga the IBTrACS data, was excluded. The extracted cyclones are shown inTable 3.4.1 and Figure 3.4.1.

Table 3.4.1 Cyclone extracted for Probable Tide Level Deviation Calculation(1947～1990)

Cyclone Name	Central Pressure (hPa)	Cyclone Radius (km)
1989GINA	995	154
1985DRENA	993	151
1982ISAAC	944	78
1981NOT_NAMED_86	997	156
1981NOT_NAMED_47	997	157
1981BETSY	997	157
1979LESLIE	989	144
1977PAT	989	144
1975BETTY	984	136
1973ELENORE	990	145
1972NOT_NAMED	997	157
1970HELEN	997	157
1970GILLIAN_100	980	129
1970GILLIAN_98	987	141

Source: JICA Study Team

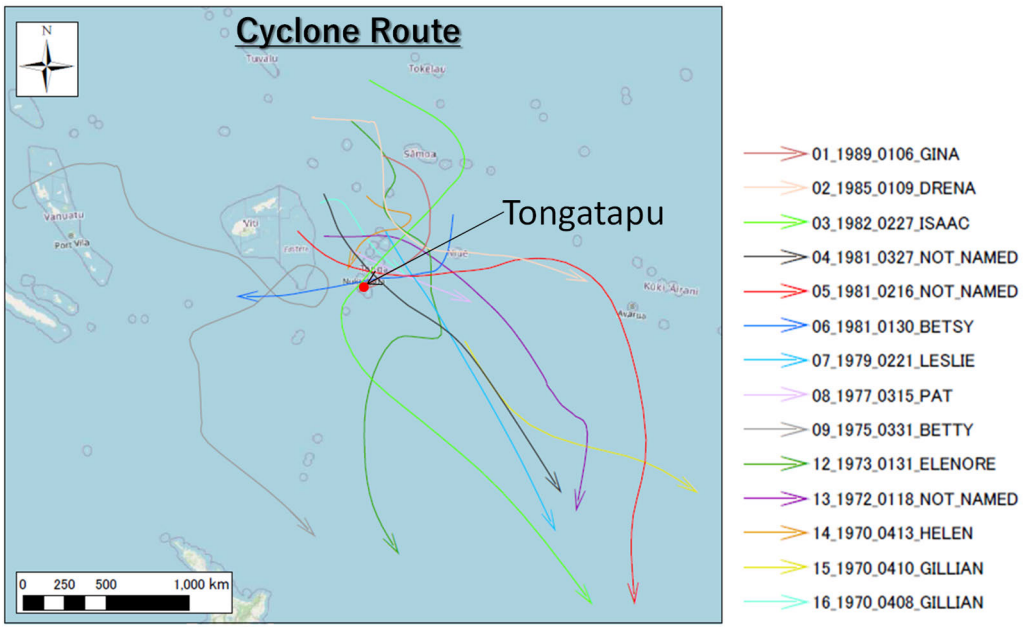

Source: JICA Study Team

Figure 3.4.1 Cyclone Course Extracted for Probabilistic Tide Level Deviation Calculation (1947～1990)

1) Calculation of the tidal height anomaly for each cyclone

Numerical calculations are carried out for the cyclones extracted in the previous section. For the calculation conditions, the calculations were carried out in a large domain with the aim of obtaining only the tidal anomalies. The calculation conditions and calculation results (storm surge anomalies) are shown below.

Table 3.4.1 Calculation Conditions (For Probabilistic Tide-Level Deviation Calculation)

Items	Calculation conditions
Mesh Compositions	Region1(135 sec (around 4050m)mesh)：Cyclone development area
Analysis method	STOC-ML(Tomita and Kakinuma, 2005)
Objective cyclone	1989GINA,1985DRENA, 1982ISAAC, 1981NOT_NAMED_86 ,1981NOT_NAMED_47 1981BETSY, 1979LESLIE, 1977PAT, 1975BETTY, 1973ELENORE, 1972NOT_NAMED 1970HELEN, 1970GILLIAN_100, 1970GILLIAN_98
Cyclone Model	Cyclone central area pressure・Cyclone course: IBTrACS Pressure dis: Myers (1954) Cyclone radius: Kato(2005)
Geological Conditions	Base on Tohoku University data
Tide conditions	M.S.L.+0m
Calculation Time	Calculated according to the start and end times of each cyclone
	Time resolution: Minimum 0.01sec
Others	Structure：Existing seawall

Source: JICA Study Team

Table 3.4.2 Calculated Tidal Deviation of each Cyclone

Year	Name of Cyclone	Max tidal anomaly at Nuku'alofa (m)
1970	Gillian	0.06
1970	Gillian	0.13
1970	Helen	0.09
1972	Not Named	0.06
1973	Elenore	0.08
1975	Betty	0.14
1977	Pat	0.13
1979	Leslie	0.08
1981	Betsy	0.16
1981	Not named	0.12
1981	Not named	0.13
1982	Isaac	0.70
1985	Drena	0.07
1989	Gina	0.16

Source: JICA Study Team

2) Calculation of Probable Storm Surge Anomaly

Probable storm surge anomalies were calculated using the tidal anomalies from 1947 to 1990 calculated in the previous section and the tidal anomalies calculated from the tidal observation data from 1991 to 2021 as extreme value data. The extreme value data used are shown in Table 3.4.4. Table 3.4.5 and Figure 3.4.2. show the calculation results of probable tide level deviation. The probable tidal anomaly was 80 cm with a probability of 100 years.

Table 3.4.3 Extreme Value Statistics Input

No.	Year	Max Storm surge deviation at Nuku'alofa (m)	No.	Year	Max Storm surge deviation at Nuku'alofa (m)
1	1970	0.13	22	2002	0.39
2	1972	0.06	23	2003	0.39
3	1973	0.08	24	2004	0.23
4	1975	0.14	25	2005	0.21
5	1977	0.13	26	2006	0.28
6	1979	0.08	27	2007	0.19
7	1981	0.16	28	2008	0.18
8	1982	0.70	29	2009	0.56
9	1985	0.07	30	2010	0.62
10	1989	0.16	31	2011	0.19
11	1991	0.24	32	2012	0.32
12	1992	0.19	33	2013	0.19
13	1993	0.20	34	2014	0.40
14	1994	0.21	35	2015	0.26
15	1995	0.12	36	2016	0.26
16	1996	0.22	37	2017	0.21
17	1997	0.50	38	2018	0.70
18	1998	0.47	39	2019	0.33
19	1999	0.23	40	2020	0.65
20	2000	0.39	41	2021	0.21
21	2001	0.35			

Source: JICA Study Team

Table 3.4.4 Extreme Value Statistics Input (Probable storm surge level deviation)

Recurrence period	Probable Storm Surge Anomaly at Nuku'alofa (m)
10 years	0.49
20 years	0.59
30 years	0.64
50 years	0.71
100 years	0.80

Source: JICA Study Team

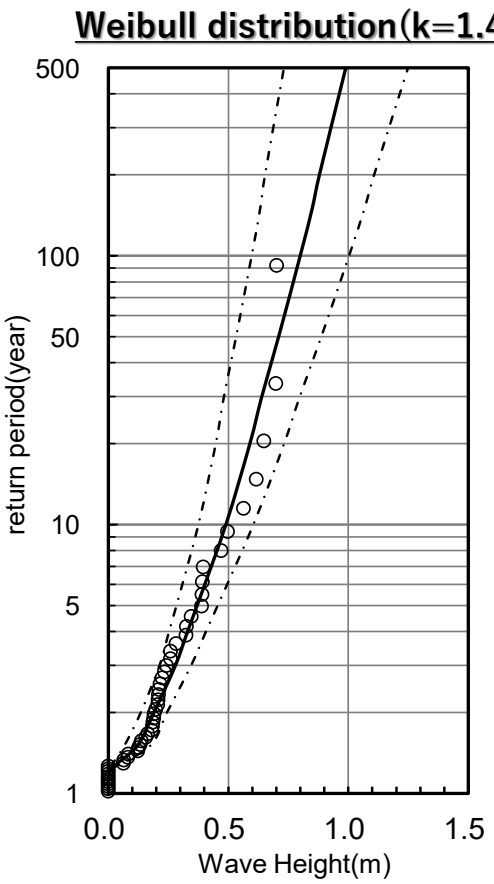

Source: JICA Study Team

Figure 3.4.2 Extreme value statistics result graph (probability storm surge tide level deviation)

3.5 Storm surge future forecasting calculations

3.5.1 Hazard level study

(1) Hazard Level of Storm Surge

Over the last 30 years (1991-2021) with observation records, the anomaly of storm surge levels due to cyclones was about 0.7m. On the other hand, the extreme value of statistical results of the storm surge deviation is calculated in even the 100-year probability deviation considering the H.W.L. Based on the results of this study, it is considered appropriate to set 100-year probability tide level deviations for hazard level 1 storm surges, which are dealt with by means of structural measures.

It should be noted that the required height of the embankment needs to consider not only the tide level but also the wave.

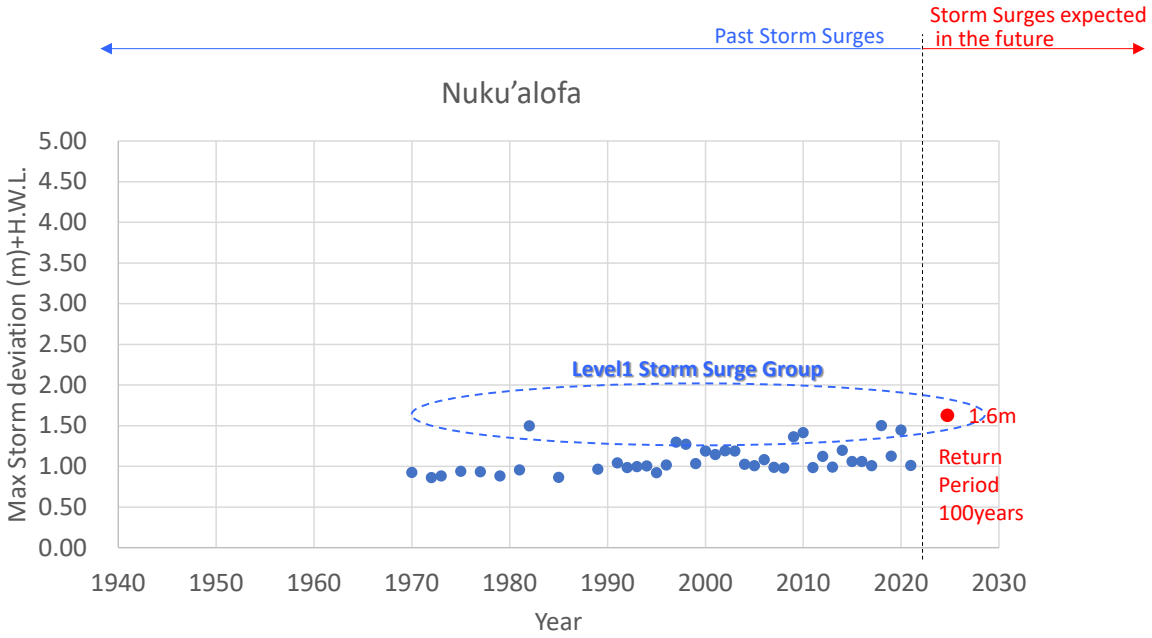

Source: JICA Study Team

Figure 3.5.1 Classification of storm surge hazard levels in Nukualofa

Table 3.5.1 Probable storm surge anomalies at Nuku'alofa during H.W.L.

Recurrence period	Probable Storm Surge Anomaly during H.W.L at Nuku'alofa (m)
10 years	0.49
20 years	0.59
30 years	0.64
50 years	0.71
100 years	0.80

Source: JICA Study Team

(2) Comparison between the design tide level of seawall and the tide level at hazard level 1

The required height of the existing seawall is set by Isaac (1982) as a design external force. It is set in consideration of waves, tide level and amount of water level rise on the reef. The outline of the study results is as follows.

Table 3.5.2 Summary of design parameters of existing seawall

Item	Set value	Rationale, etc.
Design offshore wave height	H0=11.6m	1982Isaac Willson method estimate
Design offshore wave period	T0=12.6s	−
Design offshore wave direction	NE (north-east) -	−
Wave height in front of embankment	H1/3=1.7～5.4m	−
Design tide level	H.W.L. + storm surge deviation L.W.L.+1.5+0.2=L.W.L.+1.7m =M.S.L.+1.0m	−
Water level rise above the reef	0.21～0.9m	−
Required seawall top height	L.W.L.+2.95～3.00m Example: design tide level + rise in water level above reef + required height of allowable overtopping flow ＝1.7+0.9+0.35=2.95m	Set to meet the allowable overtopping flow
Design seawall top edge height	L.W.L.+2.3～3.3m (M.S.L.+1.6～2.6m)	−

Source: JICA Study Team

If the L1 storm surge water level is assumed to be 100 years, it will be necessary to add 0.6 m to the design of the existing seawall. Since the required seawall height is determined based on the overtopping discharge, it is necessary to recalculate it.

3.5.2 Storm surge and tsunami study for Hazard Level 2

(1) Establishment of Hazard Level 2 storm surge conditions

The storm surge analysis for Hazard Level 2 is based on the course and conditions of the 1982 Isaac, which is considered to be the largest storm surge in the past, and further assumes the case of adverse conditions. The following conditions are assumed;

- The central pressure of the cyclone is assumed to be 930 Hpa, the minimum pressure at the time of Cyclone Isaac's approach to Tongatapu Island, and constant (930 Hpa) throughout the calculation period.
- The course is Cyclone Isaac's course, with the course shifted west from the centre of Tongatapu Island by the Max turning radius and winds are strongest on Tongatapu Island (Max turning radius course, Figure 3.5.2).

- Based on the situation of past cyclones with high storm surges passing close to Tongatapu Island (e.g. Cyclone Renee in 2010 and Cyclone Lynn in 2009), and the suction effect of the drop in pressure of more dominant than the blow-in effect of the wind, a course is set the centre of the cyclone A course and the centre of the cyclone passes through the centre of Tongatapu Island (straight-line course, Figure 3.5.2).
- As higher cyclone speeds result in higher wind speeds in the direction of travel speed and higher storm surges (e.g. 2020 Cyclone Harold), the cyclone speed is set to the Max (constant) speed of movement of 2020 Cyclone Harold.

The tidal conditions are set to H.W.L. (M.S.L. + 0.8 m) as adverse conditions. The calculation conditions set based on the above are shown in Table 3.2.19.

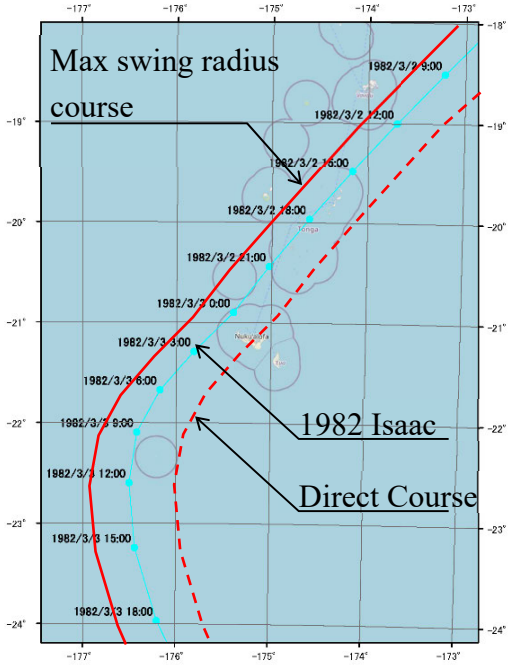

Source: JICA Study Team

Figure 3.5.2 Assumed course of the largest class of cyclone

Table 3.5.3 Calculation conditions (Hazard Level 2 storm surge)

Items	Calculation Conditions
Mesh Compositions	Region1(135sec (around 4050m)mesh)：Cyclone development range
	Region2(45sec (around 1350m)mesh)：Cyclone development range
	Region3(15sec (around 450m)mesh)：Cyclone development range
	Region4(3sec (around 90m)mesh)：Tongatapu island
	Region5(1sec (約 30m)mesh)：Tongatapu island
	Region6(1/3sec (約 10m)mesh)：Tongatapu island
Analytical method	STOC-ML(Tomita and Kakinuma, 2005)
Objective cyclone course	Same course as 2018 Zita but paralleled ・Max turning radius course ・Straight course

Items	Calculation Conditions
Cyclone Model	Cyclone central pressure: 930Hpa (constant) Cyclone speed: Harold's Max speed: 56km/h (constant) Pressure distribution: Myers (1954) Cyclone Radius: Kato (2005)
Geological conditions	Topographic data from Tohoku University
Tide conditions	M.S.L.+0.8m
Calculation time	Calculated according to the start and end times of cyclones
	time resolution：time resolution 0.01sec
Others	Structure：Exesting Seawall

Source: JICA Study Team

(2) Calculation results (hazard level 2 storm surge)

Figure 3.5.4 toFigure 3.5.5 show the storm surge inundation areas calculated with the above settings. As a result, the inundation range and depth were larger in the directly above course. Because Tongatapu does not have a topographically high raised area, the storm surge water level will not high due to storm surges (for example, a V-shaped bay).

However, in reality, not only storm surges but also high waves are involved, so caution is required for the Max gyration radius course, which tends to have larger wave heights.

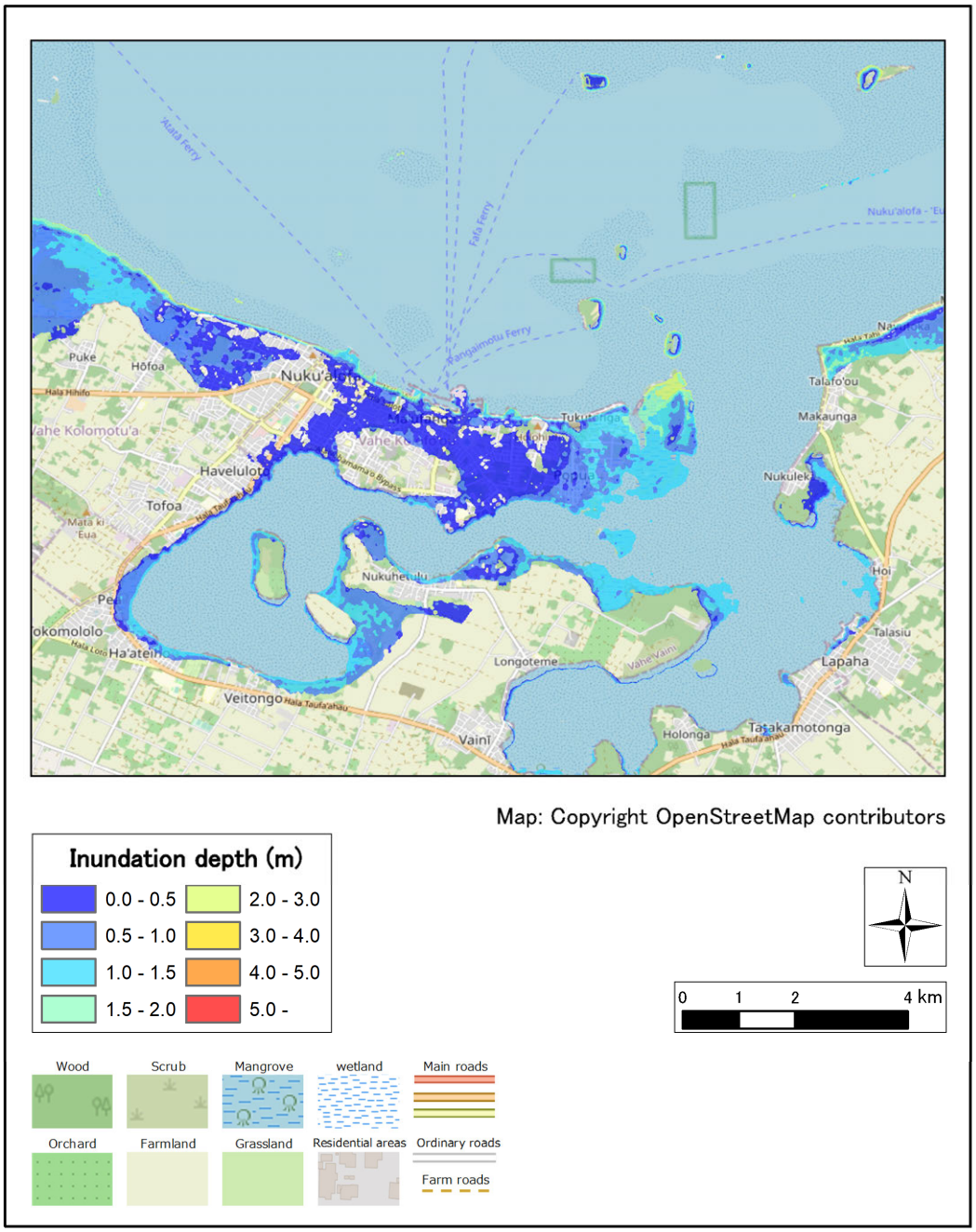

Source: JICA Study Team

Figure 3.5.3 Max Inudation Depth (Storm Surge Hazard Level 2: Max Swing Radius Course)

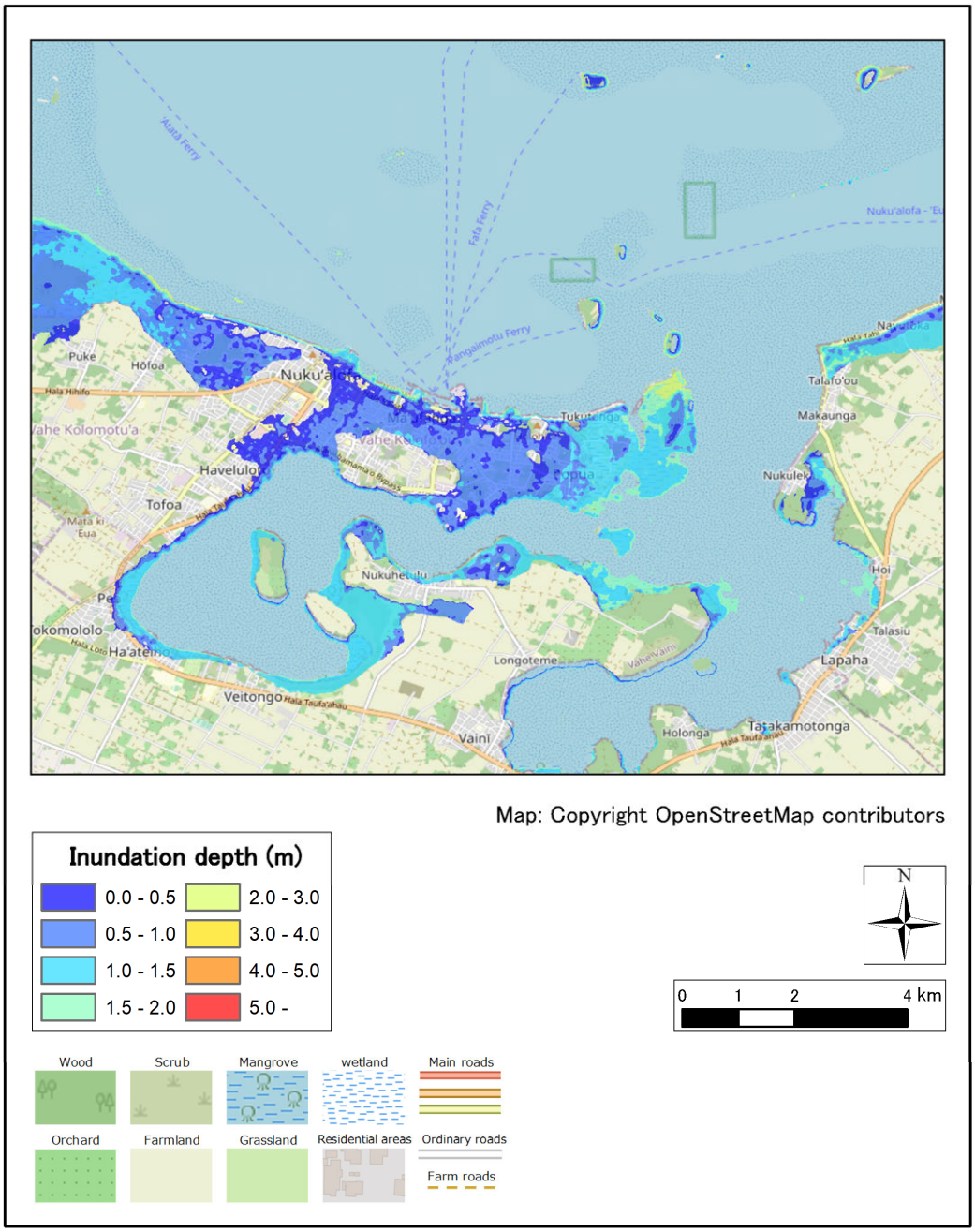

Source: JICA Study Team

Figure 3.5.4 Max Inudation Depth (Storm Surge Hazard Level 2: right above island Course)

(3) Impact of sea level rise due to climate change

Island nations like Tonga would be greatly affected by future climate change-induced sea level rise, such as increased flood damage. Therefore, based on the IPCC Sixth Assessment Report, a hazard level 2 scenario based on the amount of sea level rise in Tonga in SSP1-2-6 (scenario to keep temperature rise below 2°C in sustainable development) to consider.

The amount of sea level rise in Tonga under the SSP1-2-6 scenario is shown below. The table below shows the H.W.L. settings during sea level rise. Flooding at hazard level 2 storm surge was examined under the tide level conditions shown in the table below. The calculation conditions other than the tide level conditions are the same as those in Table 3.5.4.

The calculation results are shown in Figure 3.5.6 to Figure 3.5.7. As a matter of course, the inundation area and depth increased.

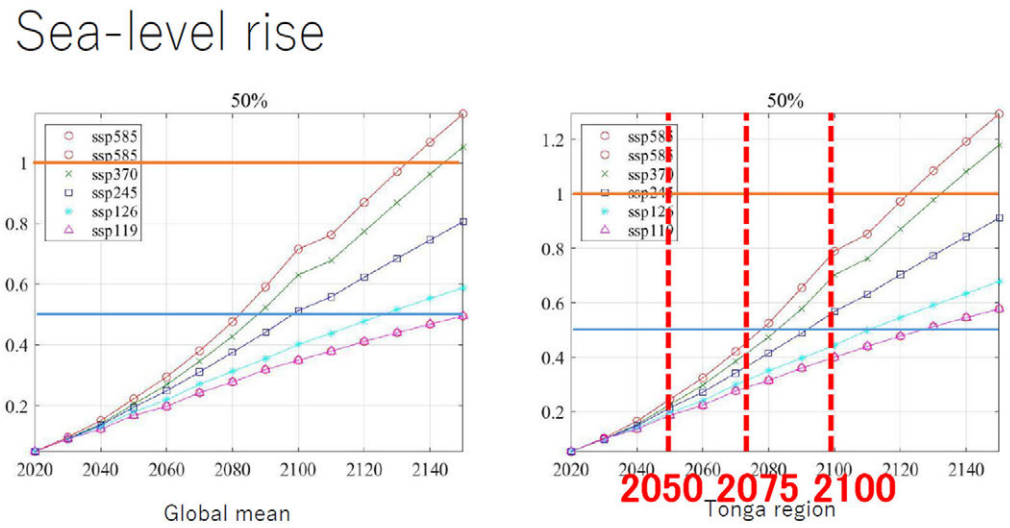

Source: Based on Domestic Support Committee, JICA Study Team made

Figure 3.5.5 Amount of sea level rise in each scenario

Table 3.5.4 H.W.L. during sea level rise at Nuku'alofa (SSP1-2-6)

Year	**H.W.L.** (M.S.L.+m)	Sea Level Rise(m)	Calculation Tide Level (M.S.L.+m)
2020	0.8	0.00	0.8
2050	0.8	0.19	0.99
2075	0.8	0.32	1.12
2100	0.8	0.44	1.24

Source: JICA Study Team

SSP1-2-6(2℃ increase scenario)

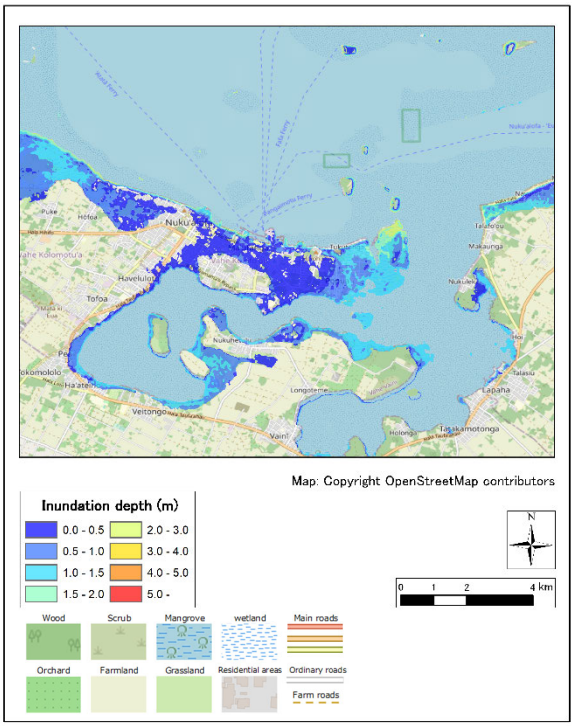

2020 H.W.L. : M.S.L.+0.8m

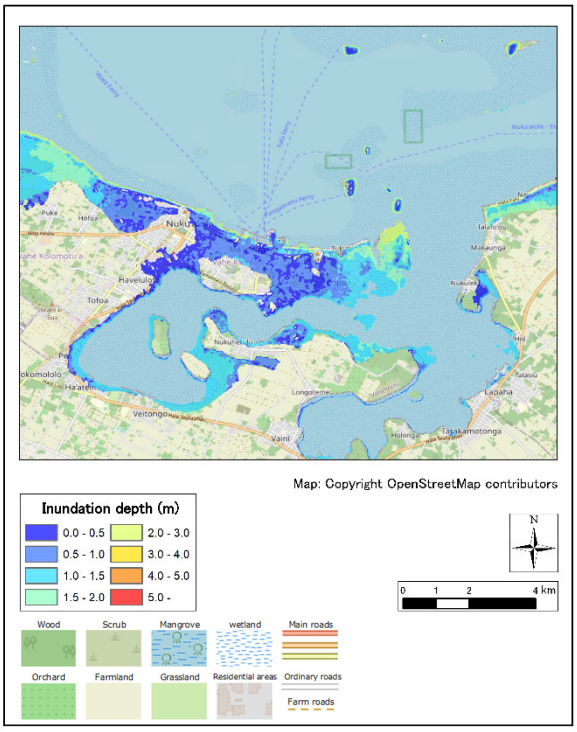

2050 H.W.L. : M.S.L.+0.99m

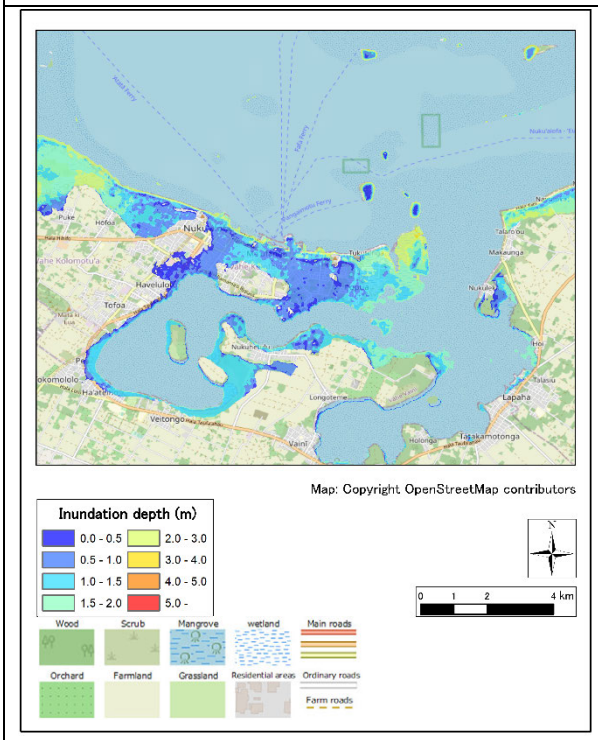

2075 H.W.L. : M.S.L.+1.12m

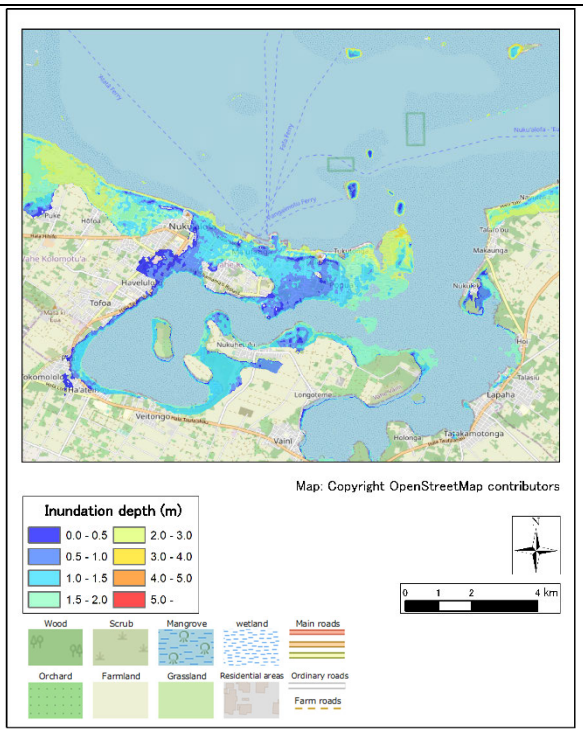

2100 H.W.L. : M.S.L.+1.24m

Source: JICA Study Team

Figure 3.5.6 Estimated inundation in case of sea level rises (storm surge hazard level 2: Max swing radius course)

SSP1-2-6(2℃ increase scenario)

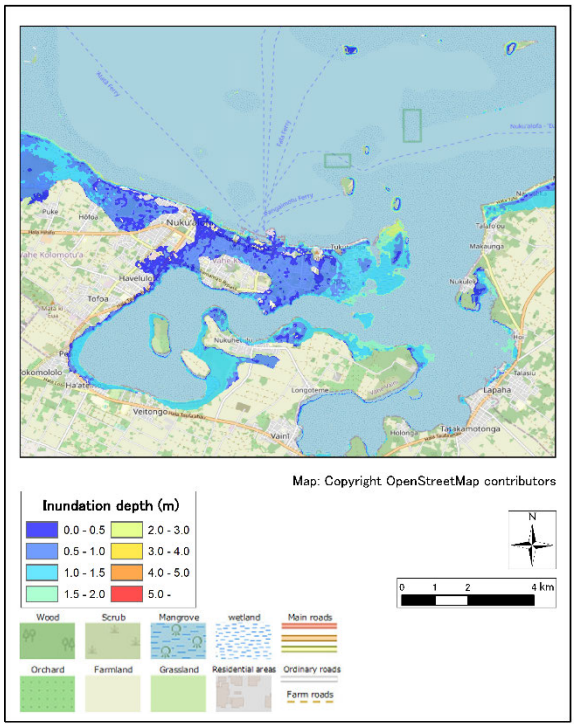

2020 H.W.L. : M.S.L.+0.8m

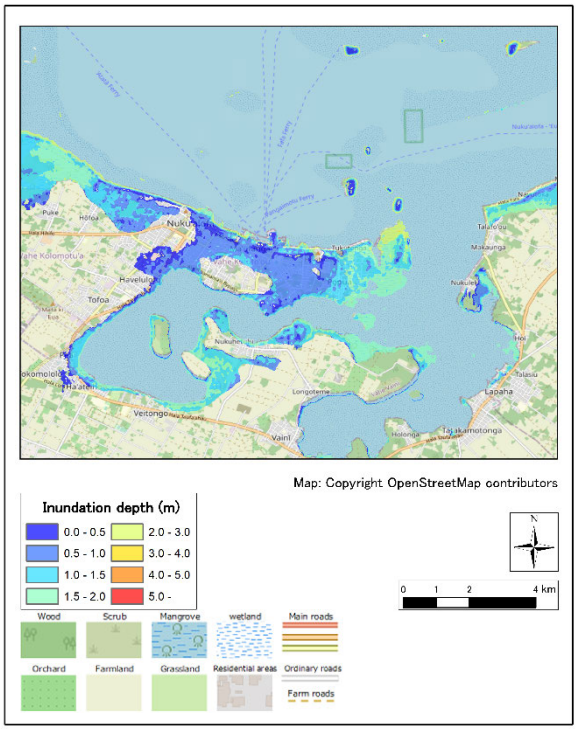

2050 H.W.L. : M.S.L.+0.99m

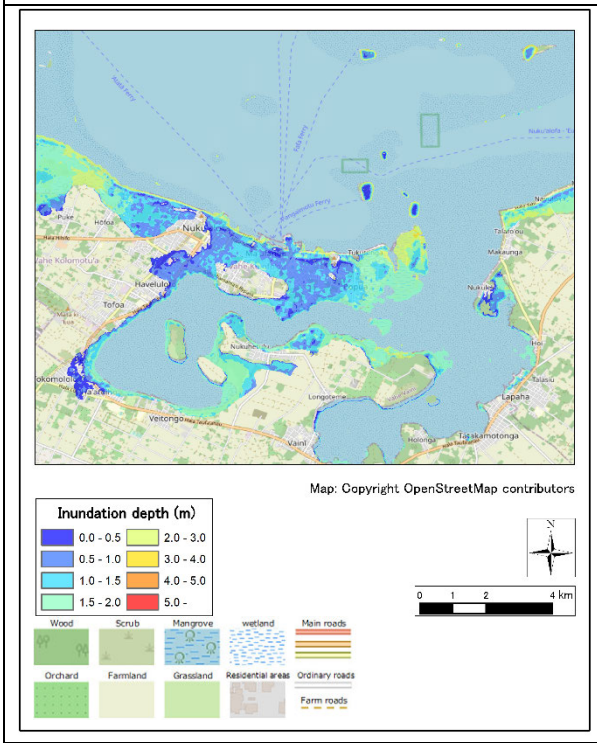

2075 H.W.L. : M.S.L.+1.12m

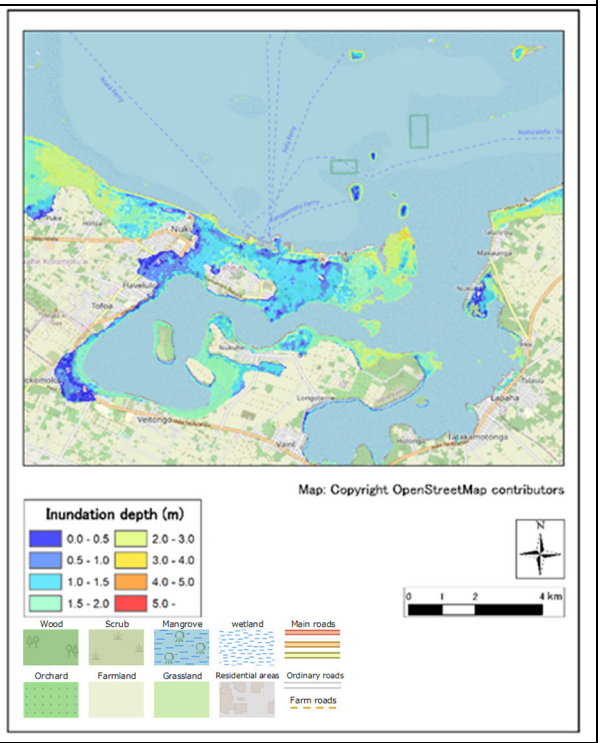

2100 H.W.L. : M.S.L.+1.24m

Source: JICA Study Team

Figure 3.5.7 Estimated inundation in case of sea level rises (storm surge hazard level 2: directly overhead course)

3.6 Analysis for seawalls

3.6.1 Seawall conditions

Tongatapu Island has a seawall of about 2m on the northern coast. As a hazard countermeasure against flood damage such as tsunami and storm surge, raising the height of the seawall is considered to have the most direct effect. Therefore, it is examined the case of raising the seawall. The height of the seawall was raised by about 1m from the current state, and a study was conducted on the case where the height was improved to M.S.L. + 3.0m. Seawall conditions are shown in Figure 3.6.1 and Figure 3.6.2.

Source: JICA Study Team

Figure 3.6.1 Existing Seawall

Source: JICA Study Team

Figure 3.6.2 Setting of raised seawall (raised to M.S.L.+3.0m)

(1) Confirmation of seawall effectiveness

Flooding calculations were carried out for the existing seawall and for the case where a raised seawall was set up.

The results showed that there was no significant difference in the extent of inundation. Further raising the seawall would increase the effect, but on the other hand, careful consideration is required, as raising the seawall by more than 1 m is expected to cause a deterioration of the landscape.

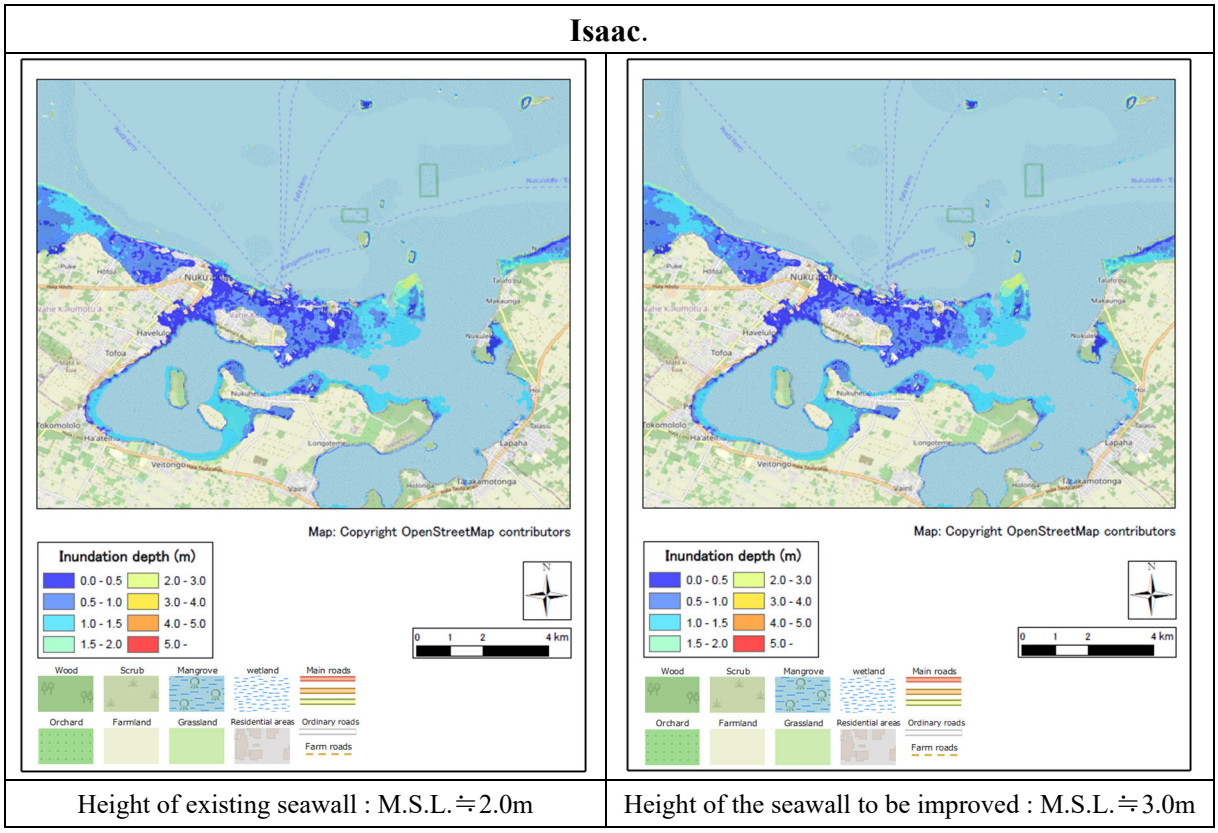

Height of existing seawall : M.S.L.≒2.0m	Height of the seawall to be improved : M.S.L.≒3.0m

Source: JICA Study Team

Figure 3.6.3 Comparison of seawall effectiveness (Isaacs)

4. Multi-hazard mapping

4.1 Method

Hazard maps were prepared for the analysed tsunami and storm surge. As hazard maps are used for evacuation, they need to show the Max hazard. Therefore, the hazard maps were created for the case showing the largest inundation area and depth among the tsunami and storm surge hazards considered in this study.

In cases where the case giving the Max inundation area differs from place to place, the Max extent and depth of inundation of the Max envelope of each case is shown.

(1) Tsunami hazard map (volcanic tsunami)

shows a hazard map based on the assumption of the largest class of volcanic tsunami considered for Hazard Level 2.

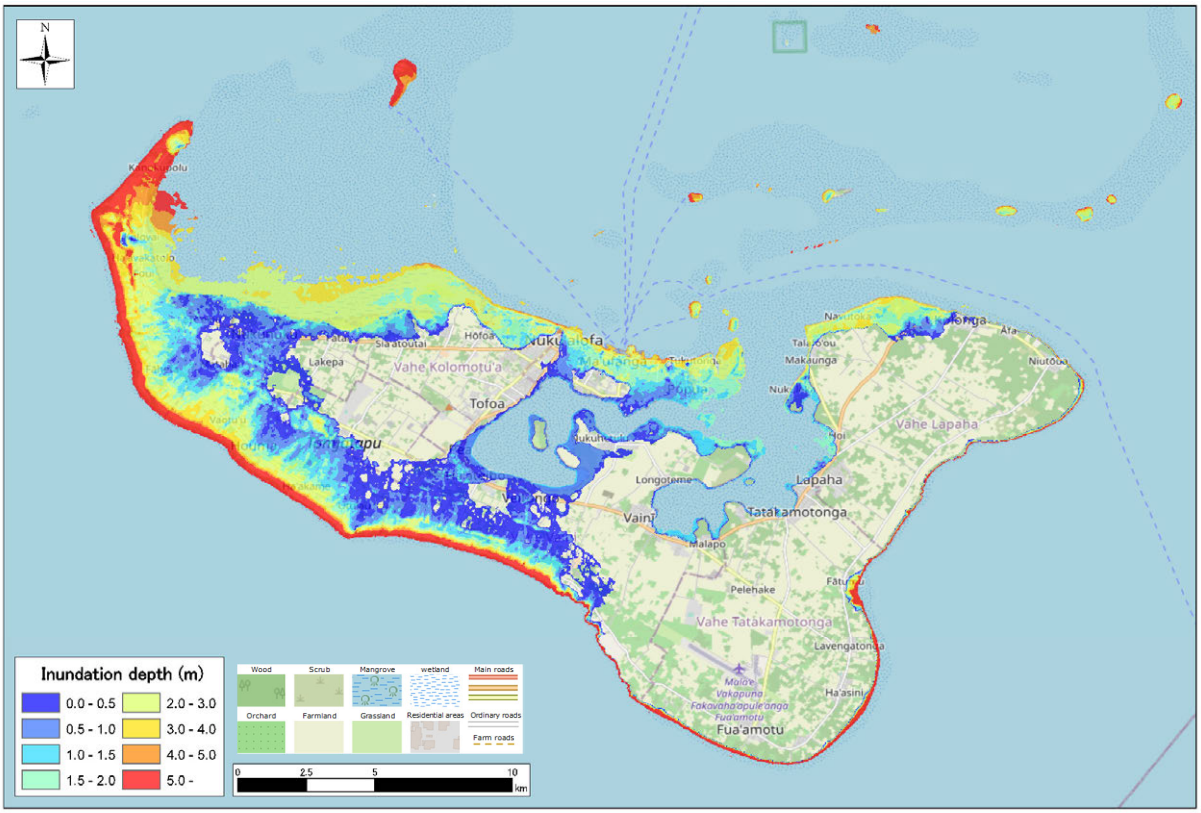

Map: Copyright OpenStreetMap contributors

Source: JICA Study Team

Figure 4.1.1 Tongatapu Island Tsunami hazard map (Volcanic Tsunami)

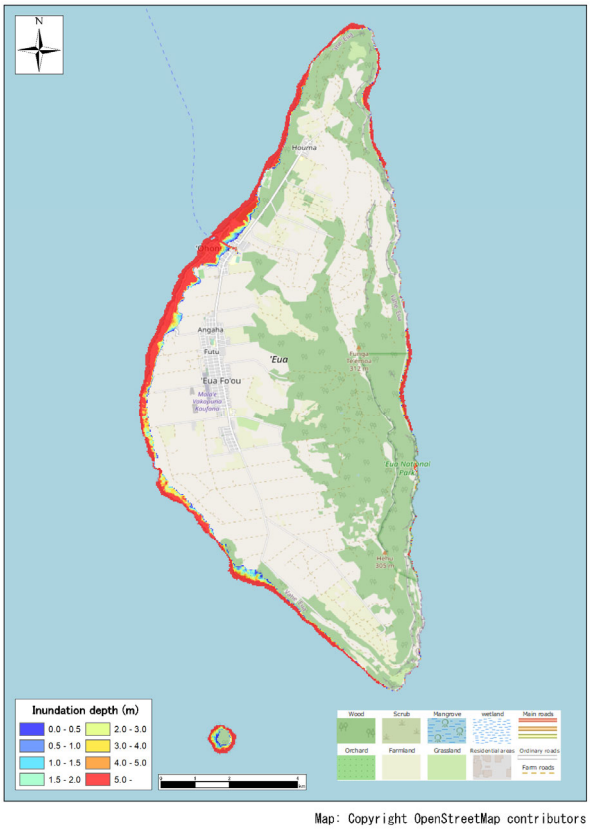

Source: JICA Study Team

Figure 4.1.2 Eua Island Tsunami hazard map (Volcanic Tsunami)

(2) Tsunami Hazard Map (Seismic Tsunami)

Figure 4.1.3 shows a hazard map based on the assumption of the largest class seismic tsunami examined at hazard level 2.

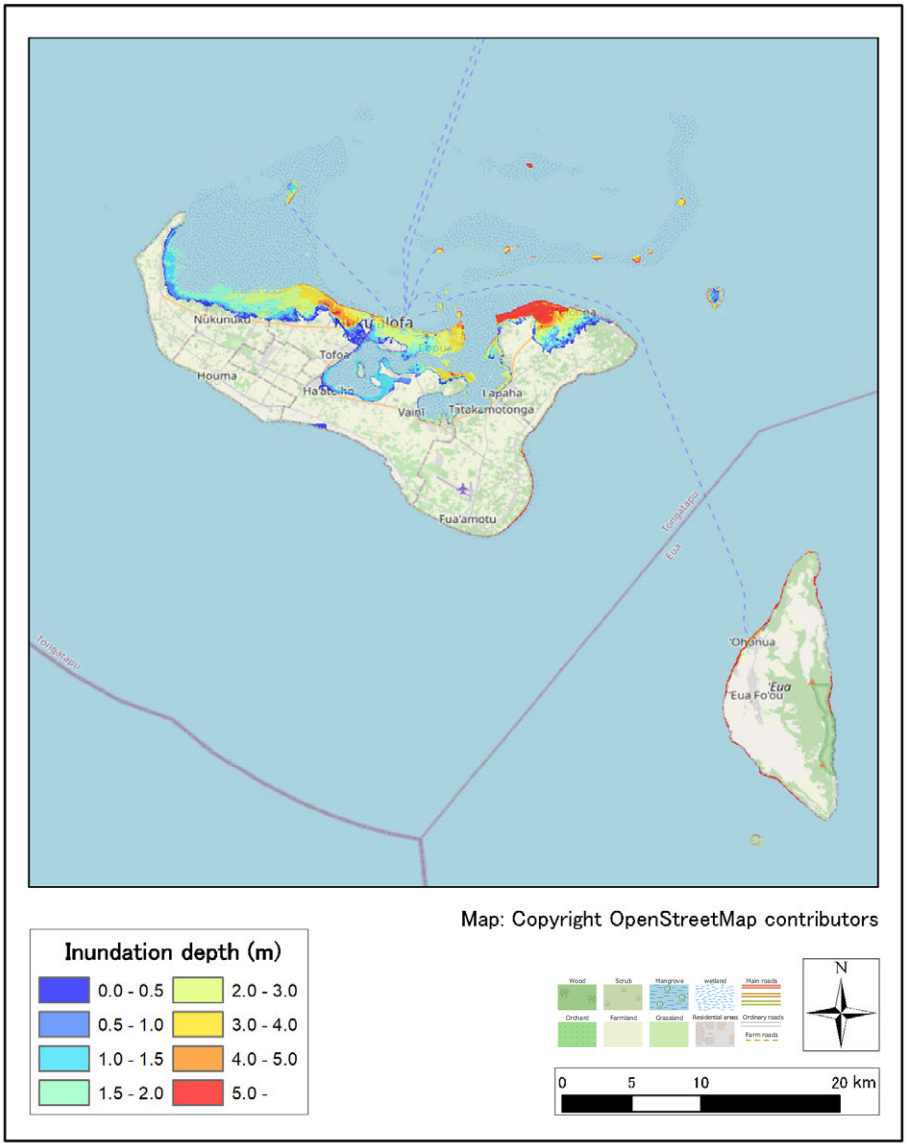

Source: JICA Study Team

Figure 4.1.3 Tsunami Hazard Map (Seismic Tsunami)

(3) Storm Surge Hazard Map

Figure 4.1.4 shows a hazard map based on the assumption of the largest class seismic tsunami examined at hazard level 2. The tidal conditions are year of 2075, which is the middle of the sea level rise cases (2050, 2075, 2100) that take into account climate change.

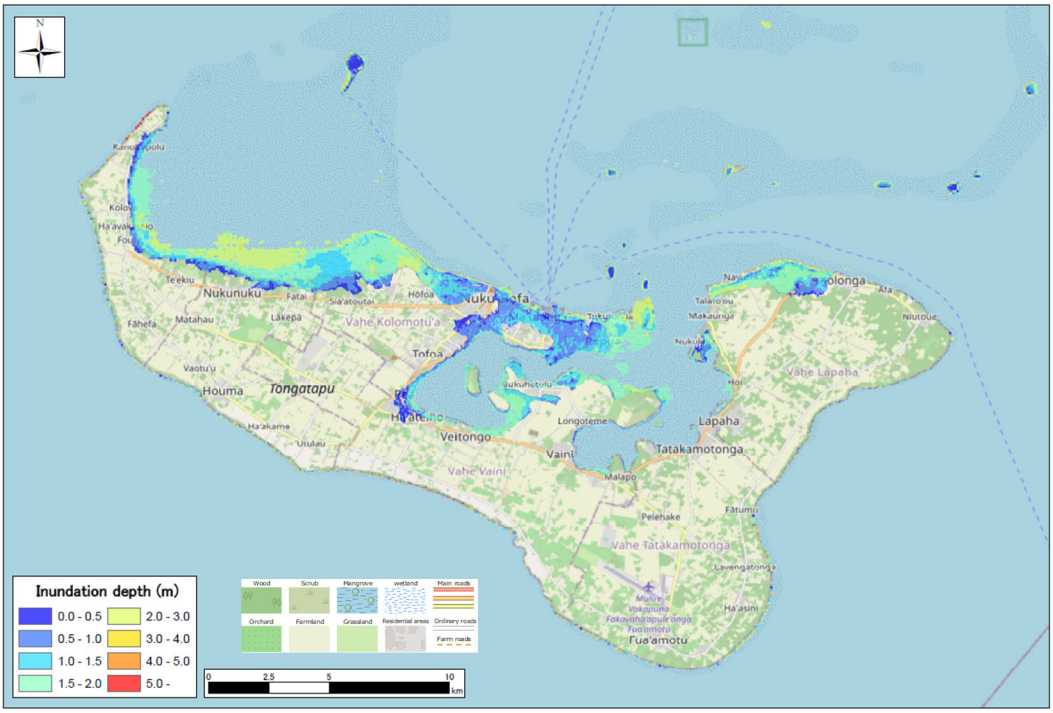

Source: JICA Study Team

Figure 4.1.4 Storm surge hazard Map

4.2 Max enveloping hazard map for tsunamis (volcanic and seismic) and storm surges

The tsunami and storm surge hazard maps were created by overlaying the hazard maps organised in (1) to (3) above. The results are shown below.

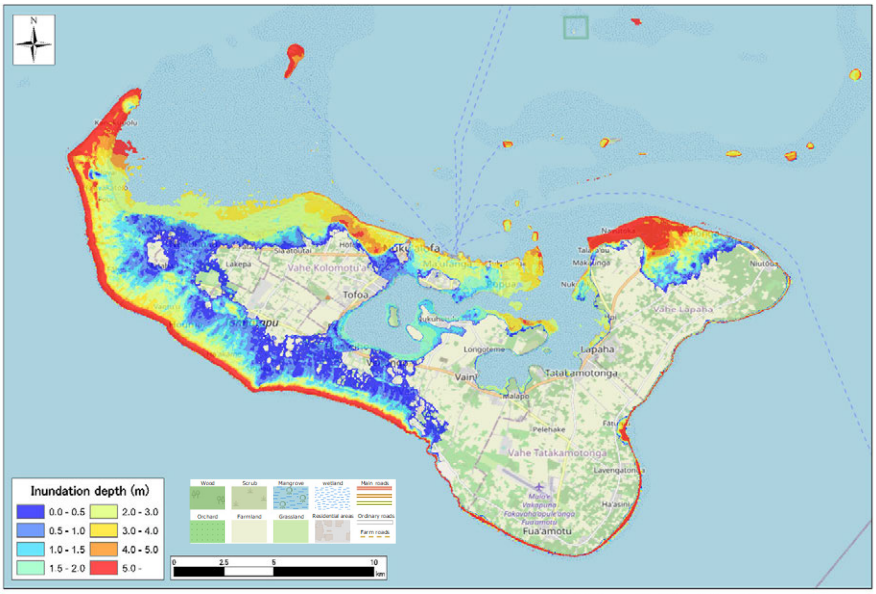

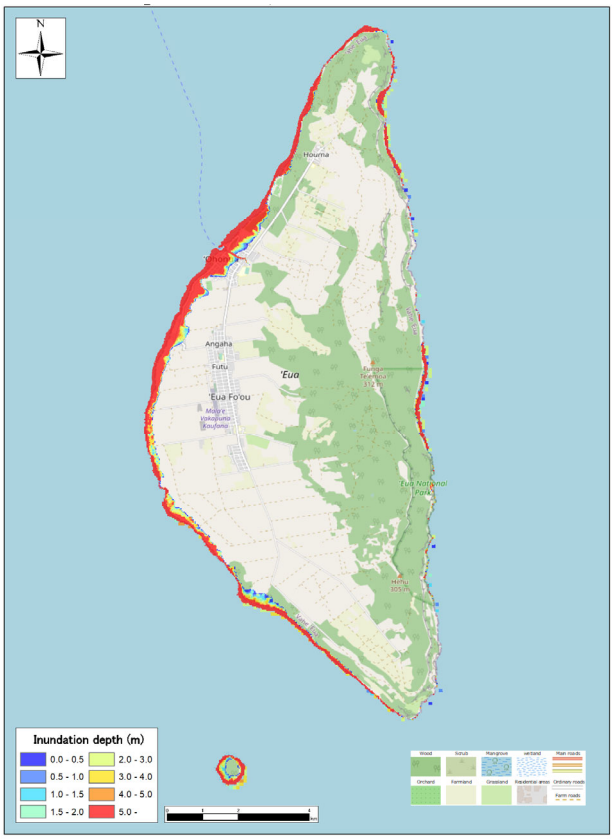

Source: JICA Study Team

Figure 4.2.1 Tsunami (volcanic and seismic tsunami) and storm surge hazard maps

5. Organisation of waveforms

5.1 Volcanic tsunami waveforms

The waveforms of volcanic tsunamis, except for Tongatapu and Eua Island, were compiled to contribute to future disaster prevention. The approximate tsunami height and arrival time can be determined from the waveforms. Waveforms are shown in Appendix 3-3.
The location map of the extracted waveforms is shown below.

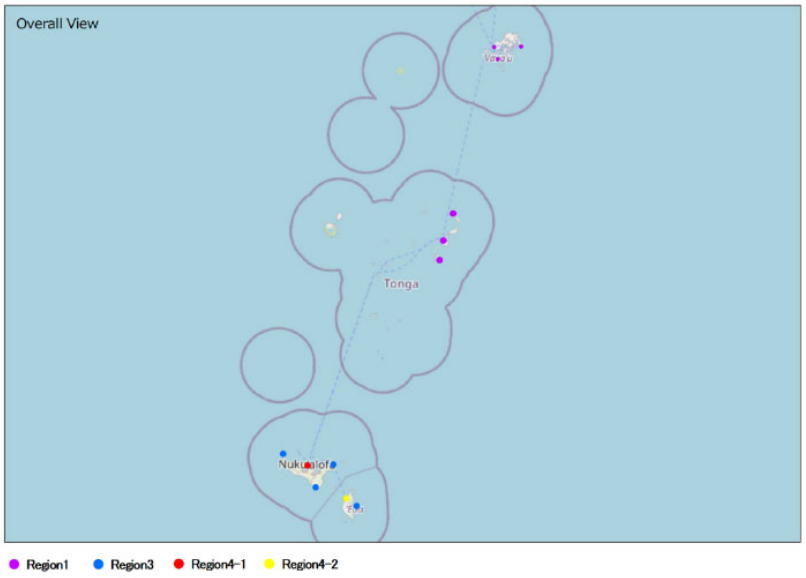

Source: JICA Study Team

Figure 5.1.1 Location map of waveform output points (general view)

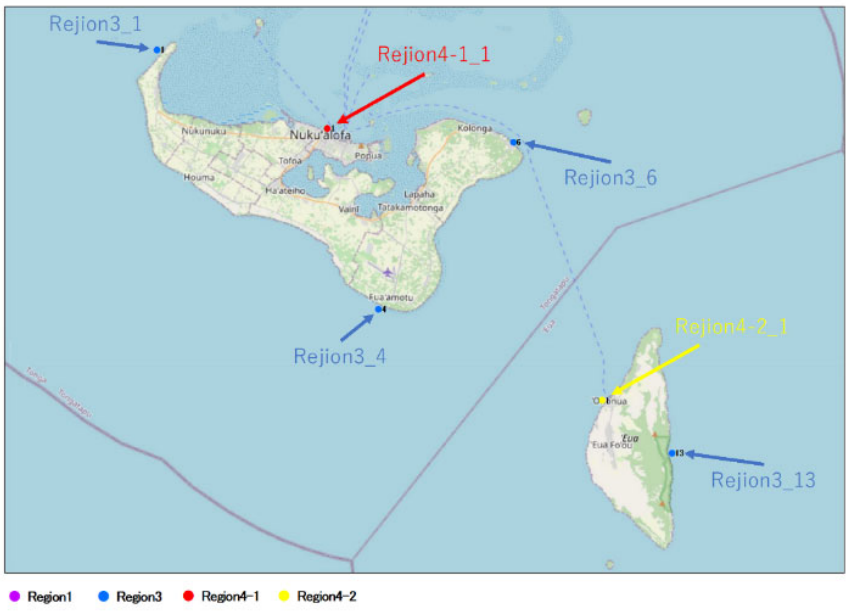

Source: JICA Study Team

Figure 5.1.2 Waveform output points (Tongatapu Island and Eua Island)

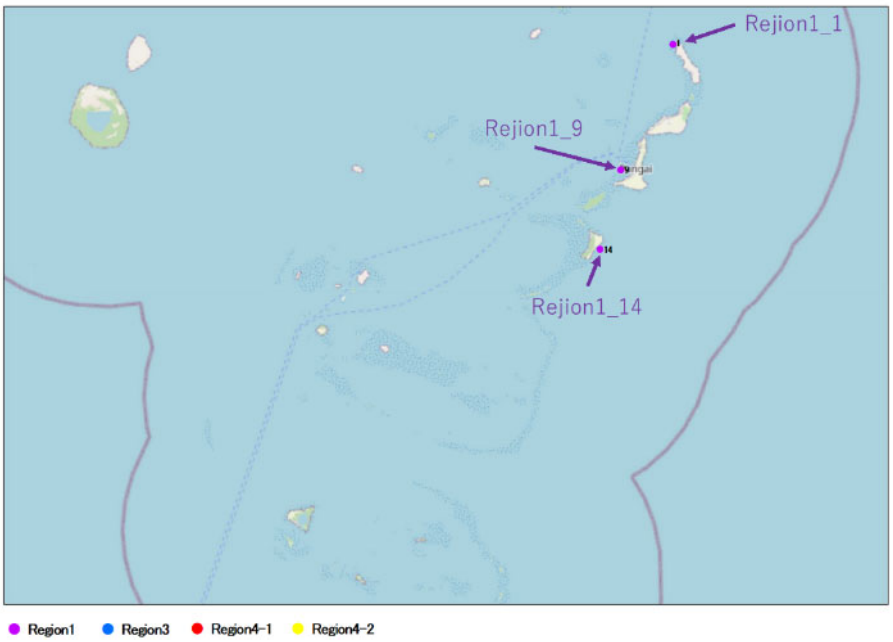

Source: JICA Study Team

Figure 5.1.3 Waveform output points (HA'APAI Islands)

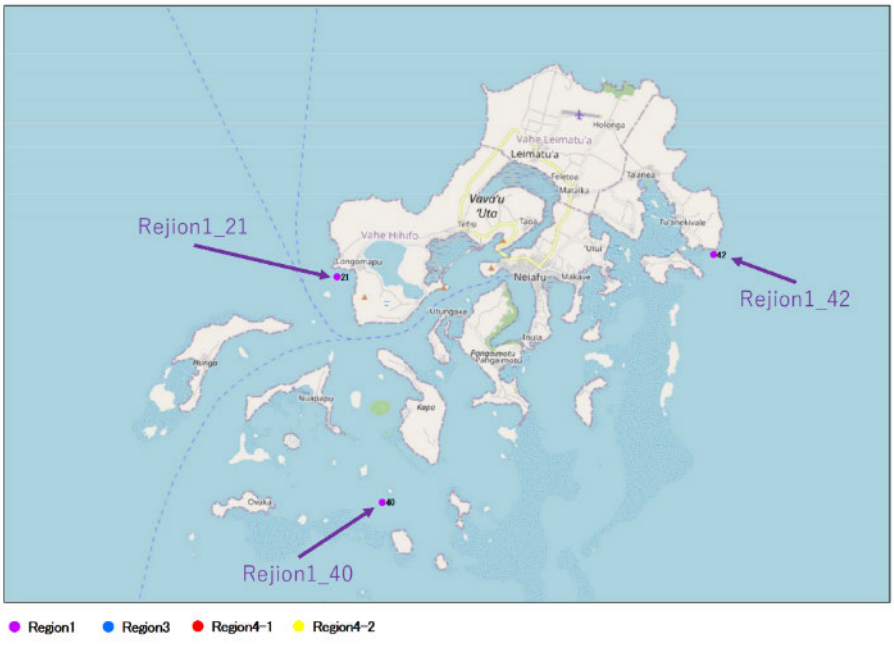

Source: JICA Study Team

Figure 5.1.4 Waveform output point (VAVA'U Islands)